National Library of Canada
Bibliothèque nationale du Canada

Canadian Theses Service
Service des thèses canadiennes

Ottawa, Canada
K1A 0N4

NOTICE

The quality of this microform is heavily dependent upon the quality of the original thesis submitted for microfilming. Every effort has been made to ensure the highest quality of reproduction possible.

If pages are missing, contact the university which granted the degree.

Some pages may have indistinct print especially if the original pages were typed with a poor typewriter ribbon or if the university sent us an inferior photocopy.

Previously copyrighted materials (journal articles, published tests, etc.) are not filmed.

Reproduction in full or in part of this microform is governed by the Canadian Copyright Act, R.S.C. 1970, c. C-30.

AVIS

La qualité de cette microforme dépend grandement de la qualité de la thèse soumise au microfilmage. Nous avons tout fait pour assurer une qualité supérieure de reproduction.

S'il manque des pages, veuillez communiquer avec l'université qui a conféré le grade.

La qualité d'impression de certaines pages peut laisser à désirer, surtout si les pages originales ont été dactylographiées à l'aide d'un ruban usé ou si l'université nous a fait parvenir une photocopie de qualité inférieure.

Les documents qui font déjà l'objet d'un droit d'auteur (articles de revue, tests publiés, etc.) ne sont pas microfilmés.

La reproduction, même partielle, de cette microforme est soumise à la Loi canadienne sur le droit d'auteur, SRC 1970, c. C-30.

NL-339 (r. 88/04)

Canada

THE UNIVERSITY OF ALBERTA

ENTHALPY OF MIXING OF CARBON DIOXIDE WITH ORGANIC SOLVENTS

by

Raul A. Hauser

A THESIS

SUBMITTED TO THE FACULTY OF GRADUATE STUDIES AND RESEARCH

IN PARTIAL FULFILMENT OF THE REQUIREMENTS FOR THE DEGREE

OF MASTER OF SCIENCE

IN

CHEMICAL ENGINEERING

DEPARTMENT OF CHEMICAL ENGINEERING

EDMONTON, ALBERTA

FALL 1988

Permission has been granted to the National Library of Canada to microfilm this thesis and to lend or sell copies of the film.

The author (copyright owner) has reserved other publication rights, and neither the thesis nor extensive extracts from it may be printed or otherwise reproduced without his/her written permission.

L'autorisation a été accordée à la Bibliothèque nationale du Canada de microfilmer cette thèse et de prêter ou de vendre des exemplaires du film.

L'auteur (titulaire du droit d'auteur) se réserve les autres droits de publication; ni la thèse ni de longs extraits de celle-ci ne doivent être imprimés ou autrement reproduits sans son autorisation écrite.

ISBN 0-315-45596-9

THE UNIVERSITY OF ALBERTA

RELEASE FORM

NAME OF AUTHOR Raul A. Hauser

TITLE OF THESIS Enthalpy of Mixing of Carbon Dioxide with Organic Solvents

DEGREE FOR WHICH THESIS WAS PRESENTED Master of Science in Chemical Engineering

YEAR THIS DEGREE GRANTED Fall 1988

Permission is hereby granted to the UNIVERSITY OF ALBERTA LIBRARY to reproduce single copies of this thesis and to lend or sell such copies for private, scholarly or scientific research purposes only.

The author reserves other publication rights, and neither the thesis nor extensive extracts from it may be printed or otherwise reproduced without the author's written permission.

(SIGNED) .....

PERMANENT ADDRESS:

Norte 87-A # 20

Colonia Claveria

Mexico, D.F. 02080 MEXICO

DATED August 16, 1988

THE UNIVERSITY OF ALBERTA

FACULTY OF GRADUATE STUDIES AND RESEARCH

The undersigned certify that they have read, and recommend to the Faculty of Graduate Studies and Research for acceptance, a thesis entitled Enthalpy of Mixing of Carbon Dioxide with Organic Solvents submitted by Raul A. Hauser in partial fulfilment of the requirements for the degree of Master of Science in Chemical Engineering.

A.E. Mather
.....
Supervisor. A.E. Mather

P.R. Tremaine
.....
Co-supervisor. P.R. Tremaine

L.G. Hepler
.....
L.G. Hepler

T.W. Forest
.....
T.W. Forest

Date August 15, 1988

TO MY PARENTS

ABSTRACT

The enthalpy of mixing of CO_2 with six physical solvents has been measured at 298.15 K and 7.5, 10.6, and 12.6 MPa. The solvents used were: N-Methyl Pyrrolidone, Propylene Carbonate, Selexol, Methanol, Methyl Cyanoacetate, and N-Formyl Morpholine. In addition to these solvents, the enthalpy of mixing of CO_2 with Toluene was determined at 298.15 and 308.15 K and pressures of 7.5 and 10.6 MPa. The enthalpy of mixing of Cyclohexane with n-Hexane was also measured at 298.15 K and 0.1, 7.0, and 14.0 MPa.

The enthalpy of mixing measurements for the systems (Cyclohexane + n-Hexane) and (CO_2 + Toluene) are in good agreement with similar measurements made by Christensen, et al. and Wormald, et al. The (CO_2 + Physical Solvent) systems exhibited exothermic enthalpy of mixing in the entire composition range. The only exception was the (CO_2 + Methanol) system which showed both exothermic and endothermic effects. The accuracy of the enthalpy of mixing measurements is about 6 per cent.

The experimental results were predicted with the Peng-Robinson equation of state. The fits obtained with the equation are approximate, even though the equation reproduces the main features observed in the enthalpy of mixing curves.

AKNOWLEDGMENTS

I am truly indebted to my supervisor, Dr. Alan E. Mather, for his patience, encouragement, guidance and support throughout the course of my graduate program.

I am grateful to Dr. Peter Tremaine for his encouragement and suggestions during the course of this work.

I wish to thank the Alberta Research Council, particularly the Oil Sands and Hydrocarbon Recovery Department, for making their equipment available and for all the assistance provided during the course of this work. Thanks are extended to Brian Wiwchar for his help in building the flow system, and to Jamey Hovey for his helpful suggestions and discussions.

Finally, financial support from the Natural Sciences and Engineering Research Council of Canada and the University of Alberta is gratefully acknowledged.

TABLE OF CONTENTS

Chapter		Page
I	INTRODUCTION	1
II	HIGH PRESSURE ISOTHERMAL FLOW CALORIMETRY	6
	2.1 General Aspects of Isothermal Calorimeters	6
	2.2 Enthalpy of Mixing Measurements for Systems involving CO_2	7
	2.2.1 Christensen et al. Apparatus	7
	2.2.2 Wormald et al. Apparatus	11
III	EXPERIMENTAL APPARATUS	16
	3.1 Tronac High Pressure Isothermal Flow Calorimeter	16
	3.1.1 Reaction Vessel	16
	3.1.2 450 Electronics Console	18
	3.1.3 550 Electronics Console	23
	3.1.4 Water Bath and Refrigeration System	28
	3.2 Flow System	29
IV	EXPERIMENTAL PROCEDURE	34
	4.1 Pumps Fill-up	34
	4.2 Equilibration	35
	4.3 System Pressurization	35
	4.4 450 and 550 Electronics Consoles Adjustments	36
	4.5 Electrical Calibration	38
	4.6 Measurement of Enthalpy of Mixing	38
	4.7 System Evacuation	39

4.8 Flow Rates 39

4.9 Materials 40

V EXPERIMENTAL RESULTS AND DISCUSSION 44

5.1 Experimental Results 44

5.2 Errors and Uncertainties 58

5.3 Regression Procedure 58

5.4 (Cyclohexane + n-Hexane) 59

5.5 (CO_2 + Toluene) 59

5.6 (CO_2 + N-Methyl Pyrrolidone), (CO_2 + Propylene Carbonate), and (CO2 + Methyl Cyanoacetate) 60

5.7 (CO_2 + Selexol) 60

5.8 (CO_2 + Methanol) 61

5.9 (CO_2 + N-Formyl Morpholine) 61

VI PREDICTED DATA WITH THE PENG-ROBINSON EQUATION OF STATE 63

6.1 General Background 63

6.2 Enthalpy Calculations 65

6.3 Interaction Parameters 66

6.4 Discussion of Results 66

6.4.1 (CO_2 + Toluene) System 67

6.4.2 (CO_2 + Physical Solvent) Systems 67

VII CONCLUSIONS 79

REFERENCES 81

APPENDIX I. Physical Properties 86

APPENDIX II. Sample Calculation 95

APPENDIX III. Calibration of Pumps 102

APPENDIX IV. Experimental and Calculated Data 106

APPENDIX V. Enthalpy Departure Formulation for the Peng-Robinson Equation of State 119

APPENDIX VI. Experimental and Predicted Data 122

APPENDIX VII. Raw Experimental Data 130

LIST OF TABLES

Table		Page
1.	Summary of {Carbon Dioxide + Hydrocarbon} Systems.	8
2.	Correspondence between the Settings of the μcal/count Switch and the Zero Adjustment Coarse Control.	27
3	Solvents Studied in this Work.	41
4.	Peng-Robinson Parameters for Various Solvents.	77
5.	Interaction Parameters for Various Systems involving Carbon Dioxide at 298.15 K.	78
A1.1	References for Vapour Pressure and Density Data for Various Solvents.	93
A1.2	Chemical Abstracts Registry Number for Various Solvents.	94
A2.1	Basic Experimental Data for the System (CO_2 + Methanol).	100
A3.1	Calibration of the ISCO LC-5000 Syringe Pump.	103
A3.2	Calibration of the ISCO 314 Syringe Pump.	104
A3.3	Coefficients for the correction of the Flow Rate by Equation (A3.1).	105
A4.1	Enthalpy of Mixing of (Cyclohexane + n-Hexane) at 298.15 K and 0.1, 7.0, and 14.0 MPa.	107
A4.2	Comparison of Calculated and Experimental Enthalpy of Mixing of (CO_2 + Toluene) at 298.15 and 308.15 K and 10.6 MPa.	108
A4.3	Comparison of Calculated and Experimental Enthalpy of Mixing of (CO_2 + Toluene) at 298.15 K and 7.5 MPa.	108
A4.4	Comparison of Calculated and Experimental Enthalpy of Mixing of (CO_2 + N-Methyl Pyrrolidone) at 298.15 K and 7.5, 10.6, and 12.6 MPa.	109
A4.5	Comparison of Calculated and Experimental Enthalpy of Mixing of (CO_2 + Propylene Carbonate) at 298.15 K and 7.5, 10.6, and 12.6 MPa.	110

A4.6 Comparison of Calculated and Experimental Enthalpy of Mixing of (CO_2 + Selexol) at 298.15 K and 7.5, 10.6, and 12.6 MPa. 111

A4.7 Comparison of Calculated and Experimental Enthalpy of Mixing of (CO_2 + Selexol) at 298.15 K and 7.5, 10.6, and 12.6 MPa. 112

A4.8 Comparison of Calculated and Experimental Enthalpy of Mixing of (CO_2 + Methanol) at 298.15 K and 7.5, 10.6, and 12.6 MPa. 113

A4.9 Comparison of Calculated and Experimental Enthalpy of Mixing of (CO_2 + Methyl Cyanoacetate) at 298.15 K and 7.5, 10.6, and 12.6 MPa. 114

A4.10 Comparison of Calculated and Experimental Enthalpy of Mixing of (CO_2 + N-Formyl Morpholine) at 298.15 K and 7.5 MPa. 115

A4.11 Comparison of the Enthalpy of Mixing of (CO_2 + Selexol) at 298.15 K and 10.6 MPa with Different Flow Rates. 116

A4.12 Coefficients for least-squares representation of the enthalpy of mixing of CO_2 with several solvents by equation (5.1). 117

A6.1 Comparison of Predicted and Experimental Enthalpy of Mixing of (CO_2 + Toluene) at 298.15 K and 308.15 K and 10.6 MPa. 123

A6.2 Comparison of Predicted and Experimental Enthalpy of Mixing of (CO_2 + Toluene) at 298.15 K and 7.5 MPa. 123

A6.3 Comparison of Predicted and Experimental Enthalpy of Mixing of (CO_2 + N-Methyl Pyrrolidone) at 298.15 K and 7.5, 10.6, and 12.6 MPa. 124

A6.4 Comparison of Predicted and Experimental Enthalpy of Mixing of (CO_2 + Propylene Carbonate) at 298.15 K and 7.5, 10.6, and 12.6 MPa. 125

A6.5 Comparison of Predicted and Experimental Enthalpy of Mixing of (CO_2 + Selexol) at 298.15 K and 7.5, 10.6, and 12.6 MPa. 126

A6.6 Comparison of Predicted and Experimental Enthalpy of Mixing of (CO_2 + Methanol) at 298.15 K and 7.5, 10.6, and 12.6 MPa. 127

A6.7 Comparison of Predicted and Experimental Enthalpy of Mixing of (CO_2 + Methyl Cyanoacetate) at 298.15 K and 7.5, 10.6, and 12.6 MPa. 128

A6.8 Comparison of Predicted and Experimental Enthalpy of Mixing of (CO_2 + N-Formyl Morpholine) at 298.15 K and 7.5 MPa. 129

A7.1 Raw Data - Enthalpy of Mixing of (Cyclohexane + n-Hexane) at 298.15 K and 0.1 MPa. 131

A7.2 Raw Data - Enthalpy of Mixing of (Cyclohexane + n-Hexane) at 298.15 K and 7.0 MPa. 132

A7.3 Raw Data - Enthalpy of Mixing of (Cyclohexane + n-Hexane) at 298.15 K and 14.0 MPa. 133

A7.4 Raw Data - Enthalpy of Mixing of (CO_2 + Toluene) at 298.15 K and 7.5 MPa. 134

A7.5 Raw Data - Enthalpy of Mixing of (CO_2 + Toluene) at 298.15 K and 10.6 MPa. 135

A7.6 Raw Data - Enthalpy of Mixing of (CO_2 + Toluene) at 308.15 K and 10.6 MPa. 136

A7.7 Raw Data - Enthalpy of Mixing of (CO_2 + N-Methyl Pyrrolidone) at 298.15 K and 7.5 MPa. 137

A7.8 Raw Data - Enthalpy of Mixing of (CO_2 + N-Methyl Pyrrolidone) at 298.15 K and 10.6 MPa. 138

A7.9 Raw Data - Enthalpy of Mixing of (CO_2 + N-Methyl Pyrrolidone) at 298.15 K and 12.6 MPa. 139

A7.10 Raw Data - Enthalpy of Mixing of (CO_2 + Propylene Carbonate) at 298.15 K and 7.5 MPa. 140

A7.11 Raw Data - Enthalpy of Mixing of (CO_2 + Propylene Carbonate) at 298.15 K and 10.6 MPa. 141

A7.12 Raw Data - Enthalpy of Mixing of (CO_2 + Propylene Carbonate) at 298.15 K and 12.6 MPa. 142

A7.13 Raw Data - Enthalpy of Mixing of (CO_2 + Selexol) at 298.15 K and 7.5 MPa. 143

A7.14 Raw Data - Enthalpy of Mixing of (CO_2 + Selexol) at 298.15 K and 10.6 MPa. 144

A7.15 Raw Data - Enthalpy of Mixing of (CO_2 + Selexol) at 298.15 K and 12.6 MPa. 145

A7.16 Raw Data - Enthalpy of Mixing of (CO_2 + Selexol) at 298.15 K and 7.5 MPa. 146

A7.17 Raw Data - Enthalpy of Mixing of (CO_2 + Selexol) at 298.15 K and 10.6 MPa. 147

A7.18 Raw Data - Enthalpy of Mixing of (CO_2 + Selexol) at 298.15 K and 12.6 MPa. 148

A7.19 Raw Data - Enthalpy of Mixing of (CO_2 + Methanol) at 298.15 K and 7.5 MPa. 149

A7.20 Raw Data - Enthalpy of Mixing of (CO_2 + Methanol) at 298.15 K and 10.6 MPa. 150

A7.21 Raw Data - Enthalpy of Mixing of (CO_2 + Methanol) at 298.15 K and 12.6 MPa. 151

A7.22 Raw Data - Enthalpy of Mixing of (CO_2 + Methyl Cyanoacetate) at 298.15 K and 7.5 MPa. 152

A7.23 Raw Data - Enthalpy of Mixing of (CO_2 + Methyl Cyanoacetate) at 298.15 K and 10.6 MPa. 153

A7.24 Raw Data - Enthalpy of Mixing of (CO_2 + Methyl Cyanoacetate) at 298.15 K and 12.6 MPa. 154

A7.25 Raw Data - Enthalpy of Mixing of (CO_2 + N-Formyl Morpholine) at 298.15 K and 7.5 MPa. 155

LIST OF FIGURES

Figure		Page
1.	Solvent absorption acid gas removal process.	3
2.	Block Diagram of the main components of the calorimeter.	9
3.	Flow System.	12
4.	Plan view of the mixing calorimeter.	14
5.	Side view of the mixing calorimeter.	15
6.	Reaction vessel and contents.	17
7.	Front Panel of the 450 Electronics Console.	19
8.	Rear Panel of the 450 Electronics Console.	20
9.	Front Panel of the 550 Electronics Console.	24
10.	Experimental Apparatus.	30
11.	Enthalpy of Mixing of (Cyclohexane + n-Hexane) at 298.15 K and 0.1 MPa.	45
12.	Enthalpy of Mixing of (Cyclohexane + n-Hexane) at 298.15 K and 7.0 MPa.	46
13.	Enthalpy of Mixing of (Cyclohexane + n-Hexane) at 298.15 K and 14.0 MPa.	47
14.	Enthalpy of Mixing of (CO_2 + Toluene) at 298.15 K and 7.5 MPa.	48
15.	Enthalpy of Mixing of (CO_2 + Toluene) at 298.15 K and 10.6 MPa.	49
16.	Enthalpy of Mixing of (CO_2 + Toluene) at 308.15 K and 10.6 MPa.	50
17.	Comparison of Calculated and Experimental Enthalpy of Mixing of (CO_2 + N-Methyl Pyrrolidone) at 298.15 K.	51
18.	Comparison of Calculated and Experimental Enthalpy of Mixing of (CO_2 + Selexol) at 298.15 K. (0.83% wt. H_2O)	52

19. Comparison of Calculated and Experimental Enthalpy of Mixing of (CO_2 + Selexol) at 298.15 K. (3.62% wt. H_2O) 53

20. Comparison of Calculated and Experimental Enthalpy of Mixing of (CO_2 + Methanol) at 298.15 K. 54

21. Comparison of Calculated and Experimental Enthalpy of Mixing of (CO_2 + Propylene Carbonate) at 298.15 K. 55

22. Comparison of Calculated and Experimental Enthalpy of Mixing of (CO_2 + N-Formyl Morpholine) at 298.15 K. 56

23. Comparison of Calculated and Experimental Enthalpy of Mixing of (CO_2 + Methyl Cyanoacetate) at 298.15 K. 57

24. Comparison of the Enthalpy of Mixing of (CO_2 + Selexol) at 298.15 K with Different Flow Rates. (0.83% wt. H_2O) 62

25. Comparison of Predicted and Experimental Enthalpy of Mixing of (CO_2 + N-Methyl Pyrrolidone) at 298.15 K. 68

26. Comparison of Predicted and Experimental Enthalpy of Mixing of (CO_2 + Selexol) at 298.15 K. (0.83% wt. H_2O) 69

27. Comparison of Predicted and Experimental Enthalpy of Mixing of (CO_2 + Methanol) at 298.15 K. 70

28. Comparison of Predicted and Experimental Enthalpy of Mixing of (CO_2 + Propylene Carbonate) at 298.15 K. 71

29. Comparison of Predicted and Experimental Enthalpy of Mixing of (CO_2 + N-Formyl Morpholine) at 298.15 K. 72

30. Comparison of Predicted and Experimental Enthalpy of Mixing of (CO_2 + Methyl Cyanoacetate) at 298.15 K. 73

31. Comparison of Predicted and Experimental Enthalpy of Mixing of (CO_2 + Toluene) at 298.15 K. 74

32. Comparison of Predicted and Experimental Enthalpy of Mixing of (CO_2 + Toluene) at 308.15 K. 75

33. Chart Recorder Output. 101

NOMENCLATURE

a	parameter in Peng-Robinson equation of state, Pa m^6/mol^2
b	parameter in Peng-Robinson equation of state, m^3/mol
v	volumetric flow rate, ml/s
w	weight fraction
x	mole fraction
B	constant defined by equation (A5.9)
C	coefficient in equation (5.1)
D	coefficient in equation (5.1)
E	energy per count defined by equation (A2.2), (J/s)/count
H	enthalpy, J/mol
M	molar flow rate, mol/s
P	pressure, Pa
Q	heat of the interaction defined by equation (A2.4), Watts
R	gas contant, J/mol K
T	temperature, K
V	specific volume, m^3/kg
W	heating power defined by equation (A2.1), Watts
Z	compressibility factor

Greek letters

β_T	isothermal compressibility, m^2/N
δ	interaction parameter in the Peng-Robinson equation of state
ρ	density, g/cm^3
σ	standard deviation

v	molar volume, m^3/mol

Subscripts

i	component i
j	component j
r	reduced property

Superscripts

E	excess property
*	ideal gas state

CHAPTER I

INTRODUCTION

In acid gas removal, the most common impurities are CO_2 and H_2S which often occur in quite large concentrations in industrial processes such as hydrogen manufacture, ammonia production, and natural gas purification. Some processes (e.g., ammonia manufacture from natural gas), require removal of just one acidic impurity, CO_2. Others such as natural gas purification often require the simultaneous removal of several impurities such as CO_2, H_2S, and COS.

The cleanup target, the allowable extent of the impurity in the treated gas to meet product specifications, varies from process to process and with the nature of the acidic impurity. The cleanup target for H_2S is particularly severe. Such a severe target is necessary due to the toxicity and corrosiveness of H_2S and its ability to poison catalysts. The CO_2 specifications are set to prevent catalyst poisoning and to reduce the amount of CO_2 acting as a diluent in the treated gas.

The most common method for acid gas removal has been absorption into a liquid agent, either physical absorption or absorption into a solution of a chemical base.

The solvent must have several important properties in order to be considered useful in the absorption process. The solvent should have a high capacity for the acid gas under absorption conditions but have a significantly lower capacity under regeneration conditions. The difference in solubility between the two stages determines the circulation rate of the solvent which in turn affects the equipment sizes and heat requirements for regeneration. The solvent must have a low vapour pressure to reduce solvent losses and a low capacity for hydrocarbons which, if absorbed with the acid

gas, may lead to catalyst fouling in the sulphur recovery unit. The solvents for acid gas removal may be classified in terms of the mechanism of absorption. In a first group we have the chemical solvents, which are characterized by liquid phase reactions between the acid gas and the soluble base. Some of these chemical solvents are aqueous solutions of monoethanolamine (MEA), diethanolamine (DEA), and diglycolamine (DGA). The second group are the physical solvents, in which the absorption process takes place strictly by physical dissolution. Some of the solvents in this group are N-methyl pyrrolidone, propylene carbonate, dimethylether of polyethylene glycol (Selexol) and methanol, to mention just a few of them. Another group of absorbents are the mixed solvents which consist of a chemical reactive component and a physical solvent with a high capacity for acid gases. The development of mixed solvents arises from an attempt to combine the desirable features of chemical and physical solvents.

The principal differences between physical and chemical solvents can be summarized as follows:

Physical Solvents.	Chemical Solvents.
Solubility proportional to acid gas partial pressure in feed gas	Capacity not highly sensitive to acid gas partial pressure
Low heat of absorption	High heat of absorption
Desorb by flashing (sometimes)	Need low-level steam for desorption
Difficult to remove acid gas completely (need many stages)	Easily reduces acid gas to low level in treated gas

Acid gas removal processes based on solvent absorption all use variations on a basic process flowsheet shown in Figure 1. The raw gas is contacted countercurrently with regenerated (lean) solvent in an absorber tower which usually operates at low temperature and high pressure. Treated gas leaves overhead from the absorber,

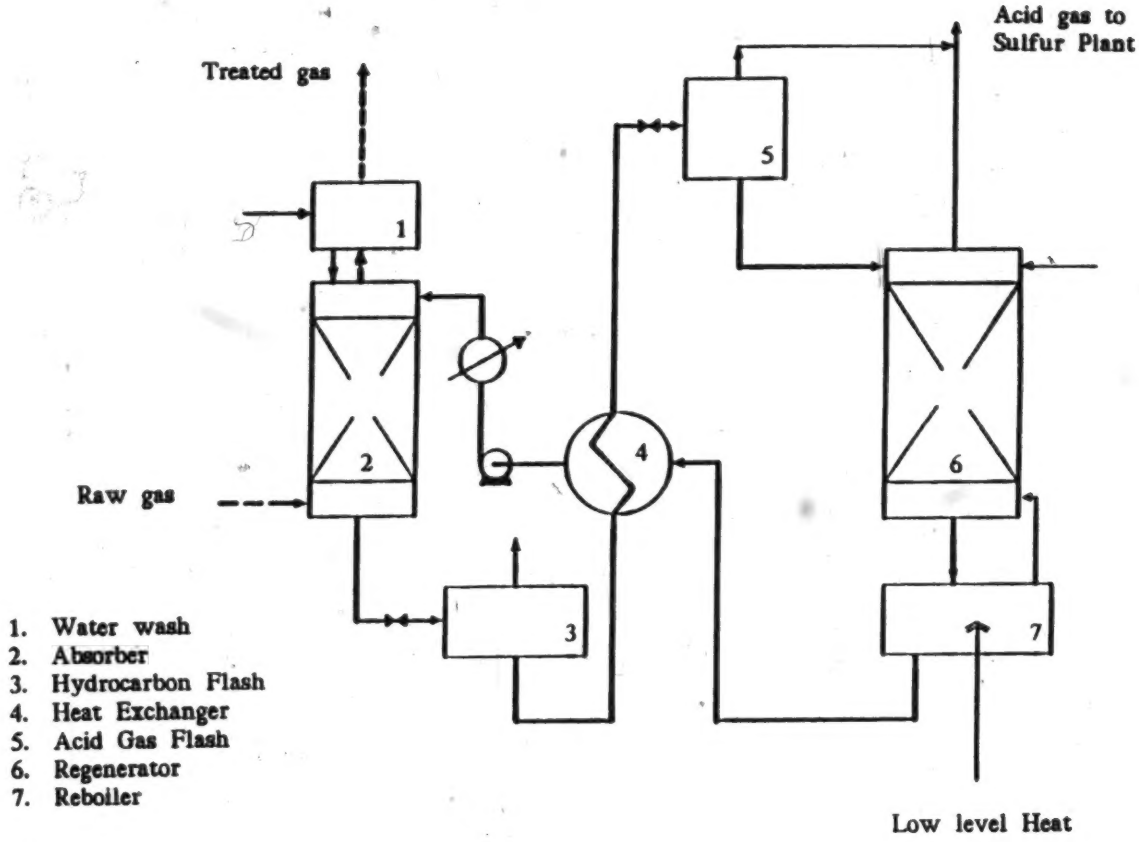

Figure 1. Solvent absorption acid gas removal process.
Modified from Ref. [2]

sometimes after water wash to prevent carryover of solvent components. The loaded (rich) solvent leaving the bottom of the absorber is reduced in pressure, sometimes in stages, to flash off dissolved hydrocarbons and a portion of the acid gases. The rich solvent may also be heated against the returning hot regenerated lean solvent in a rich/lean heat exchanger. The regenerator is usually a low pressure countercurrent tower in which the remaining dissolved acid gases are stripped out with steam generated by reboiling the lean solution.

No gas treating process is a stand-alone operation. Every gas treating unit is integrated into a larger process. When H_2S is present in the acid gas, the separated acid gas must go directly to a sulfur plant to minimize emissions of H_2S to the atmosphere. In CO_2 removal, particularly in connection with ammonia manufacture, the separated CO_2 may become the feedstock for making urea, or it may be recovered as a pure product.

More research is being carried out in order to achieve an efficient removal of these acid gases and to satisfy the need of accurate and reliable data required in the design of the equipment involved in the process, (i.e. the enthalpy of mixing is required to determine the temperature profile in the absorber).

Direct calorimetric measurements at high pressure, such as those performed in this work, are difficult and only a few laboratories are able to make them. A high pressure flow calorimeter is required to carry out these measurements.

The purpose of this work was to determine experimentally the enthalpy of mixing of CO_2 with the major physical solvents used in gas processing. The solvents studied were: N-Methyl Pyrrolidone, Propylene Carbonate, Selexol, Methanol, Methyl Cyanoacetate, and N-Formyl Morpholine. The enthalpy of mixing was measured at 298.15 K and pressures up to 12.6 MPa. A secondary objective was to test the usefulness of a typical cubic equation of state in fitting the CO_2 + solvent experimental data.

Chapter II presents some general aspects of isothermal calorimeters together with a brief overview of the measurements of enthalpy of mixing for systems involving CO_2. Chapter III provides a complete description of the experimental apparatus employed for the determination of the enthalpy of mixing. The experimental procedure is given in Chapter IV. The experimental results and those predicted with the Peng-Robinson equation of state are presented in Chapters V and VI respectively.

CHAPTER II

HIGH PRESSURE ISOTHERMAL FLOW CALORIMETRY

2.1 General Aspects of Isothermal Calorimeters.

A calorimeter is an instrument which measures the energy involved in a known change in state of a material. This can involve a change in phase, temperature, pressure, volume, chemical composition, or any other property of the material which is associated with the change in energy.

A calorimeter can measure the heat involved either directly by comparison with a known electrical energy or indirectly by comparison with materials with known properties. Direct measurement usually involves the addition of a known amount of electrical energy in the form of heat, because with modern techniques, electrical energy can be measured more accurately and conveniently than other forms of energy.

Calorimeters may be classified in several ways. One method of classification is according to which physical variables are kept constant. Thus isothermal calorimeters, as the name implies, are those in which there is ideally no temperature change during the experiment. The general usage of the term isothermal here implies constancy of temperature with time of any part of the calorimeter, rather than the uniformity of temperature over the calorimeter at any one time. Several methods have been used to maintain a constant temperature during the experiment; some of them include the use of electric heating to balance removal of heat and electric cooling (Peltier effect) to balance the addition of heat. The isothermal calorimeter has an advantage that its heat capacity does not affect the results since its temperature does not change.

2.2 Enthalpy of Mixing Measurements for Systems involving CO_2.

The available information in this field is rather scarce and not many people have worked on it. Only two other laboratories have reported high pressure measurements near or above room temperature. Interest in mixtures containing carbon dioxide has led Christensen and co-workers to make measurements on several mixtures containing (carbon dioxide + hydrocarbon). Recently, Wormald and co-workers, with the development of a new flow calorimeter, determined the excess molar enthalpies for the systems (carbon dioxide + toluene) and (carbon dioxide + ethane). In addition, Wallis et al. have made measurements below 230 K using a cryogenic batch calorimeter. Table 1 gives a summary of the systems (carbon dioxide + hydrocarbon) that have been studied up to date.

2.2.1 Christensen et al. Apparatus.

An isothermal titration calorimeter [16], an isothermal titration microcalorimeter [17], an isothermal high pressure flow calorimeter [13], and two isothermal, elevated temperature, high pressure flow calorimeters [14, 15] have been described by Christensen et al. The following description corresponds to that of one of the isothermal, elevated temperature, high pressure flow calorimeters [14], which is a more recent refinement of the low temperature unit [13] used in our study.

The main components of the calorimeter are the reaction vessel containing the isothermal plate and the equilibration coil, the isothermal shields, the air bath, the flow circuit which contains the high pressure pumps and flow controller programmer, and the isothermal control unit. A block diagram showing the main components of the unit is given in Figure 2.

TABLE 1

SUMMARY OF {CARBON DIOXIDE + HYDROCARBON} SYSTEMS

AUTHOR.	SYSTEM.	REFERENCES.
Christensen, et al.	CO_2 + Cyclohexane	[5] [9] [20]
Christensen, et al.	CO_2 + Decane	[8] [37]
Christensen, et al.	CO_2 + n-Hexane	[4] [11]
Christensen, et al.	CO_2 + Pentane	[7] [36]
Christensen, et al.	CO_2 + Pyridine	[6] [10]
Christensen, et al.	CO_2 + Toluene	[3] [19] [35]
Christensen, et al.	CO_2 + Toluene + n-Hexane	[21]
Wallis, et al.	CO_2 + Ethane	[46]
Wormald, et al.	CO_2 + Toluene	[48]
Wormald, et al.	CO_2 + Ethane	[49]

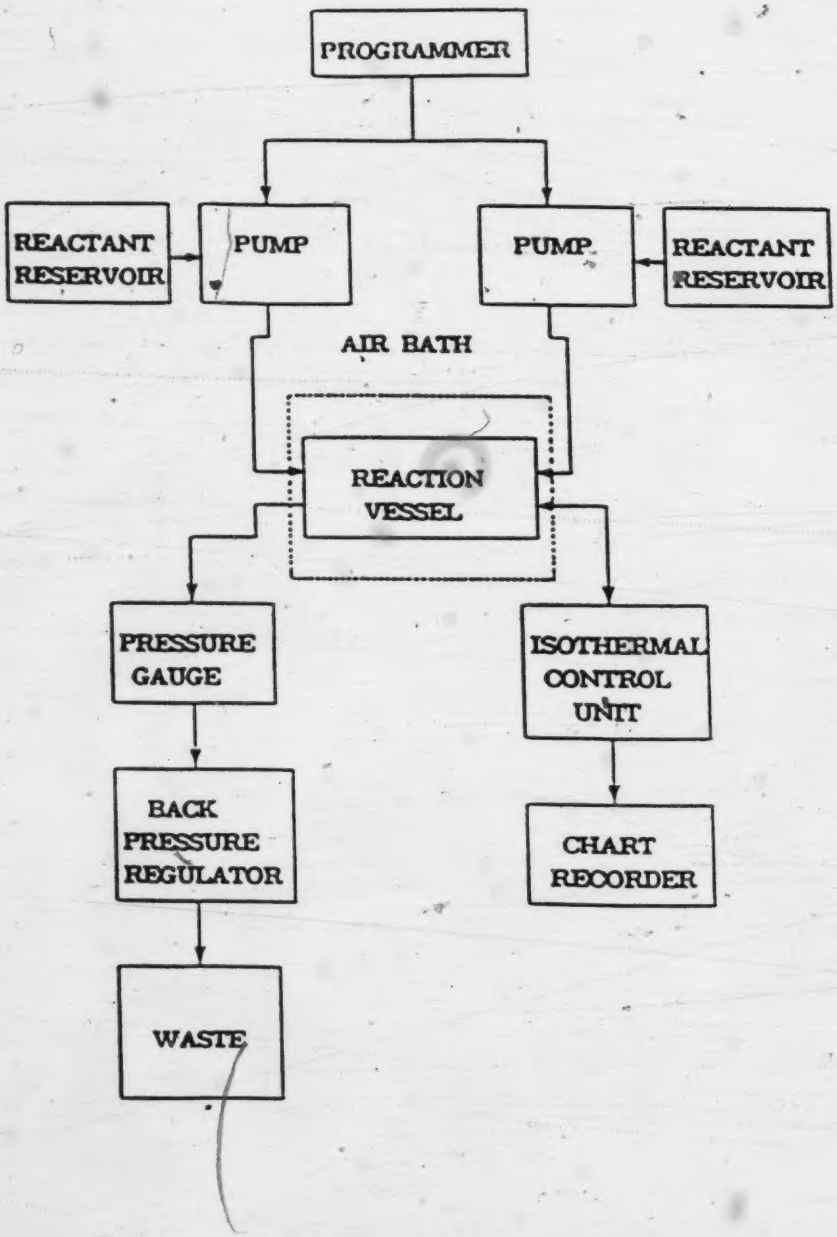

Figure 2. Block diagram of the main components of the calorimeter. Modified from Ref. [14]

A) Reaction Vessel and Shields.

The reaction vessel contains the isothermal plate and equilibration coil. Under the plate are a control heater and a Peltier thermoelectric cooler. The isothermal plate consists of two round brass plates with the equilibration coil soldered between the plates. After entering the reaction vessel and before entering the coil, the reactants are equilibrated with the products from the coil in a countercurrent heat exchanger. The two reactant streams run coaxially for approximately 1 turn of the equilibration coil before the smaller inlet tube ends and mixing begins. Thermistors are used to monitor continuously the reaction vessel temperature and to control the plate at a constant temperature.

The thermal shields consist of two cans surrounding the reaction vessel. The inner shield is temperature controlled, whereas the outer shield is not, but is allowed to assume a steady state temperature between that of the inner shield and the air bath.

B) Flow Circuit.

Three different pump systems, a Waters model 6000 series, a Varian, Inc. 8700 series, and an ISCO model 314 series can be used in the operation of the unit. The unit can be run in either the variable or fixed mode.

The pressure in the system was controlled by a back pressure regulator placed in the exit line from the reaction vessel. The control gas to the back pressure regulator was supplied by a compressed nitrogen gas cylinder and the pressure was monitored with a Heise gauge.

C) Air Bath.

The air bath consists of a Precision Scientific Co. model L8 oven which has been modified for better temperature control by using a Tronac PTC-36 temperature

controller and probe modified to operate in the proportional mode. The reaction vessel, shields, and accompanying lines are suspended in the air bath. The air bath is capable of temperature control to better than ±1 K over the temperature range 298 to 473 K.

D) Isothermal Control Unit.

The isothermal plate and attached equilibration coil are held at a constant temperature by maintaining the Peltier cooler at a constant cooling rate while varying the energy input with the control heater.

2.2.2 Wormald et al. Apparatus.

A) Flow System.

The main features of Wormald's apparatus [48] are shown in Figure 3. Mixing calorimeter 1 and densimeter 2 were mounted in thermostatted bath 3. Fluids were supplied to the calorimeter by the pumping system shown to the left of the figure, and were collected in the receiver shown on the right. A second refrigerated bath 4, contained two stainless steel cylinders 5 and 6 filled with the liquids to be supplied to the calorimeter. The liquids to be pumped were confined over mercury contained in two similar stainless-steel cylinders 7 and 8. The mercury was displaced from 7 and 8 by solvent drawn from reservoirs 9 and 10 or burettes 11 and 12 and pumped by two Gilson type 302 metering pumps 13 and 14. Electrical contacts 15 and 16 switched off the metering pumps when the mercury in 5 and 6 reached the top of the cylinders. The two fluids passed through heat exchange coils 17 and 18 before entering calorimeter 1. On leaving the calorimeter the fluid mixture passed through a shut-off valve 19 and a further heat exchange coil 20 before entering densimeter 2. Mixture leaving the densimeter was collected in a stainless steel receiver 21. The

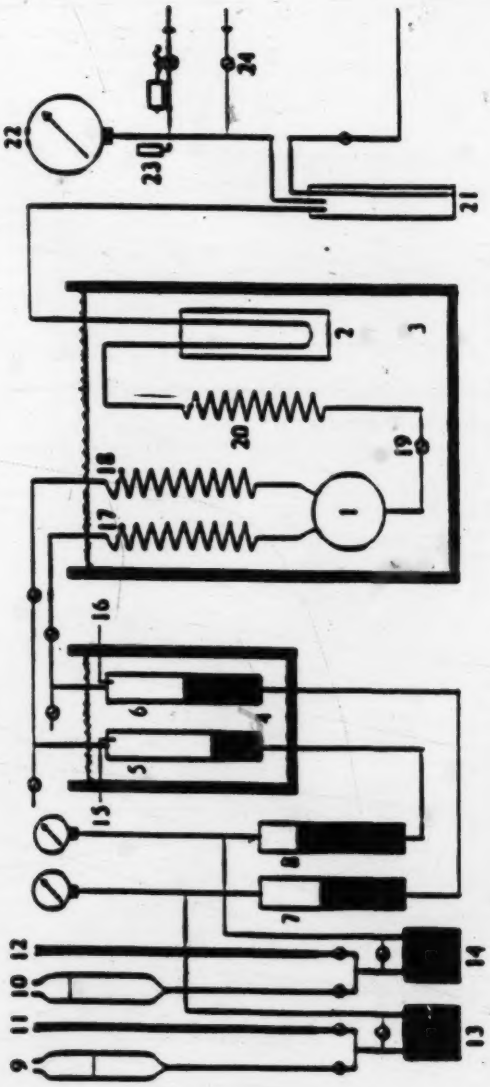

Figure 3. Flow system. Modified from Ref. [48]

pressure in the receiver was indicated on gauge 22 and sensed by pressure transducer 23. To pressurize the system a nitrogen cylinder was connected to valve 24.

B) Calorimeter.

A plan view of the calorimeter is shown in Figure 4 and a side view in Figure 5. The calorimeter was mounted on brass disk 1. A brass cover 2 which enclosed the calorimeter was secured to disk 1 by 8 bolts and sealed with a neoprene gasket 3. Stainless-steel inlet tubes 4 and 5 and outlet tube 6 passed through holes in disk 1 and were sealed to the disk. Electrical leads were ducted through a copper tube 7. Mixing was accomplished in a 1.5 m length of stainless steel tube.

A brass ring 8, was placed over two Peltier cooling elements 11 and was held firmly against them by a Tufnol strip bolted to disk 1. The position of the cooling elements is shown in Figure 5; they were connected in series. The temperature of the liquid mixture leaving the calorimeter was sensed by platinum resistance thermometer 12. The temperature of the incoming liquids was sensed by platinum resistance thermometer 13.

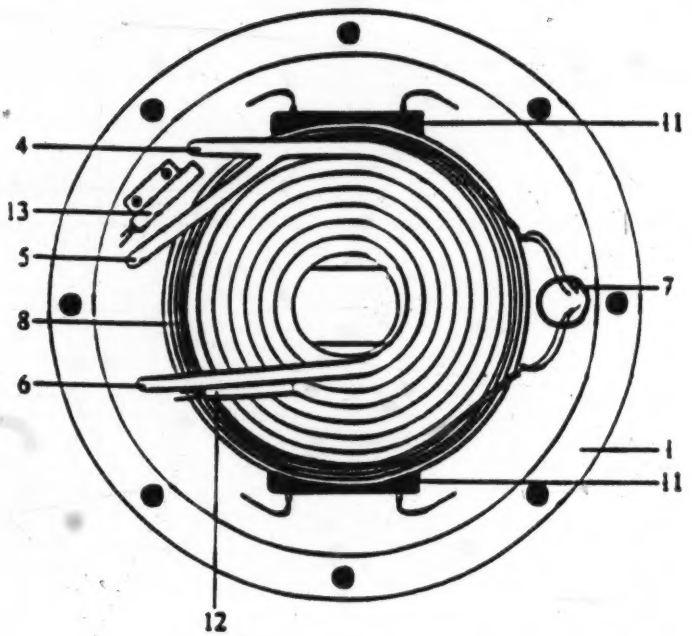

Figure 4. Plan view of the mixing calorimeter. Modified from Ref. [48]

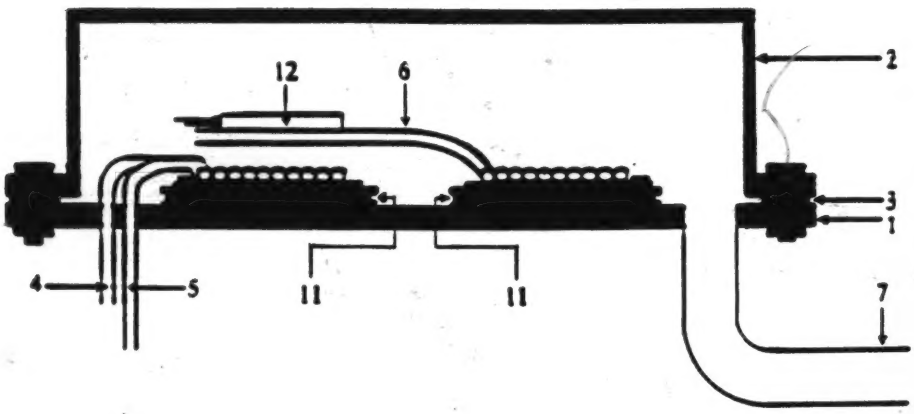

Figure 5. Side view of the mixing calorimeter. Modified from Ref. [48]

CHAPTER III

EXPERIMENTAL APPARATUS

3.1 Tronac High Pressure Isothermal Flow Calorimeter.

The experimental apparatus employed throughout this work was a Tronac Isothermal Flow Calorimeter with high pressure capability. The main components of the calorimeter are the 450 and 550 electronics consoles, the water bath, the reaction vessel, and the flow system. The flow system was designed and built during the course of this work.

3.1.1 Reaction Vessel.

The reaction vessel, shown in Figure 6, consists of a water-tight stainless steel canister containing the isothermal plate and equilibration coil. Under the plate are a 100 Ω wafer control heater and a Peltier thermoelectric cooler. They are located adjacent to each other to minimize the heat flow path between them. The cooler is in contact with the bottom of the stainless steel container to facilitate transfer of heat from the cooler to the water bath. The canister is fitted with an O-ring seal to prevent water leaks and the lid is attached by stainless steel screws. The unit is suspended 25 cm below a mount situated on the top of the water bath by four stainless steel rods. The isothermal plate consists of a triangular aluminum plate with the equilibration coil attached to the top. The equilibration coil consists of a 1.83 m length of 0.159 cm (1/16 in) o.d., thin wall (0.13 mm) stainless steel tubing coiled in a flat helical shape. The tubing is filled 1.52 m of its length with 12.7 cm long

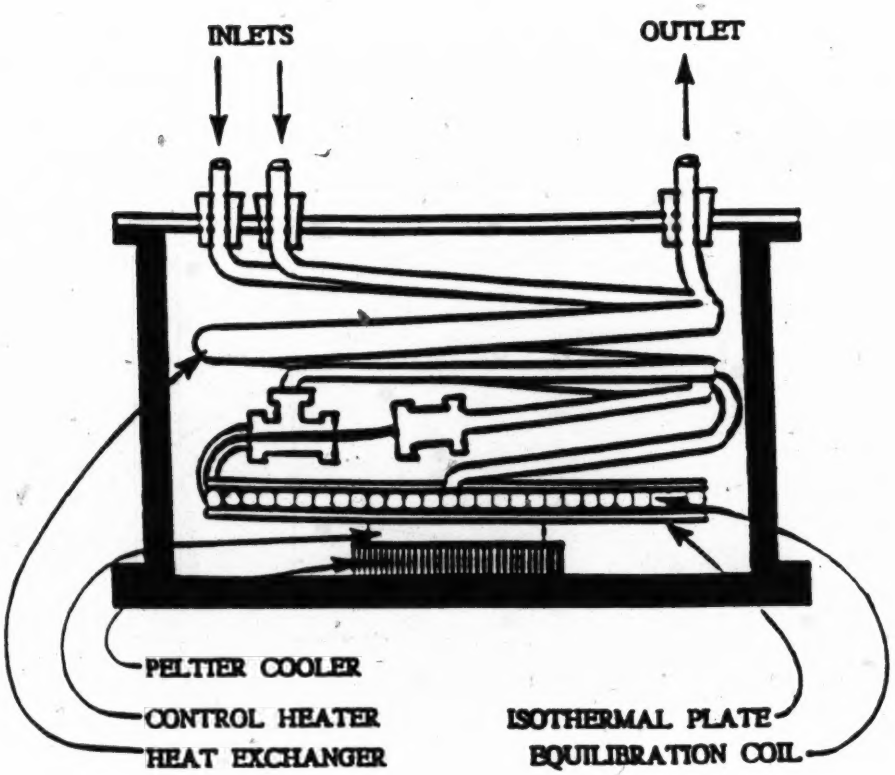

Figure 6. Reaction vessel and contents.
Modified from Ref. [14]

segments of crimped stainless steel wire. The wire promotes thorough mixing of the reactants as they flow through the coil. After entering the reaction vessel and before entering the coil, the reactants are equilibrated with the products from the coil in a countercurrent heat exchanger. This exchanger consists of 0.30 m lengths of the inlet and exit tubing which are soldered together, so that the two inlet streams run countercurrent to the exit stream. The tube diameter of one stream is reduced from 0.159 cm (1/16 in) to 0.0794 cm (1/32 in). The smaller tube is fitted inside the larger tube and the two reactant streams run coaxially for approximately 1 turn of the equilibration coil before the smaller inlet tube ends and mixing begins. Two thermistors are epoxied in grooves cut into the top surface of the aluminum plate. The thermistors are used to continuously monitor the reaction vessel temperature and to control the plate at a constant temperature. The plate is attached to the bottom of the can by three small plastic screws. Plastic spacers are used to reduce thermal contact between the plate and the can. The plate is tightened down against the Peltier cooler and control heater to give good thermal contact.

3.1.2 450 Electronics Console.

The 450 electronics console contains the electrical components necessary for temperature sensing and calibration heating. The front and rear panel controls, connectors, and indicators are shown in Figures 7 and 8. A description of these controls will now be given.

A) Standby-On Switch.

The standby-on switch is located below the heater switch. When the switch is in the standby position only the most important bath functions such as the temperature controller and the bath stirring motor are left on. The power supply for the

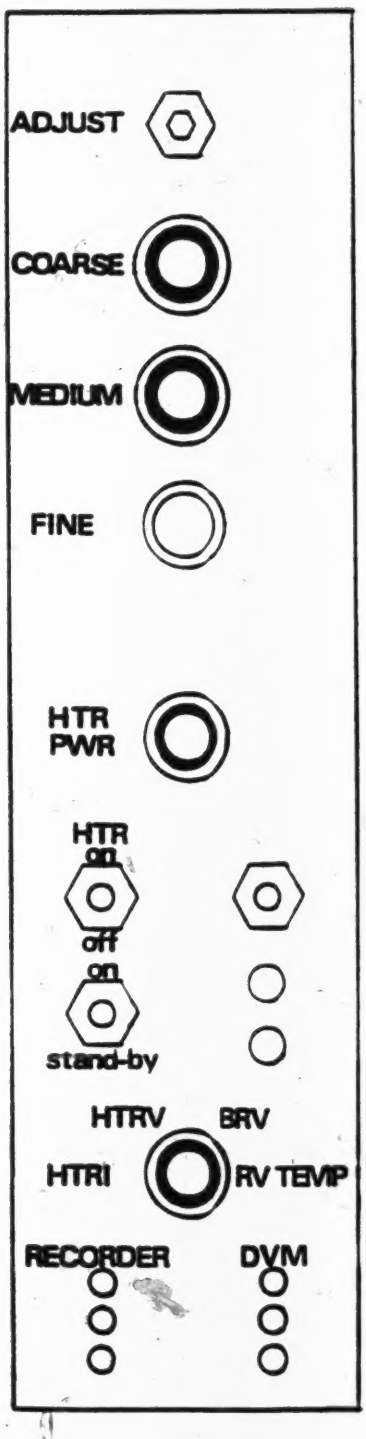

Figure 7. Front Panel of the 450 Electronics Console. Modified from Ref. [44]

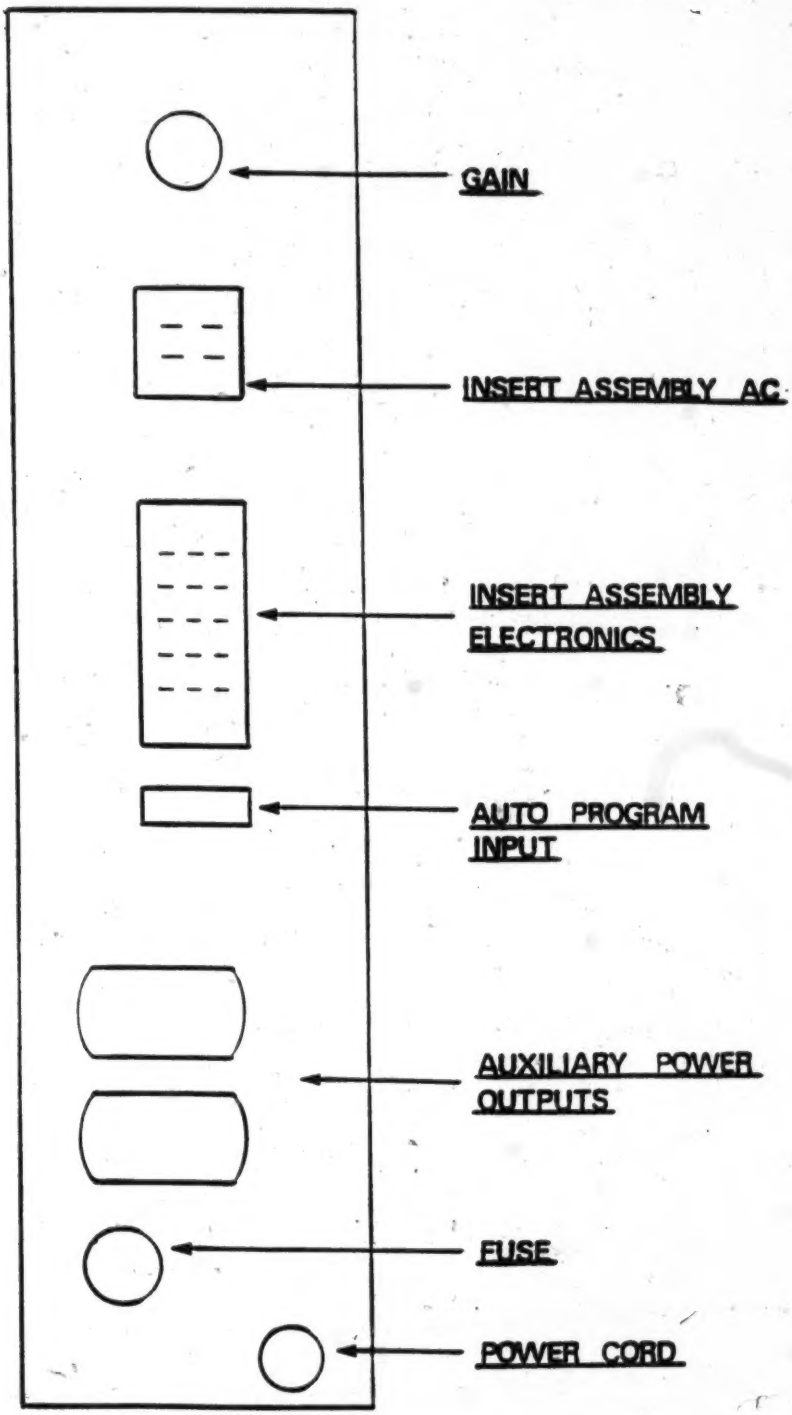

Figure 8. Rear Panel of the 450 Electronics Console. Modified from Ref. [44]

Wheatstone bridge which gives the read out of the reaction vessel temperature is left on as well so that it will remain stable. The remaining functions of the calorimeter are turned off. Once the switch is in the on position, the calorimeter is ready to use. The lights to the right of the switch in the control panel indicate whether the calorimeter has been turned on or not.

B) Bridge controls.

The bridge controls consist of four knobs located at the top of the front panel of the 450 electronics console. The controls adjust the bridge potential and the reference point of the Wheatstone bridge. The bridge voltage adjust (ADJ) is a lock nut screw driver adjustable control. The voltage is adjustable in the range of 1.5 to 15 volts. The voltage may be monitored on the digital voltmeter (DVM) by setting the DVM select switch to the bridge voltage position (BRV) while adjusting the ADJ control. When the desired voltage is obtained, the lock nut should be tightened. A higher thermistor sensitivity is achieved when increasing the bridge voltage. A voltage between 5.0 and 7.0 volts is recommended for optimum results. The coarse, medium, and fine adjustments and bridge balance adjust vary the set point for the readout of the reaction vessel temperature. The coarse and medium controls are ten-turn controls with ten-turn indicating locking dials. The fine adjust is a ten-turn control with a plain knob. The medium adjust has about 1/100 of the range of the coarse adjust and the fine adjust has about 1/100 of the range of the medium adjust.

C) HTR PWR Switch.

This switch selects the voltage across the calibration heater and therefore the amount of heat that is dissipated by the calibration heater when the heater switch (HTR ON-OFF) is turned ON. There are 11 heating rates available for selection. These rates are: 0.1, 0.2, 0.5, 1.0, 2.0, 5.0, 10.0, 20.0, 50.0, 100.0, and 200.0 mcal/s.

D) HTR ON-OFF Switch.

This is a toggle switch with an on and off position indicated. It is located below the HTR PWR switch. When the switch is in the on position and the standby-on switch is turned on, there will be power dissipated from the calibration heater corresponding to the power setting on the heater power (HTR PWR) switch. No power will be dissipated in the heater if the switch is in the off position. Every time the heater is manually turned on or off, there is a momentary voltage offset put into the (RV TEMP) temperature outputs to the recorder and voltmeter to cause a mark to show up on the strip chart recorder indicating that the heater has been turned on or off. When the heater is turned on, the voltage offset is a positive voltage on the positive or increasing temperature direction. Conversely, when the heater is turned off, the offset is a negative voltage in the negative or decreasing temperature direction. The offset in the output voltage is momentary and does not affect the data in any other way.

E) DVM Select Switch.

The DVM select switch is located on the bottom of the control panel. This switch has 4 positions: HTRI, HTRV, BRV and RV TEMP which select the output to the digital voltmeter (DVM) output terminals.

In the HTRI position, the voltage to the DVM output terminals is a measure of the current going to the calibration heater in the reaction vessel by means of a standard resistor. In the next position, heater voltage (HTRV), the voltage measured at the DVM terminals is the voltage across the calibration heater.

The bridge voltage position (BRV) allows the voltage across the Wheatstone bridge to be measured at the DVM terminals. The RV TEMP position of the switch allows the output of the Wheatstone bridge unbalance potential to be measured by the DVM. Simultaneous recording of the reaction vessel temperature on a chart recorder and the

DVM monitoring may be done.

F) Bridge Output.

Two sets of three miniature banana jack terminals are located at the bottom of the 450 electronics console front panel. The recorder output is on the left and the DVM select switch output is on the right. Each output has a red (high), black (common), and green (guard) terminals. A digital voltmeter (DVM) can be connected on the DVM terminals to read the voltages. The recorder terminals provide the output voltage from the Wheatstone bridge which indicates the change in temperature from the set point for the contents of the reaction vessel. A strip chart recorder with a suitable span should be connected across these terminals.

3.1.3 550 Electronics Console.

The 550 electronics console is commercially available as a Tronac 550 Isothermal Calorimeter Adaptor and is used in conjunction with the 450 electronics console. The adaptor holds the temperature of a reaction vessel constant within $\pm 2 \times 10^{-5}$ °C and can display in a digital and/or analog way the heat input or output required to maintain the reaction vessel at a constant temperature. Details of the control panel are shown in Figure 9. A description of each of the controls is given below.

A) ON Switch.

The instrument is always on when the plug is inserted into the auxiliary power outlet provided at the rear of the 450 electronics console.

B) Meter Select Switch.

The meter, 6, at the top of the front panel is provided to make the adjustment

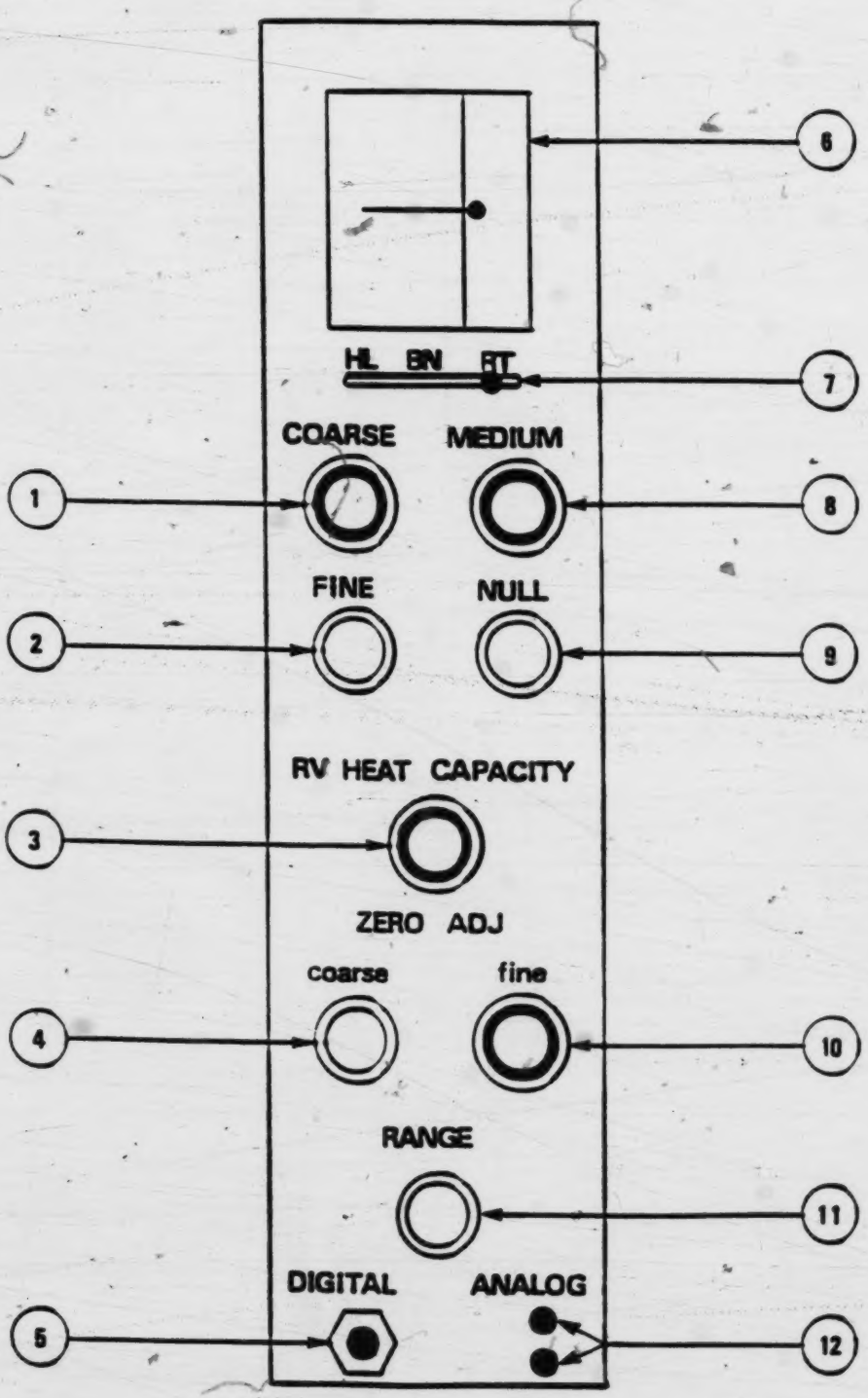

Figure 9. Front Panel of the 550 Electronics Console. Modified from Ref. [44]

of the control bridge easier. It is assumed that the set point of the reaction vessel temperature readout bridge on the 450 electronic console has already been adjusted. The meter select switch, 7, allows monitoring of three functions in the isothermal control bridge. These functions are: HT LOSS, BDG NULL, and RV TEMP.

In the RV TEMP position the meter indicates the departure of the reaction vessel temperature from the set point temperature. The set point temperature gives a zero reading at the center of the meter scale. This position is used for a relative indication only, and one should not attempt to determine the reaction vessel temperature from this reading.

The BDG NULL position is used to make the final adjustment of the bridge controls when nulling the bridge at the set point. In this position the meter reads the magnitude of the bridge signal prior to rectification in the keyed clamp. The BDG NULL position, therefore, shows the magnitude of the component of the bridge signal voltage which is out of phase with the bridge excitation voltage as the desired in phase signal.

The HT LOSS position allows the operator to read the output of the integrator (or analog output signal) before it goes to the voltage-to-frequency converter.

C) Bridge Controls.

The COARSE, 1, MEDIUM, 8, and FINE, 2, controls are ten-turn potentiometers used to adjust the desired set point in the ac Wheatstone bridge of the control circuit for the isothermal calorimeter. The NULL control, 9, is a variable capacitor used to null the out-of-phase component of the bridge signal.

D) μcal/count & mcal/volt Switch (RANGE).

This switch, 11, controls the energy per pulse that is put into the reaction vessel through the control heater. There are nine positions available: 0.05, 0.1, 0.2, 0.5, 1.0,

2.0, 5.0, 10.0 and 20.0 μcal/count. Trim potentiometers for adjusting each position are located under the dust cover. There are about 24000 counts per second available when the heater is operating at its upper limit.

E) RV Heat Capacity Switch.

The RV Heat Capacity switch, 3, controls the gain of the reaction vessel temperature control amplifier. This switch holds the total loop gain of the reaction vessel temperature control loop nearly constant as the heat capacity of the reaction vessel changed. There is a wide latitude in this adjustment, and the settings in cal/°C are only approximate. In operation, the switch should be set on the highest position that gives stable operation. Too high a setting will cause the reaction vessel temperature to oscillate. Too low a setting will give a sluggish response to any change in heat.

F) The Zero Adjustment.

These controls adjust the current in the Peltier cooler and make the instrument capable of controlling a variety of reaction vessels at different cooling rates.

The zero adjustment coarse control, 4, makes step adjustments in the Peltier cooler's cooling rates by adjusting the current in the Peltier cooler. Table 2 shows which step corresponds to different position settings on the μcal/count switch for standard reaction vessels. If the coarse setting is in the wrong position the control circuitry cannot control the temperature in the reaction vessel and the temperature will either constantly rise (cooling rate too low, alphabet letter too high) or constantly cool (cooling rate too large, alphabet letter too low).

The FINE ZERO ADJ control, 10, is adjusted to compensate for the heat inputs. This adjustment takes a while since a change in the ZERO ADJ controls varies the cooling rate in the Peltier cooler and the reaction vessel must reach thermal

TABLE 2

CORRESPONDENCE BETWEEN THE SETTINGS OF THE μcal/count SWITCH AND THE ZERO ADJUSTMENT COARSE CONTROL

POSITION OF μcal/count SWITCH.	POSITION OF ZERO ADJUSTMENT COARSE CONTROL.
20.0	A
10.0	B
5.0	C
2.0	D
1.0	E
0.5	F
0.2	G
0.1	H
0.05	I

equilibrium after each adjustment of the ZERO ADJ.

3.1.4 Water Bath and Refrigeration System.

The constant temperature water bath consists of a thermally insulated container with a motor driven stirrer, a cooled heater assembly, a bath temperature control probe, and a PTC-41 precision temperature controller. The bath is constructed of ABS plastic, silicone rubber, and stainless steel. The bath has a volume of 95 liters and requires a source of external cooling for operation. Distilled water should be used for maximum temperature controller stability and to reduce the growth of algae in the water bath.

The Tronac refrigeration system is a closed loop refrigeration system capable of being adjusted to a wide range of temperatures as well as cooling capacities. The system incorporates a 1/8 hp condensing unit. The expansion valve is of the automatic type which controls the pressure and hence the evaporating temperature. The capacity of the system is controlled by two back pressure valves which limit the mass flow of the system. High and low side pressures are monitored on gauges provided on the system. A solenoid operated equilization valve is connected between the high and low sides in order to provide easy starting in case of power failure. Without this valve, the compressor may not restart due to high pressures in the system. The cooled heater is an integral heating and cooling unit. The outside stainless steel tubing is heated electrically and is controlled by the temperature controller. The refrigeration system provides cooling by evaporating the refrigerant within the inner lining of the cooled heater. A filter drier and liquid moisture indicator are provided to control system moisture and for charging refrigerant into the system.

The Tronac PTC-41 temperature controller is a general purpose precision temperature controller with excellent short and long term stability. It was developed to provide a control accuracy of better than ±0.0003 °C/week when used with well

designed, well stirred fluid baths.

3.2 Flow System.

As mentioned before, the flow system was built by us. We tried several arrangements; in one of them the solvent collection vessel was a pressure vessel which contained a piston. On one side of the piston the (CO_2 + solvent) mixture was collected, whereas the other side was filled with water. The outlet port of the vessel in the water side was connected to the back pressure regulator. Before starting an experimental run, the vessel was evacuated and the piston was brought up to the top of the vessel, and filled with water. The (CO_2 + solvent) mixture flowing into the vessel pushed the piston down and water was displaced on the other side of the piston. The main problem we had with this arrangement was with the piston and its O-rings. Some solvents (i.e. toluene) caused the O-rings to swell; therefore, the movement of the piston was not smooth enough to achieve a steady pressure. In the worst case the piston would be stuck. To avoid these problems we decided to pressurize the system with a N_2 bottle, eliminating the need for the piston.

The final arrangement of all the components of both the flow system and the calorimeter is shown in Figure 10.

Two different pump systems, a ConstaMetric model and an ISCO, Inc. 314 and LC-5000 model, were used in the operation of the calorimeter. The ConstaMetric Pumps were used only for the runs with the test system (Cyclohexane + n-Hexane), while the ISCO pumps were used to obtain the remaining of the experimental information reported in this work. The ISCO LC-5000 syringe pump was used for delivering CO_2 while the ISCO 314 pump delivered the physical solvent.

The ConstaMetric pumps were always operated in conjunction with the Laboratory

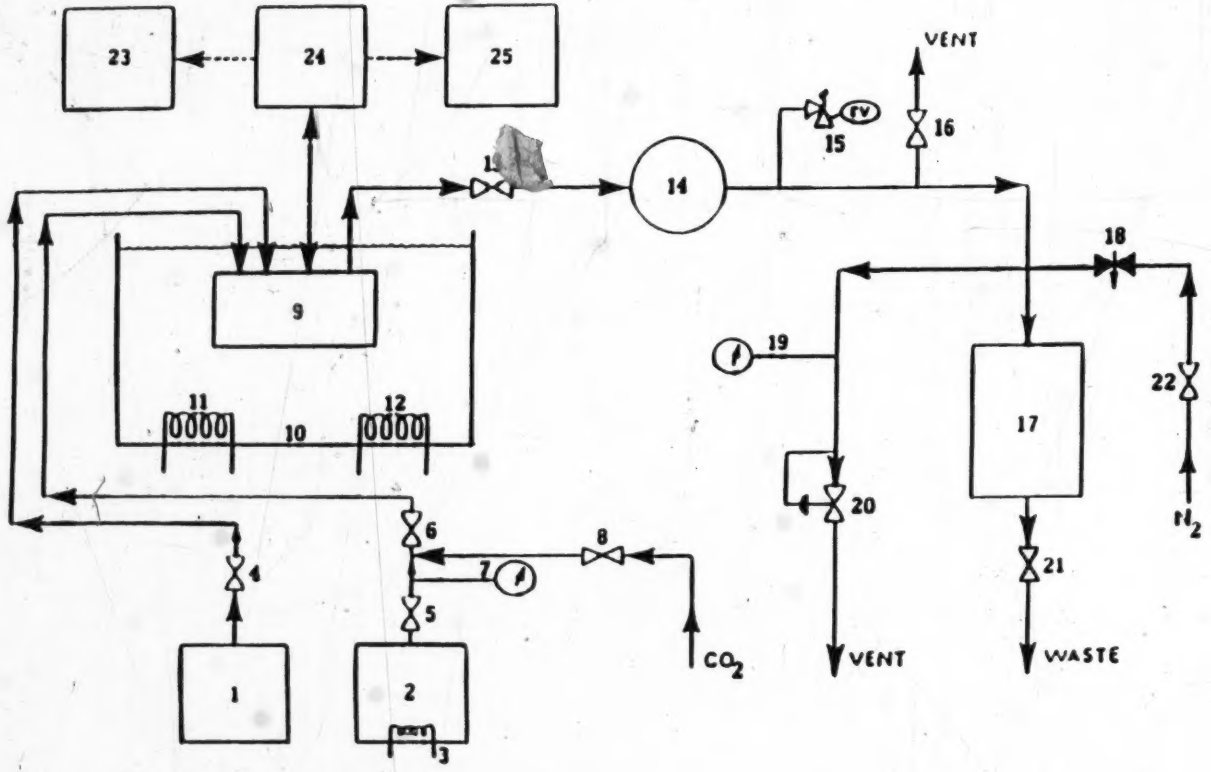

LEGEND

1. Solvent Pump
2. CO_2 Pump
3. Cooling for CO_2 Pump
4. Shut-Off Valve
5. Shut-Off Valve
6. Shut-Off Valve
7. Pressure Gauge
8. Shut-Off Valve for CO_2 Cylinder
9. Reaction Vessel
10. Water Bath
11. Cooling for Water Bath
12. Heat Input for Water Bath
13. Shut-Off Valve
14. Heise Gauge
15. Pressure Relief Valve
16. Shut-Off Valve
17. Solvent Collection Vessel
18. Needle Valve for N_2
19. Pressure Gauge
20. Back Pressure Regulator
21. Shut-Off Valve
22. Shut-Off Valve for N_2 Cylinder
23. Printer
24. 450 and 550 Electronics Consoles
25. Strip Chart Recorder

—— Fluid Lines

------ Electrical Lines

Figure 10. Experimental Apparatus.

Data Control model 1601 Gradient Master, which provided a means of changing continuously the flow delivery rate of each pump according to a preselected program allowing us to scan the entire mole fraction range for the heat of mixing curve. The ISCO pumps were run in the fixed composition mode.

The ISCO pumps have the advantage that the delivered flow rates are consistent from run to run and thus the pumps need only be calibrated once, while the ConstaMetric pumps present some problems with the proper functioning of the check valves with some fluids.

It is known that in the vicinity of the critical point the properties of CO_2 exhibit large fluctuations; in order to avoid them a cooling coil was placed around the cylinder of the LC-5000 syringe pump. The coil was connected to an oil bath which was kept at a constant temperature of 6°C.

A) ConstaMetric Pumps.

The ConstaMetric solvent delivery pumping system features constant flow under all presures up to 5000 psig. The flow rate is adjustable from 0.1 to 10 ml per minute by a turncounting dial adjustment on the pump panel. The flow rate is controlled by an accurate phase-locked loop controller with repetitive accuracy of better than ±0.3 %. Pulsefree operation at all flow rates is achieved through the use of a computer designed cam which drives two positive displacement sapphire pistons. The cam is designed so that the sum of the delivery from the two liquid outputs is always constant. The liquid discharge system has a minimum of dead volume to permit rapid solvent changeover.

B) ISCO Pumps.

The ISCO model 314 metering pump is a positive displacement syringe type pump and produces a fixed rate flow stream at pressures up to 2850 psi. The flow rate is

controlled by the settings of two selectors on the control unit. The pump has a flow rate range of 0.1 ml/h to 200 ml/h. It has a stainless steel cylinder with a volume of 375 ml. A stainless steel piston is pushed up the cylinder forcing the liquid out the port at the top of the cylinder. A pressure actuated graphite-filled Teflon seal is used to make the seal between the piston and the cylinder wall.

The ISCO LC-5000 is a syringe pump with a 500 ml capacity, flow rate range of 0.1 ml/h to 400 ml/h, and a 3700 psi pressure rating. The pump operates in a constant flow mode and has a digital display of pressure in psi or MPa. The syringe barrel and piston are made of 304 stainless steel. The pump seals are graphite-filled Teflon. The pump is designed for applications requiring precise, pulse free delivery of liquids.

The calibration of the ISCO syringe pumps is presented in Appendix III.

C) Pressure Control.

The pressure in the system was controlled by a Tescom 26-3200 series back pressure regulator with a pressure range of 0-3500 psi placed in the exit line from the reaction vessel. The pressure was monitored with a 0-3000 psi Heise gauge. The control gas to the back pressure regulator was supplied by a compressed nitrogen gas cylinder.

The Tescom 26-3200 series regulator is a handknob adjustable spring-loaded back pressure regulator. The regulator utilizes a soft-seated main valve for bubble tight shut-off and a piston sensor for high pressure service. The manual adjusting mechanism incorporates needle bearings to maintain low operating torque throughout the adjustment range. The standard materials of construction of different parts of the regulator in contact with fluid media are as follows:

Seats	Kel-F-81
Regulator body	303 SS

O-Rings	Viton A
Back-up rings	Teflon
Remaining parts	303 SS & 17-4 PH SS

D) Mechanical Set-up.

The inlet and outlet ports of the reaction vessel are located at the top of it and consist of three 1/16 in stainless steel Swagelok fittings; two of them are the inlets and one is the outlet as labeled. Each one of the two inlet ports is connected by 1/16 inch tubing to the pumps.

All tubing used for the fluid lines throughout the system was 1/16 inch (0.159 cm) o.d. stainless steel to avoid corrosion from the CO_2 solution.

CHAPTER IV

EXPERIMENTAL PROCEDURE

A detailed schematic diagram of the experimental apparatus is shown in Figure 10. The procedures given below refer to this figure as well as to some of the components of the calorimeter described in Chapter III.

4.1 Pumps Fill-up.

At this time the oil bath is turned on, valves 4 and 6 are closed, and valves 5 and 8 are opened. Once the CO_2 reaches the pump, the DELIVER-REFILL switch and the RUN-STOP switch in the controller of the LC-5000 pump are set to the REFILL and RUN positions, respectively. The refill rate is determined by the settings of the REFILL RATE adjustment screw on the back of the controller. For ending the refill process the RUN-STOP switch is set to the STOP position and valve 8 is closed.

The refill process for the 314 pump, 1, is not as automatic as in the LC-5000 pump. The pump cylinder is filled by setting the pump in the manual crank mode. The piston is raised to the top of the cylinder with the manual crank. The outlet port of the pump is connected to the solvent reservoir and using the manual crank a suction is applied by cranking the piston down the cylinder. The piston should not be lowered too rapidly because the piston-to-cylinder wall seal may leak air into the cylinder when too much suction is applied. Once the cylinder is full, the piston should be run up to see if bubbles come out the outlet. Finally, the outlet port is connected to the system.

4.2 Equilibration.

The temperature of the water bath is set to the desired value and once it has stabilized, the reaction vessel may be immersed in the bath. All the electrical connectors of the reaction vessel should be disconnected until thermal equilibration has been achieved.

The temperature of the reaction vessel must be constant and stable; therefore it should be immersed in the bath at least a couple hours before the operation of the calorimeter starts. For optimum results it is advisable to immerse the reaction vessel in the water bath 24 hours prior to making measurements.

4.3 System Pressurization.

After the pumps have been filled and the thermal equilibration of the reaction vessel has been achieved, the next step is to build up the pressure in the system. At this time valve 4 is opened and pump 1, containing the solvent, is turned on, allowing the solvent to flow through the system. Valves 6, 16, and 21 remain closed. To pressurize the system, valve 22 is opened and nitrogen starts to flow through the system. The flow rate of nitrogen is regulated with valve 18 and the pressure in the system is controlled with a back pressure regulator, 20. The pressure is monitored with a Heise gauge, 14. However, there are two other pressure gauges, 7 and 19, located at different points along the system. Up to now, all the system is under the same pressure except the pump containing CO_2. Then pump 2 is turned on and the pressure starts to rise. Once the pressure reading in the gauge, 7, is close to that of the entire system valve 6 is opened and proper adjustments with the back pressure regulator are made in order to maintain the pressure in the system at the desired level. The CO_2 is allowed to flow through the system and a few minutes later the pump is turned off.

Both the solvent and CO_2 are collected in a stainless steel vessel, 17, with an approximate capacity of 750 cm^3 and capable to withstand the operating pressure of the system. In case that for any reason (i.e., excessive accumulation of solvent and CO_2 in the collection vessel) the pressure in the system builds up to undesirable levels, a pressure relief valve, 15, was placed on line and was set to operate when the pressure in the system exceeded 2100 psi. The solvent pump is kept running and the pressure in the system should be quite stable. Then one can proceed to adjust the settings in the 450 and 550 electronics consoles.

4.4 450 and 550 Electronics Consoles Adjustments.

Determining the proper rate of the Peltier cooler and the proper energy per count for the control heater might require some trial and error and may need to be changed for each system under study. The cooling rate is adjusted with the ZERO ADJ control knobs and the energy per count released by the heater is controlled by the RANGE knob both located in the front panel of the 550 electronics console. When the heater is working at its maximum, it is able to supply up to 25000 counts (pulses) per second; thus we have to find the proper cooling rate which can be balanced by a convenient heater pulse rate.

The RV Heat Capacity switch has to be adjusted as well. This switch controls the response of the heater. The higher the setting the quicker the response. However, too high of a setting may cause significant fluctuations. Settings are typically between 30 and 70 cal/°C.

The HTR PWR knob in the front panel of the 450 electronics console should be adjusted so that its setting in mcal/s is ten times the setting in μcal/count of the RANGE knob on the 550 electronics console.

The typical settings for all these controls which were used throughout the course of this work are given below.

RV HEAT CAPACITY	ZERO ADJUST	RANGE	HTR PWR
30	D	5	50
50	C	5	50
30	D	2	20

The STANDBY-ON switch in the front panel of the 450 electronics console is turned on and now we can proceed to establish the temperature set point of the reaction vessel. In doing so, the 15 pin connector from the reaction vessel is plugged into the back panel of the 450 electronics console and the bridge controls (COARSE, MEDIUM, and FINE) are adjusted rapidly in order to produce a reading of 0.0 V in the digital voltmeter.

Next, control is established by plugging the 12 pin connector from the reaction vessel into the back panel of the 550 electronics console and by connecting the BNC control heater cable from the reaction vessel to the 550 electronics console. The bridge controls (COARSE, MEDIUM, and FINE) are quickly adjusted so that the meter in the front panel, with the meter select switch in the RV TEMP position, zeros. When control is achieved the meter settles near zero.

At this point, with the solvent flowing through the calorimeter only, and all the adjustments done, we should be able to get a base line. If the calorimeter is controlling well, the number of heat pulses per second that the control heater is supplying, must remain just about constant without any significant fluctuations and may be checked as they are recorded and printed every 15 seconds. If this is the case, then the strip chart recorder should be drawing a relatively straight base line. Usually 15 to 20 minutes

were enough time to obtain an acceptable base line; then we can move onto the next step which is the electrical calibration.

4.5 Electrical Calibration.

Once the strip chart recorder has drawn the base line, the counts per second that the control heater is supplying should be recorded and the HTR ON-OFF switch located in the front panel of the 450 electronics console may be turned on. Within a minute, the strip chart recorder should begin moving to the left, which is an indication that the calibration heater is supplying power to the reaction vessel. In about 20 minutes, the strip chart recorder should have stabilized to a straight line and the readings of HTRV and HTRI should be taken at this point by setting the DVM select switch at the bottom of the front panel to the HTRV and HTRI positions. The counts per second should be recorded again. The heater is then turned off and the strip chart recorder should indicate a return towards the original base line and once more the counts per second are recorded.

The value of HTRI is the voltage drop across a standard resistor in series with the calibration heater and the value of HTRV is the voltage drop measured across the calibration heater.

4.6 Measurement of Enthalpy of Mixing.

To measure the heat of the interaction between the solvent and CO_2, a base line is obtained by pumping just solvent through the system at the desired rate and the counts per second supplied by the control heater are recorded. Then the CO_2 pump is turned on and the pump settings that control the flow rate in each pump are changed in order to obtain the desired composition at which the enthalpy of mixing will be

determined. When the reaction under study is exothermic, the strip chart recorder should move to the left (direction of increasing temperature) and if the reaction is endothermic should move to the right. After a few minutes the strip chart recorder should stabilize to a straight line. Then the counts per second are recorded. One has to make always sure that all combinations of different settings of both pumps give the same total flow rate. Now the settings in the pumps may be changed again to determine the enthalpy of mixing at another point of different composition and the procedure is repeated until the entire heat of mixing curve has been swept and a base line with CO_2 flowing through the system is obtained. There should not be much difference between the counts per second recorded for the base line with the solvent and those for the base line with CO_2.

4.7 System Evacuation.

Once the run is completed, the calorimeter is turned off by setting the STANDBY-ON switch to the standby position. The 15 and 12 pin connectors pluged into the 450 and 550 electronics consoles as well as the BNC control heater cable are disconnected. Both pumps and the oil bath must be turned off and the flow of nitrogen is halted by shutting off valve 22. Valve 21 is then opened and the solvent is drained out of the solvent collection vessel, 17. Once all the solvent has left the collection vessel, valve 16 may be also opened to help bleed off the pressure faster.

4.8 Flow Rates.

All experimental runs were carried out at a total flow rate of 0.4 ml/min. In order for us to be certain that there was no flow rate dependence in our measurements, we made a separate run for the system (CO_2 + Selexol) at 298.15 K

and 10.6 MPa with a total flow rate of 0.2 ml/min.

4.9 Materials.

Table 3 gives a list of all the solvents used in this work along the supplier and literature values for some of their physical properties. All chemicals were used without further purification.

The carbon dioxide and nitrogen were supplied by Linde and had purities of 99.5% and 99.998% respectively.

Selexol was the only solvent of those studied that was not pure. An analysis was performed by the Microanalytical Laboratory of the Chemistry Department at this University for water content and molecular weight of the Selexol. The analysis reported 0.83% by weight of H_2O and a molecular weight of 287 g/mol. The method used for the determination of water was the Karl Fischer reaction. The molecular weight was determined by osmometry. The solvent used for the molecular weight determination was benzene. We prepared a second mixture by adding more water and the analysis reported 3.62% by weight of H_2O. The enthalpy of mixing was measured for both mixtures of Selexol-water. This was done in order to facilitate the extrapolation of the data to 0% of H_2O.

The refractive index was determined for all the solvents studied in this work at 25°C using a sodium lamp refractometer.

TABLE 3

SOLVENTS STUDIED IN THIS WORK

SOLVENT	STRUCTURAL FORMULA	SUPPLIER
N-Methyl Pyrrolidone	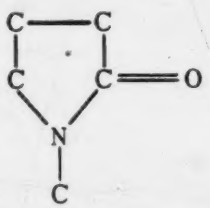	Fisher Scientific
Propylene Carbonate	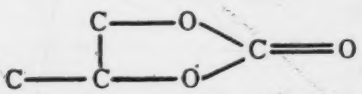	Aldrich Chemicals
Selexol	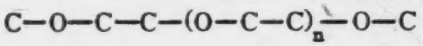	Harrisons and Crosfield, Ltd.
N-Formyl Morpholine		BASF
Methyl Cyanoacetate	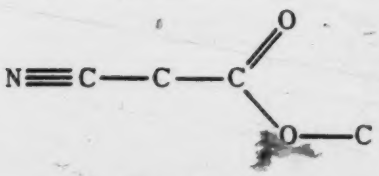	Aldrich Chemicals
Methanol	$C-O-H$	BDH Chemicals
Toluene	$C_6H_5CH_3$	Fisher Scientific
n-Hexane	C_6H_{14}	Fisher Scientific
Cyclohexane	C_6H_{12}	Fisher Scientific

TABLE 3 (continued)

SOLVENTS STUDIED IN THIS WORK

SOLVENT	PURITY (%)	MOLECULAR WEIGHT	DENSITY[+,a] (g/cm^3)	VAPOUR[+,a] PRESSURE (mm Hg)
N-Methyl Pyrrolidone	*	99.1	1.023	0.4130
Propylene Carbonate	99.0	102.1	1.189	0.0900
Selexol	**	287.0	1.027	0.0008
N-Formyl Morpholine	99.0	115.1	1.144	0.0080
Methyl Cyanoacetate	99.0	99.1	1.103	0.2000
Methanol	99.8	32.0	0.787	126.2050
Toluene	99.8	92.2	0.861	28.3250
n-Hexane	88.0	86.2	0.660	97.4570
Cyclohexane	99.0	84.2	0.779	98.4040

* Purified grade.
** Not applicable, the solvent is a mixture.
+ Literature values from Appendix I.
a Values of the property are at 25°C.

TABLE 3 (continued)

SOLVENTS STUDIED IN THIS WORK

SOLVENT	ISOTHERMAL COMPRESSIBILITY (m^2/N) [*,▲]	REFRACTIVE INDEX [▲]
N-Methyl Pyrrolidone	4.67×10^{-10}	1.4617
Propylene Carbonate	3.72×10^{-10}	1.4210
Selexol	3.72×10^{-10}	1.4373
N-Formyl Morpholine	4.67×10^{-10}	1.4810
Methyl Cyanoacetate	11.84×10^{-10}	1.4168
Methanol	12.58×10^{-10}	1.3275
Toluene	9.28×10^{-10}	1.4922
n-Hexane	16.72×10^{-10}	1.3762
Cyclohexane	11.40×10^{-10}	1.4250

* Literature values from Appendix I.
▲ Values of the property are at 25°C.

CHAPTER V

EXPERIMENTAL RESULTS AND DISCUSSION

5.1 Experimental Results.

The experimental data for all the systems studied is presented in Tables A4.1 to A4.10 of Appendix IV.

The system (Cyclohexane + n-Hexane) was previously studied by Christensen, et al. [12] and provided a test system under pressure for the calorimeter. The enthalpy of mixing for this system was measured at 298.15 K and 0.1, 7.0, and 14.0 MPa. The data is plotted in Figures 11 to 13.

The enthalpy of mixing of (CO_2 + Toluene) was previously measured by Wormald, et al. [48] and Christensen, et al. [35], allowing us to test the calorimeter with CO_2 at high pressure. The enthalpy of mixing for this system was determined at 298.15 K and 7.5 and 10.6 MPa, and at 308.15 K and 10.6 MPa. The experimental data is shown in Figures 14 to 16.

The enthalpy of mixing of CO_2 with the physical solvents studied here was measured at 298.15 K and 7.5, 10.6, and 12.6 MPa. The solvents used were the following: N-Methyl Pyrrolidone, Propylene Carbonate, Selexol, Methanol, Methyl Cyanoacetate, and N-Formyl Morpholine. The enthalpy of mixing of CO_2 with any of these solvents has not been determined before.

The experimental enthalpy of mixing data for the systems (CO_2 + Physical Solvent) is plotted in Figures 17 to 23.

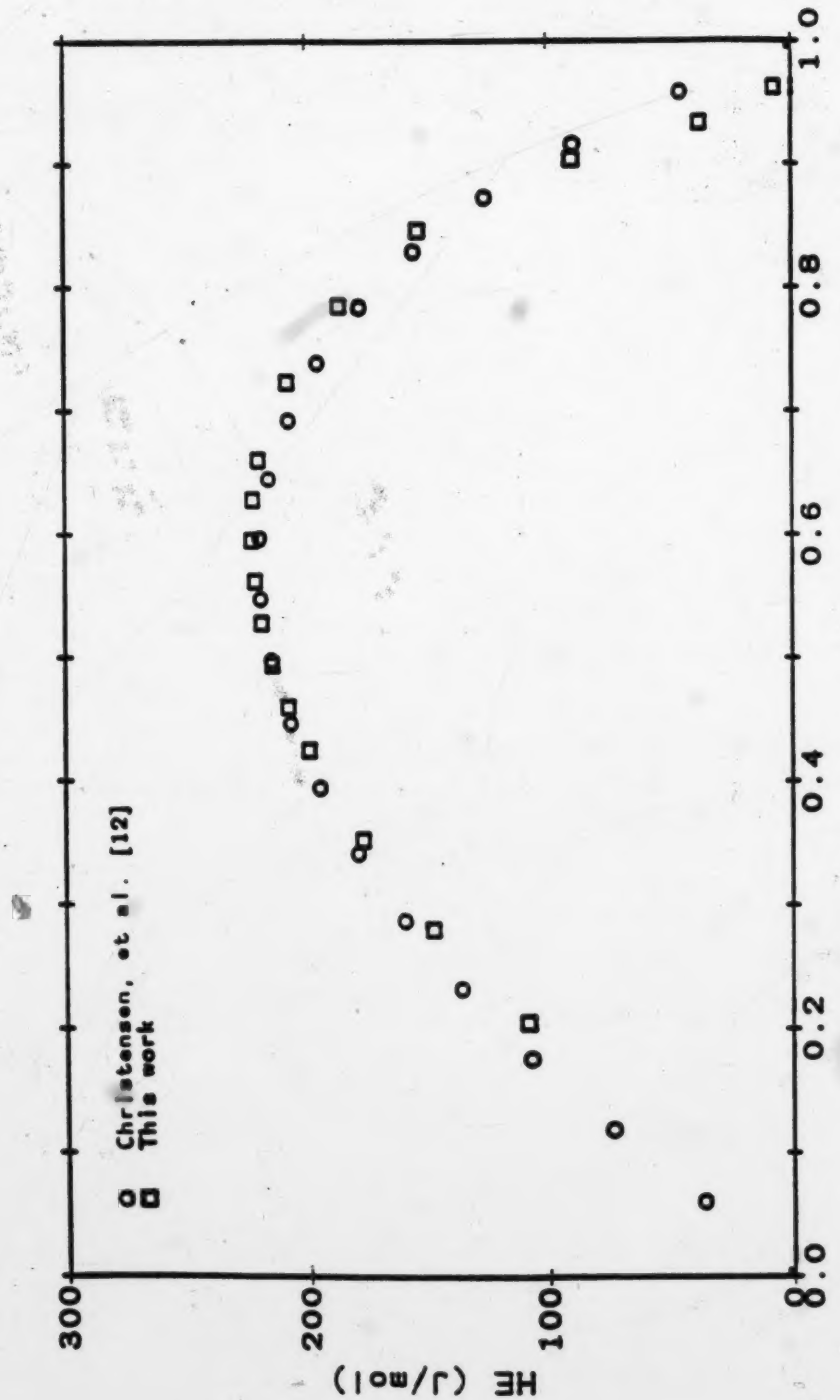

Figure 11. Enthalpy of Mixing of (Cyclohexane + n-Hexane) at 298.15 K and 0.1 MPa

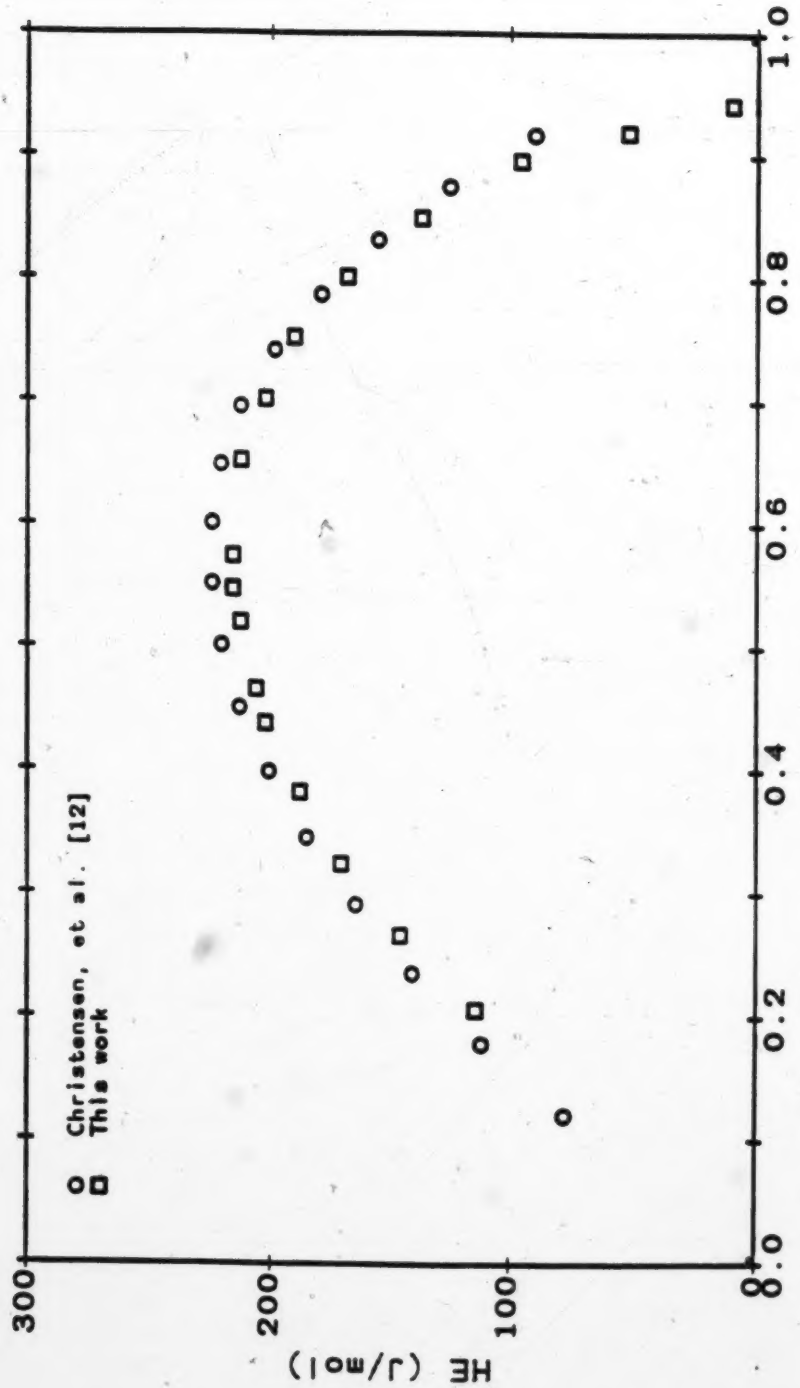

Figure 12. Enthalpy of Mixing of (Cyclohexane + n-Hexane) at 298.15 K and 7.0 MPa

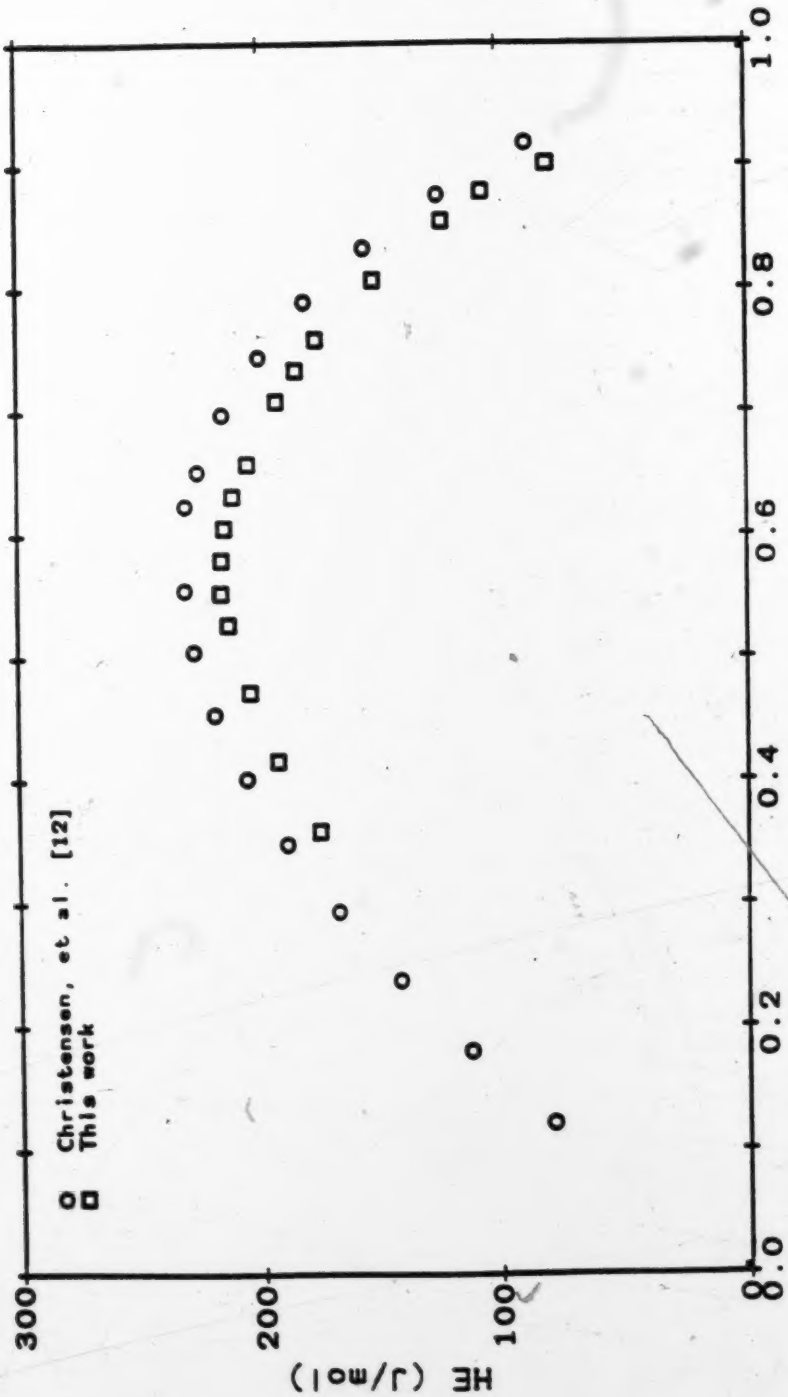

Figure 13. Enthalpy of Mixing of (Cyclohexane + n-Hexane) at 298.15 K and 14.0 MPa

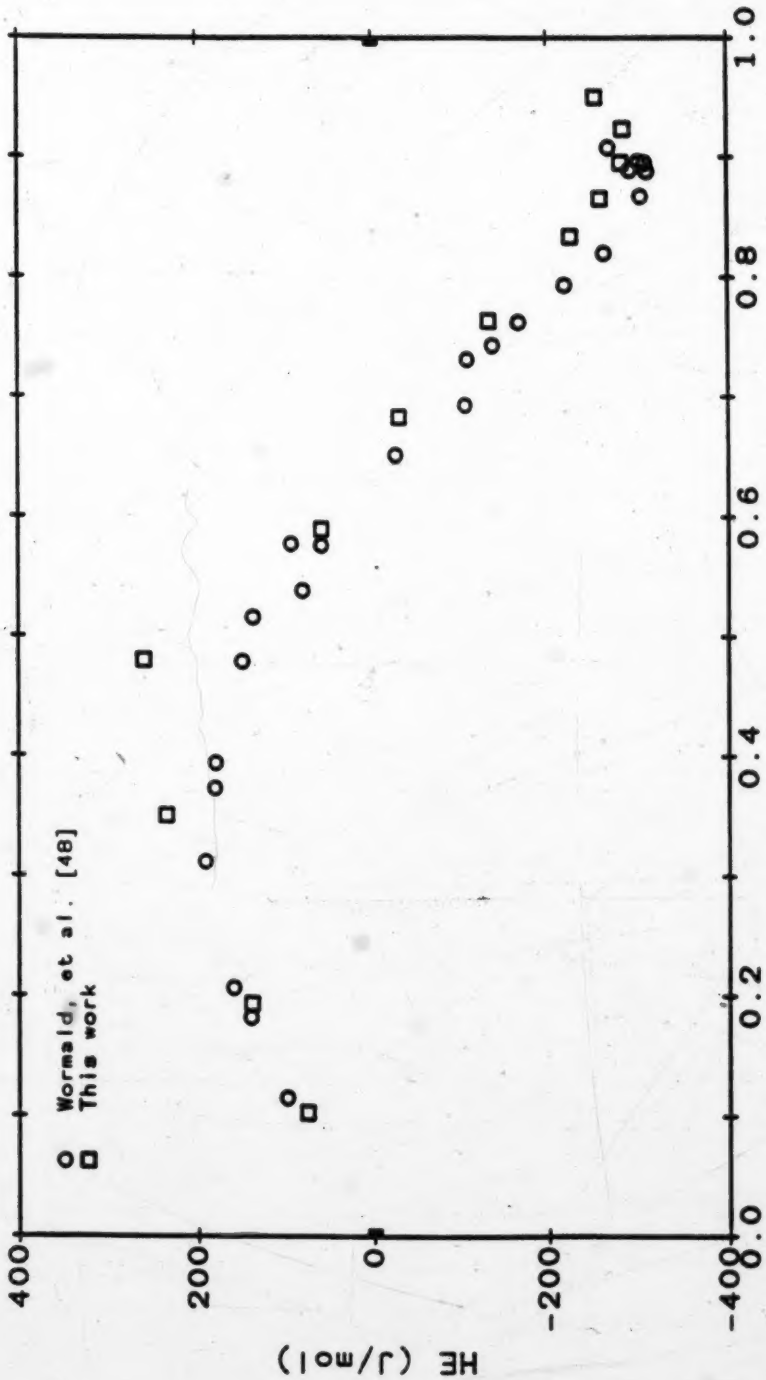

Figure 14. Enthalpy of Mixing of (CO_2 + Toluene) at 298.15 K and 7.5 MPa

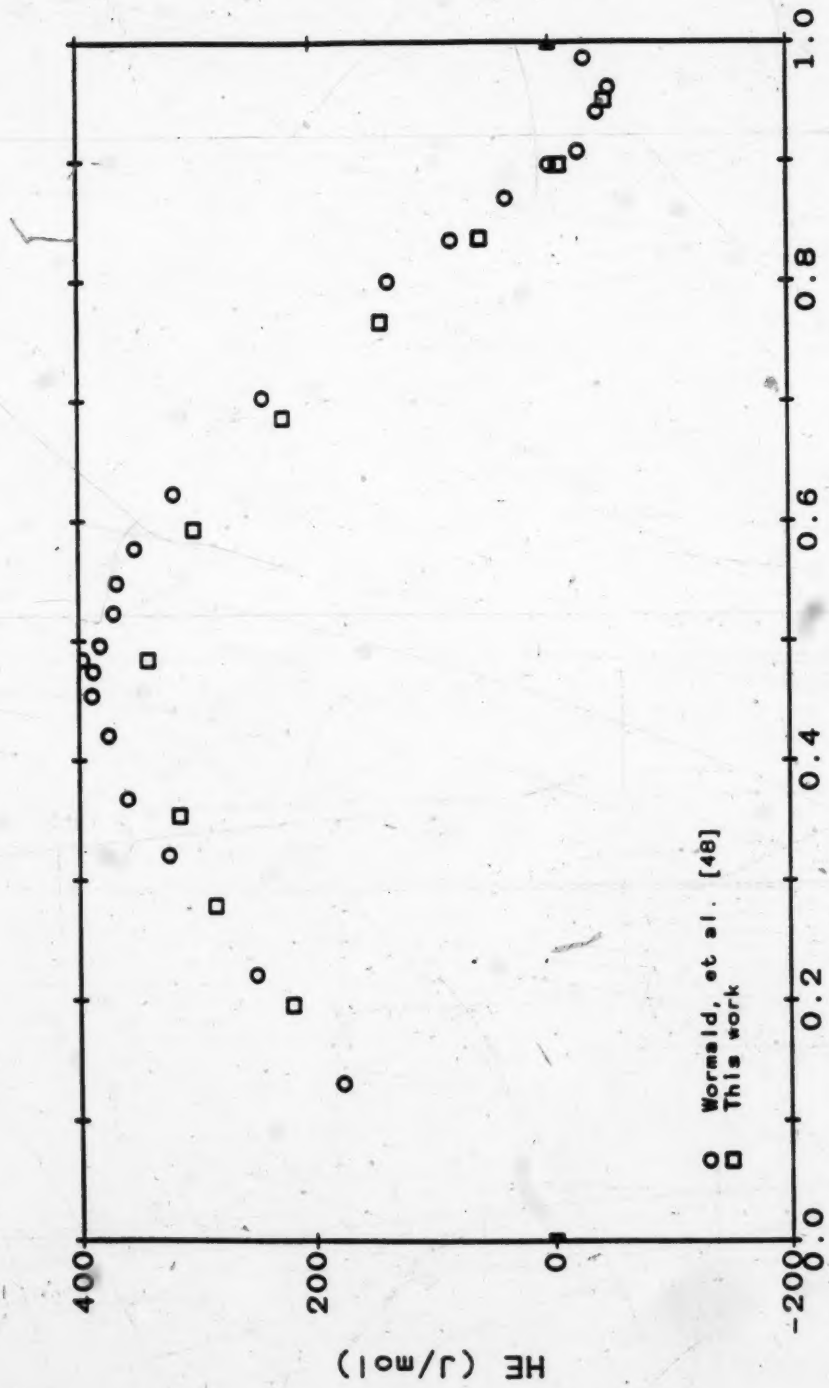

Figure 15. Enthalpy of Mixing of (CO_2 + Toluene) at 298.15 K and 10.6 MPa

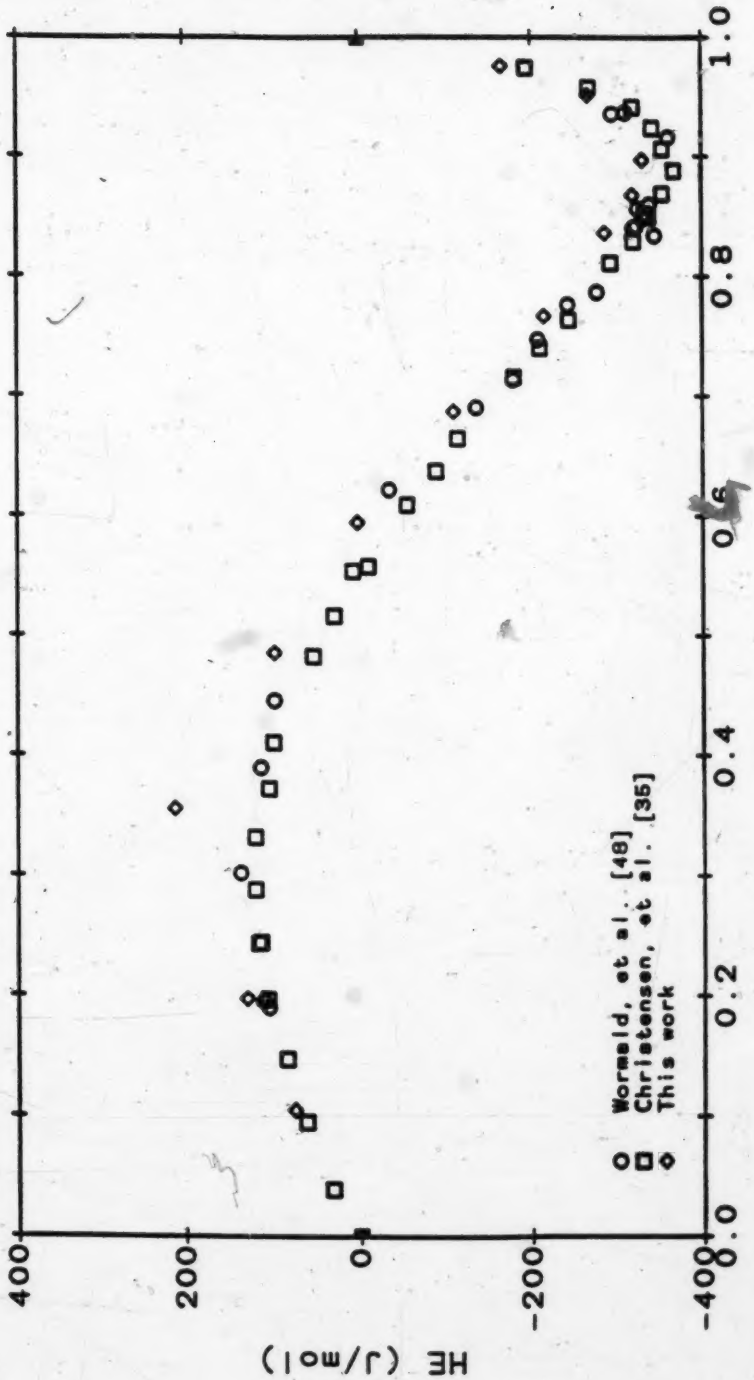

Figure 16. Enthalpy of Mixing of (CO_2 + Toluene) at 308.15 K and 10.6 MPa

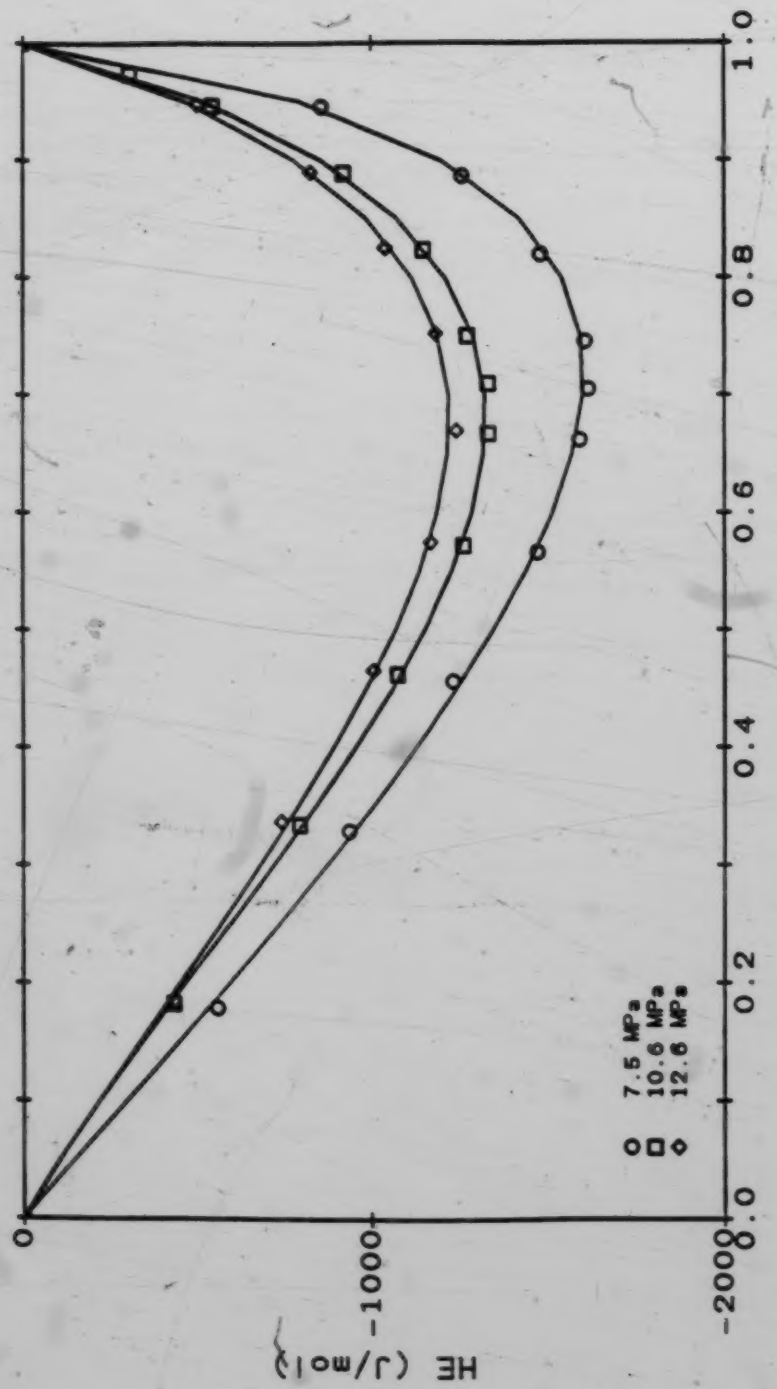

Figure 17. Comparison of Calculated and Experimental Enthalpy of Mixing of (CO_2 + N-Methyl Pyrrolidone) at 298.15 K

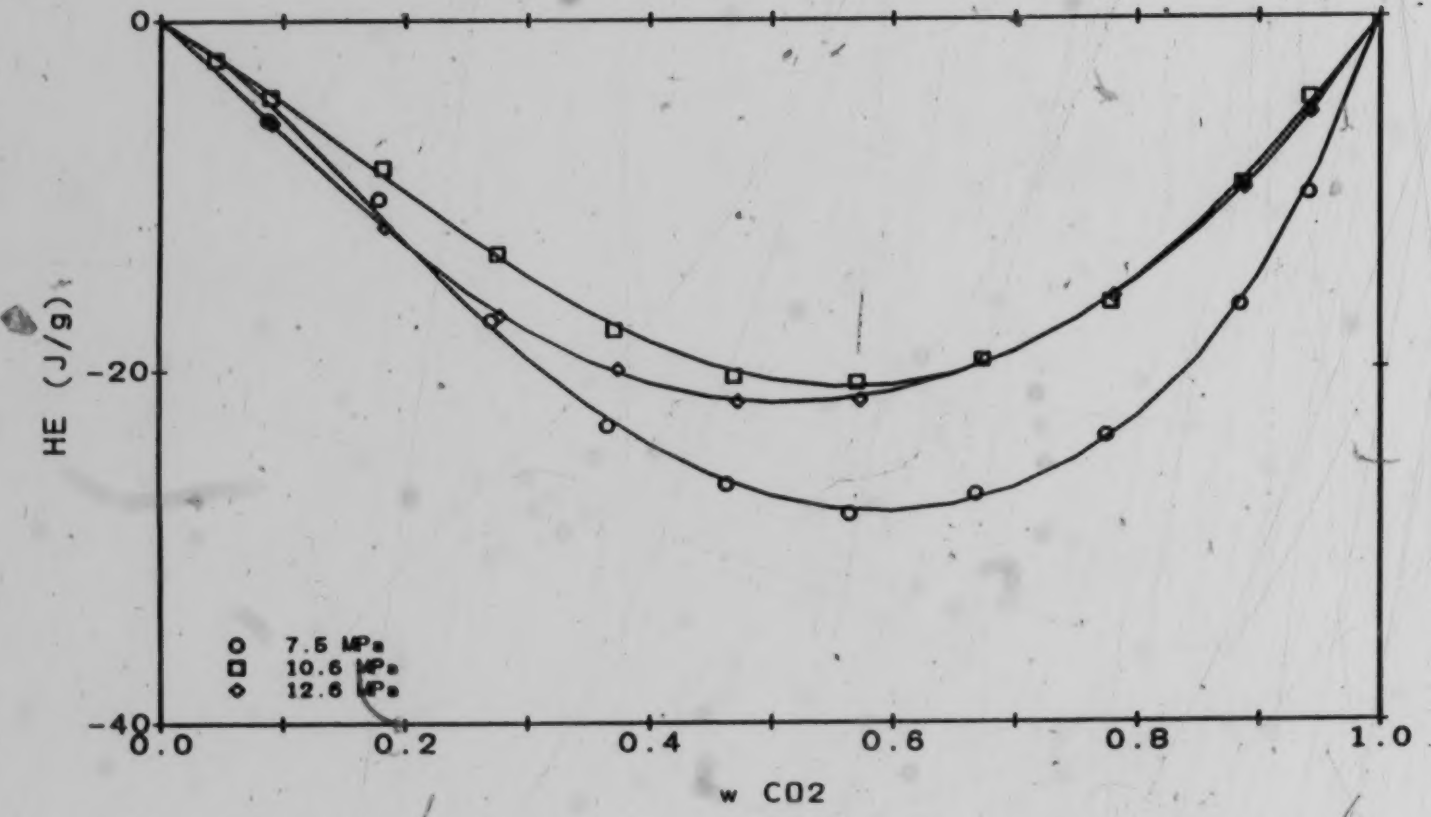

Figure 18. Comparison of Calculated and Experimental Enthalpy of Mixing of (CO_2 + Selexol) at 298.15 K. (0.83% wt. H_2O)

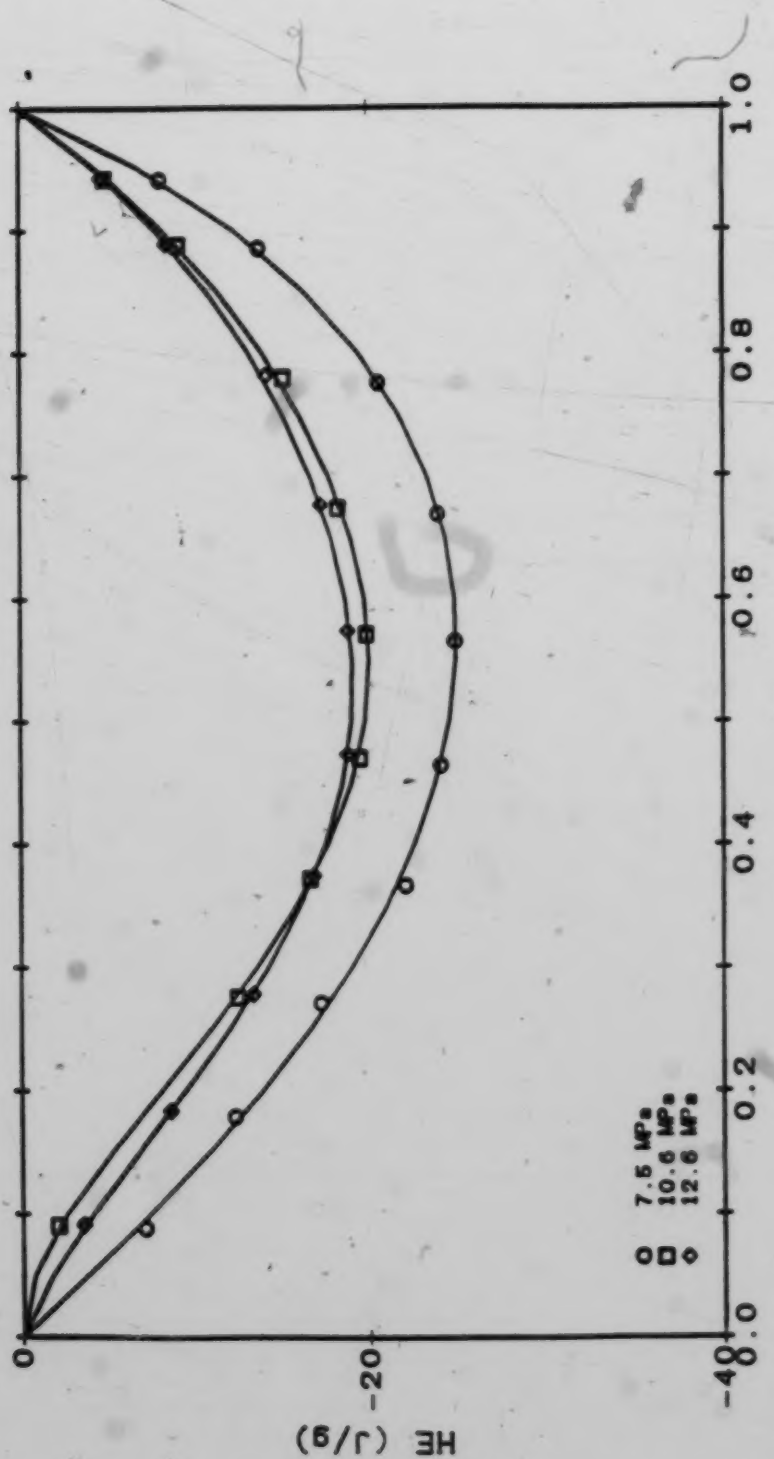

Figure 19. Comparison of Calculated and Experimental Enthalpy of Mixing of (CO_2 + Selexol) at 298.15 K. (3.62% wt. H_2O)

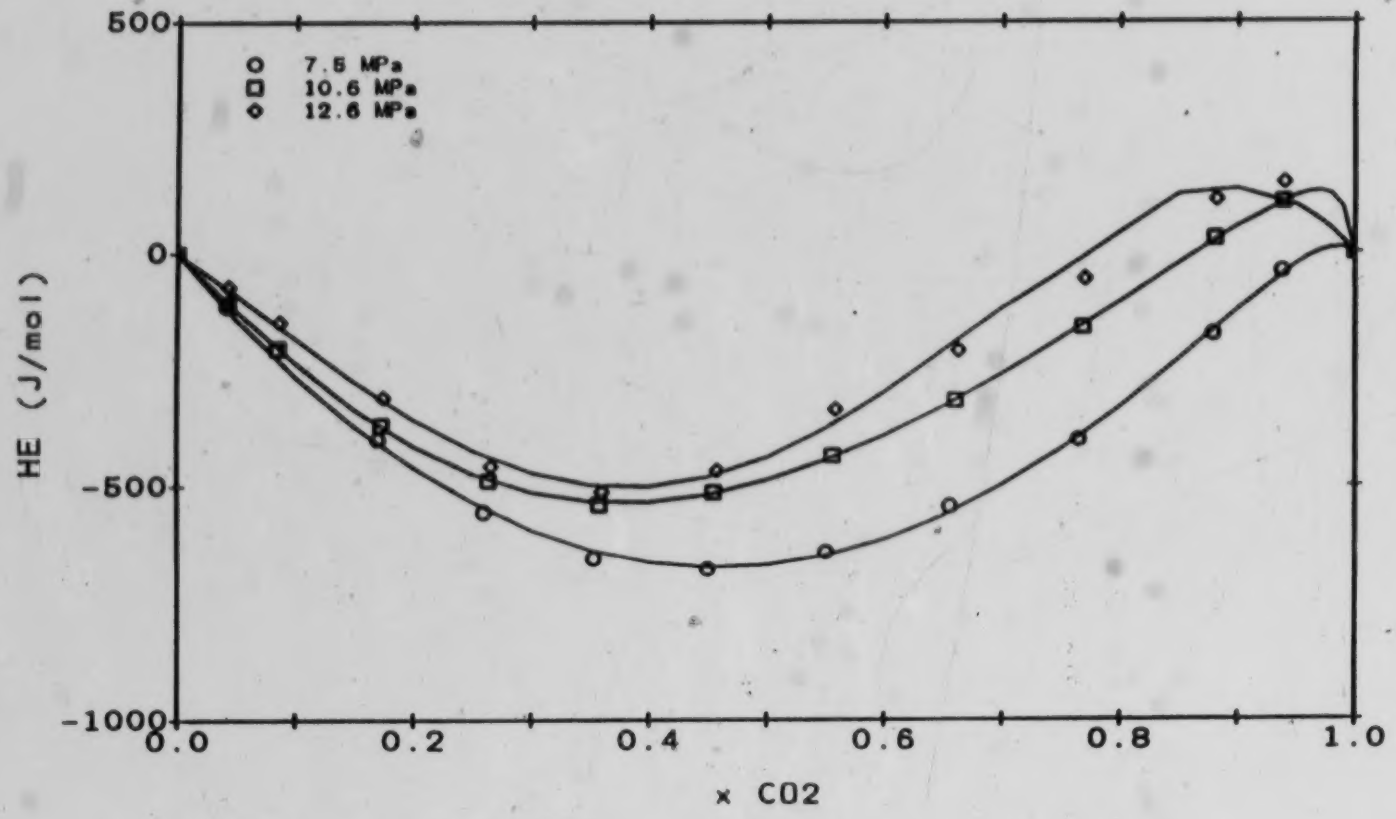

Figure 20. Comparison of Calculated and Experimental Enthalpy of Mixing of (CO_2 + Methanol) at 298.15 K

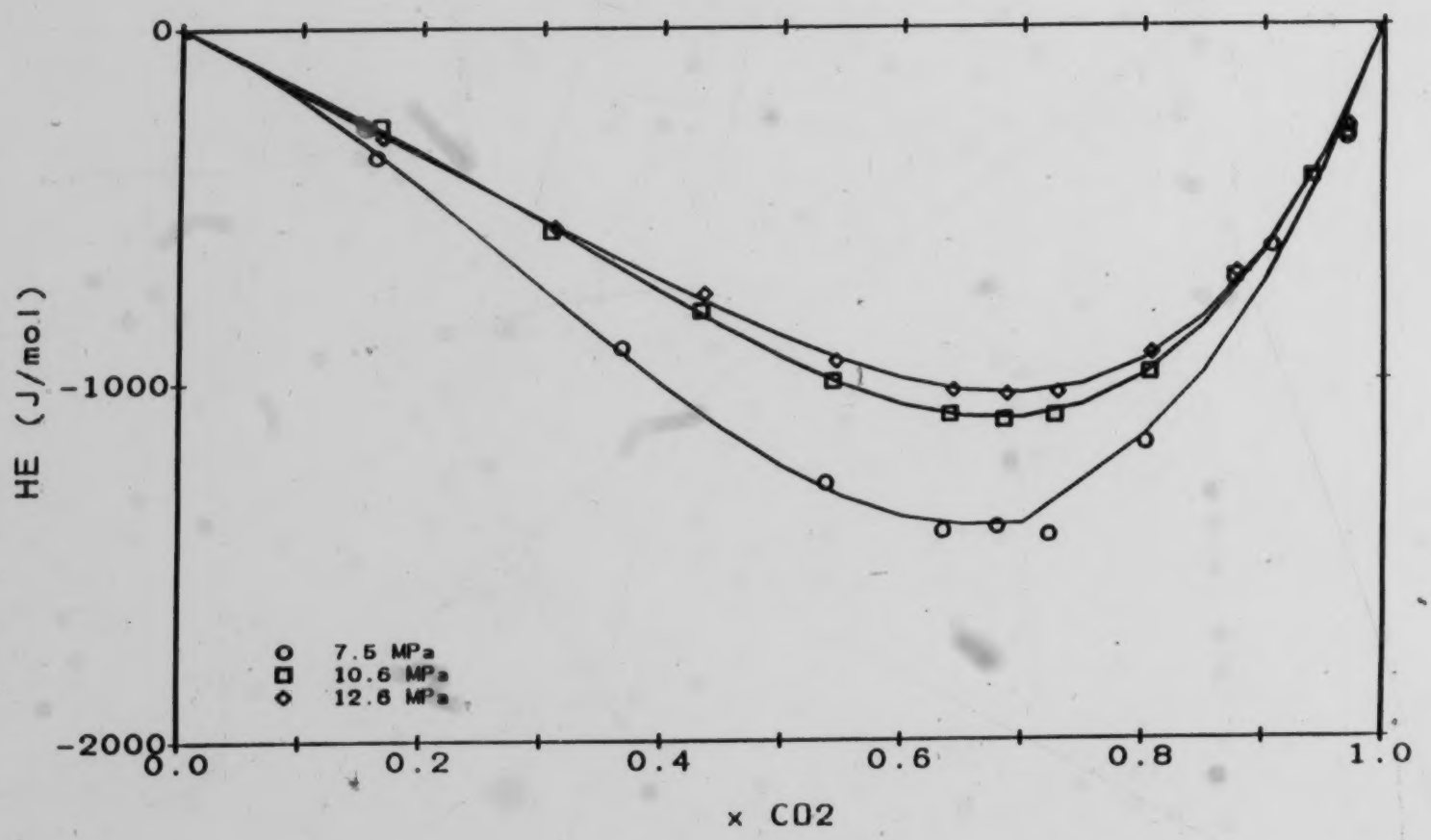

Figure 21. Comparison of Calculated and Experimental Enthalpy of Mixing of (CO_2 + Propylene Carbonate) at 298.15 K

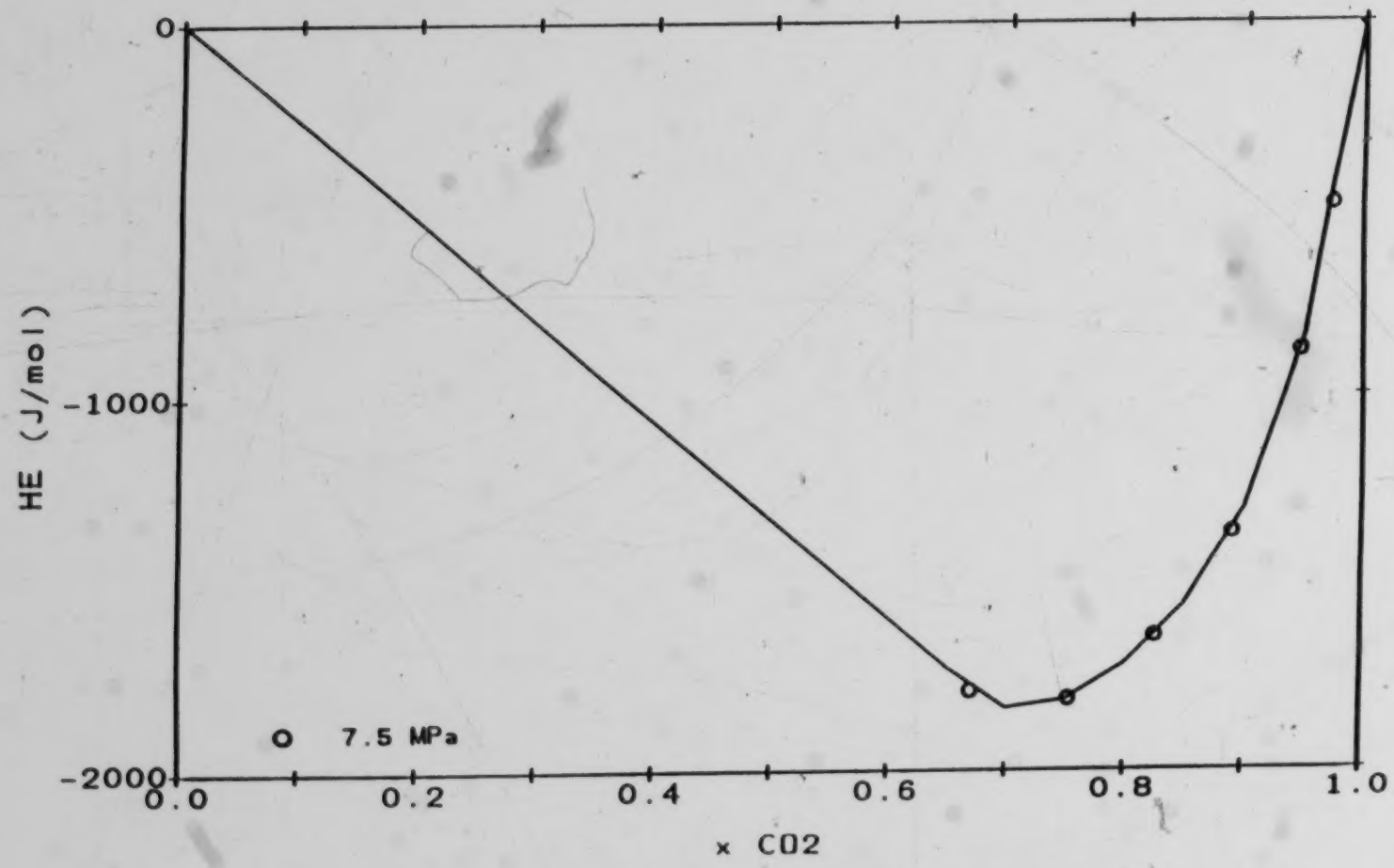

Figure 22. Comparison of Calculated and Experimental Enthalpy of Mixing of (CO_2 + N-Formyl Morpholine) at 298.15 K

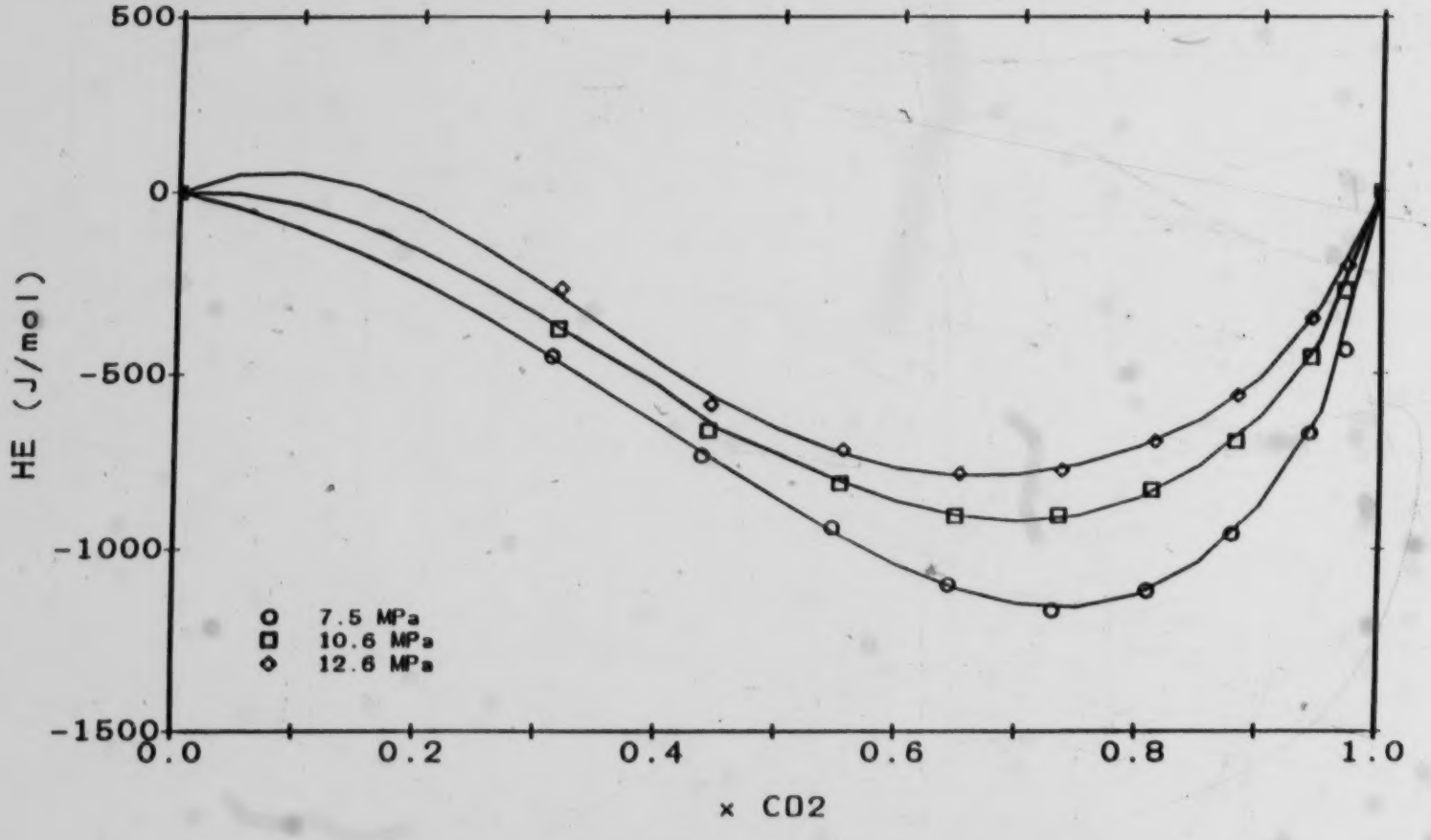

Figure 23. Comparison of Calculated and Experimental Enthalpy of Mixing of (CO_2 + Methyl Cyanoacetate) at 298.15 K

5.2 Errors and Uncertainties.

There are different types of errors and they can be classified as random and non-random. The random errors may be caused by electronic problems, flow rate control, temperature control, mixing problems, etc. The non-random errors arise when we have problems of non-equilibration of the chemical compounds (i.e. equilibrium not reached).

The criterion used for determining if equilibrium was reached was to decide upon looking at the plot from the chart recorder if the flowing chemical components equilibrated in a reasonable interval of time. Once the mixing starts, the pen in the chart recorder moves in the appropriate direction depending on whether the interaction of the two chemical components exhibits endothermic or exothermic effects, and eventually it levels off. The appearance of this plateau gives us an indication that equilibrium has been attained. If this was not the case or the shape of the plot was much different from the other points, then we had a reason to believe that the point was suspect.

In some of the tables in Appendix IV there are some experimental values of the enthalpy of mixing shown in brackets. These are points that according to the criteria given above were questionable. They were not included in the least-squares regression, neither plotted.

We estimate that the combined uncertainties in pump flow rate control, electrical calibration, and temperature control to be about 3%. Hence, the total uncertainty in the enthalpy of mixing values listed in Appendix IV is approximately ($3\% + 2\sigma$).

5.3 Regression Procedure.

Equation (5.1) was fit to the experimental data; the coefficients satisfy the principles of least-squares.

$$H^E = \left[\frac{x(1-x)}{1+\sum_{i=1}^{B} D_i(1-2x)^i}\right]\sum_{i=0}^{A} C_i(1-2x)^i \qquad (5.1)$$

This type of least-squares representation for the enthalpy of mixing was suggested by Christensen, et al. [3-11], [19], [20], and enables us to perform the interpolation of data at a given pressure. The coefficients C_i and D_i are given in Table A4.12 of Appendix IV. The solid lines in Figures 17 to 23 show the data obtained with this regression.

5.4 (Cyclohexane + n-Hexane).

This was the only system for which the ConstaMetric pumps were used. The agreement of our results at 0.1 and 7.0 MPa with Christensen, et al. is within 3%, but at 14.0 MPa there is a systematic difference of approximately 10 J/mol. This difference lies within combined uncertainties of our work (6%) and of Christensen, et al. (2%), and possibly due to a malfunction of the check valves in the pumps.

5.5 (CO_2 + Toluene).

Our data for this system exhibited the same trend as Wormald's [48] and Christensen's [35] with the exception of two points near x = 0.4 in the data at 298.15 K and 7.5 MPa and at 308.15 K and 10.6 MPa which differ by up to 60 J/mol. These points reached steady state very slowly compared to the remaining points, and we believe this behaviour was due to some problems in the flow system, but we were unable to confirm them.

The (CO_2 + Toluene) system was the only one of the systems studied involving CO_2 for which we had some experimental data available for comparison, and the agreement was good enough to give us an indication of an adequate operation of the flow system and of the calorimeter as well.

The enthalpy of mixing of this system showed both endothermic and exothermic

effects. The mole fraction range at which the change from endothermic to exothermic of the enthalpy of mixing took place varied according to the conditions of pressure and temperature. In general, we can say that the occurrence of the endothermic effect was in the CO_2 rich region of the curve, while that of the exothermic effect was in the Toluene rich region.

5.6 (CO_2 + N-Methyl Pyrrolidone), (CO_2 + Propylene Carbonate), and (CO_2 + Methyl Cyanoacetate).

These three systems showed exothermic enthalpy of mixing throughout the entire composition range. The standard deviation of the data for these systems was approximately 3% for (CO_2 + N-Methyl Pyrrolidone) and (CO_2 + Propylene Carbonate), and 2% for (CO_2 + Methyl Cyanoacetate).

5.7 (CO_2 + Selexol).

The observed trend of increasing enthalpy of mixing with decreasing pressure was not observed for this system. In the Selexol rich region of the enthalpy of mixing curve, the values at 12.6 MPa were larger than those at 10.6 MPa, while in the CO_2 rich region there was almost no difference at all between the values at 10.6 and 12.6 MPa. This trend was observed for both of the mixtures of Selexol used with different contents of water (0.83% and 3.62% weight of H_2O). The enthalpy of mixing curve for the mixture containing 0.83% weight of H_2O at 10.6 MPa was repeated twice in order to confirm the behaviour observed in the Selexol-rich region. The results for both runs were the same. We can say that the data for the mixture containing 3.62% weight of H_2O is the same at 10.6 and 12.6 MPa, because the experimental error may account for the very small difference observed between the two curves. The fact of Selexol not being a pure solvent because of the presence of water led us to think that this may be the cause of this effect. Looking at Figures 18 and 19, we can see that

the amount of water in the solvent does affect the enthalpy of mixing. The mixture containing 0.83% weight of H_2O showed a larger enthalpy of mixing, than the one containing 3.62% weight of water. The standard deviation of the data for both mixtures of Selexol was approximately 3%.

The enthalpy of mixing for this system was determined in a mass basis rather than in a molar basis due to the fact that Selexol is a polymer and its molecular weight might change between different samples, provided they were not obtained from the same lot. Another reason for doing this was to make easier the comparison of data from other studies.

The results obtained for the test on flow rate dependence with the system (CO_2 + Selexol) at 298.15 K and 10.6 MPa are given in Table A4.11 of Appendix IV and plotted in Figure 24.

5.8 (CO_2 + Methanol).

This was the only (CO_2 + Physical Solvent) system of those studied that did not exhibit an exothermic effect throughout the whole composition range. The endothermic effects appeared at 10.6 and 12.6 MPa in the region of the enthalpy of mixing curve where $x > 0.9$. The standard deviation of the data was approximately 3%.

5.9 (CO_2 + N-Formyl Morpholine).

The enthalpy of mixing for this system was determined only at 298.15 K and 7.5 MPa because of freezing problems with the N-Formyl Morpholine. The melting point of the N-Formyl Morpholine is 23°C and when we attempted to obtain the data at 10.6 MPa the solvent froze in the pump. We believe that part of the odd behaviour noticed at 7.5 MPa at high mole fractions of N-Formyl Morpholine may be due to some freezing problems as well. The standard deviation of the data was approximately 4%.

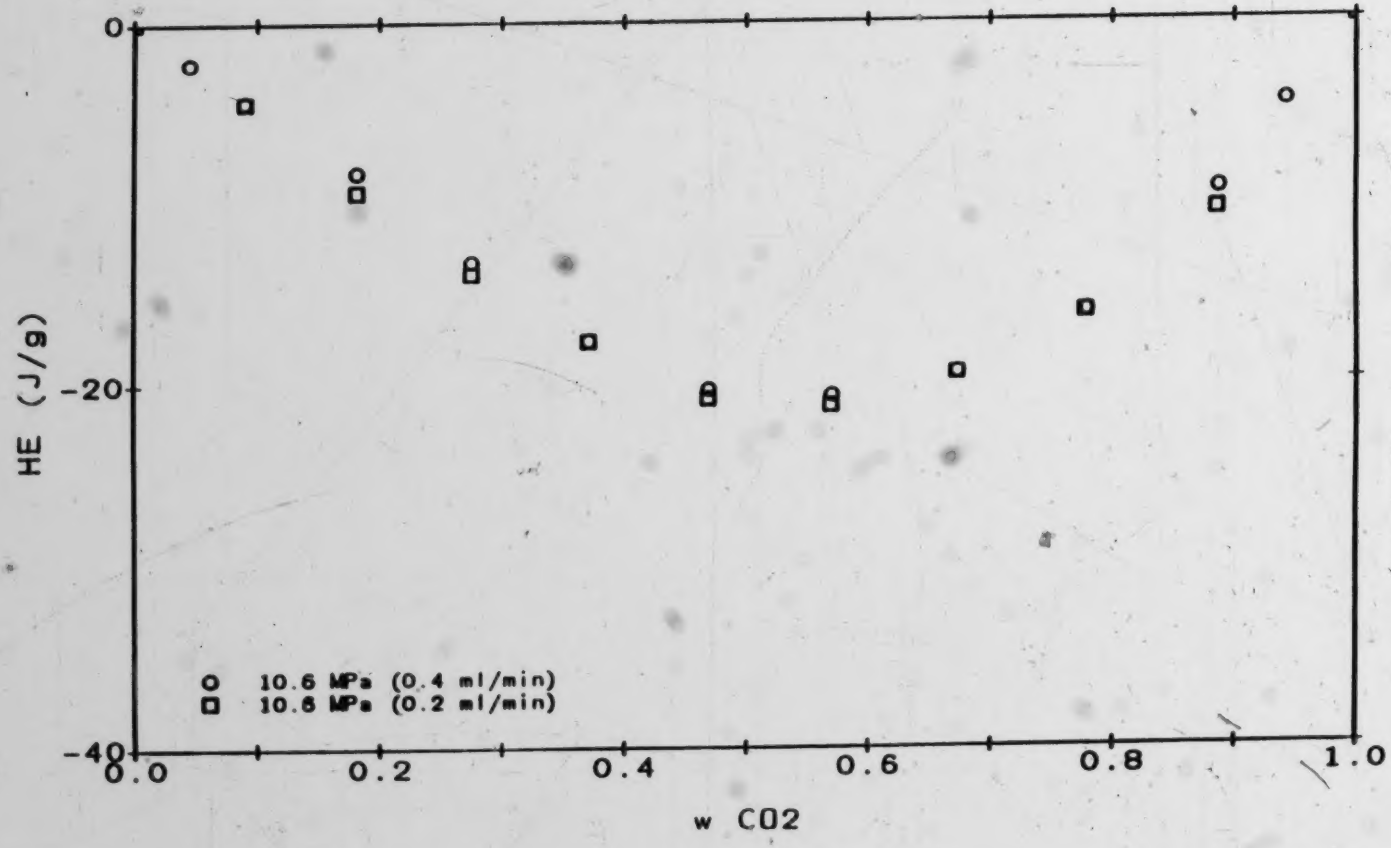

Figure 24. Comparison of the Enthalpy of Mixing of (CO_2 + Selexol) at 298.15 K with Different Flow Rates. (0.83% wt. H_2O)

CHAPTER VI

PREDICTED DATA WITH THE PENG-ROBINSON EQUATION OF STATE

6.1 General Background.

For any substance, regardless of whether it is pure or a mixture, all thermodynamic properties of interest in phase equilibria can be calculated from thermal and volumetric measurements. Thermal measurements give information on how some thermodynamic properties vary with temperature, whereas volumetric measurements give information on how thermodynamic properties vary with pressure or density at constant temperature.

The mathematical relation between volume, pressure, temperature, and composition is called the equation of state; many forms of the equation of state are of the pressure-explicit type.

Thousands of equations of state have been proposed, though the usefulness has not been the same for all of them. Among the most widely used equations of state are the Redlich-Kwong equation and its modifications, the Benedict-Webb-Rubin equation, and the Peng-Robinson equation. All these equations of state have been used for correlating both liquid and vapour thermodynamic and volumetric data, and for predicting vapour-liquid equilibria and other thermodynamic properties.

The general behaviour of the enthalpy of mixing for binary mixtures in the critical region can be explored using an equation of state. The Peng-Robinson equation of state has been used widely and successfully in the gas processing industry, this being the reason why we chose that equation to perform the predictions of the enthalpy of mixing data.

The Peng-Robinson equation of state has the form:

$$P = \frac{RT}{v-b} - \frac{a(T)}{v(v+b)+b(v-b)} \qquad (6.1)$$

The determination of the pure component parameters, a and b, requires the knowledge of the critical properties and acentric factor for each one of the components involved in the calculation. For most of the solvents studied those properties were not available in the literature. These solvents decompose at high temperatures; therefore, we had to look for other alternatives to overcome this problem.

One of these alternatives was to estimate the critical properties using the methods given by Reid, et al. [39]. Once we had the critical properties, we could proceed to calculate the acentric factor and then evaluate the pure component parameters required in the equation of state using the original mixing rules proposed by Peng and Robinson [38]. We believed that the estimation of the critical properties was not the best alternative, mainly because of problems with the characterization of each of the solvents (i.e. group contributions).

Having some vapour pressure data was not of much help either, because we needed to know, for calculating the acentric factor, the temperature at whcih $T_r = 0.7$ occurs, and for this the critical temperature was required again.

Another alternative was to find the pure component parameters, a and b, directly such that they satisfy the equation of state and the fugacity equality.

Panagiotopoulos and Kumar [34], presented a generalized technique to obtain pure component parameters for two-parameter equations of state, which included the Van der Waals, Redlich-Kwong, and Peng-Robinson equations of state. The method requires as input data the vapour pressure and saturated liquid volume of a component at a given temperature.

The values of the pure component parameters for the Peng-Robinson equation of state obtained using the method mentioned above are given in Table 4. Values for CO_2 are also given in this table; they were obtained from the equations presented in the original paper.

The sources from which the vapour pressure and saturated liquid density data were obtained for each solvent are given in Table A1.1 of Appendix I.

6.2 Enthalpy Calculations.

In the Peng-Robinson equation, parameter a is a function of temperature while parameter b is not. Using the approach outlined in the previous section both, a and b, are functions of temperature. The fact that b varies with temperature led us to modify the expression for the enthalpy departure given by Peng and Robinson [38]. The final form of the modified expression derived by us is:

$$H - H^{*} = RT(Z-1) + \frac{a - T\left(\frac{da}{dT}\right)}{2\sqrt{2}b}\ln\left(\frac{Z-0.414B}{Z+2.414B}\right)$$

$$+\frac{aT\left(\frac{da}{dT}\right)}{b}\left[\frac{\frac{ZP}{RT}}{Z^2+2BZ-B^2} - \frac{1}{2\sqrt{2}b}\ln\left(\frac{Z-0.414B}{Z+2.414B}\right)\right] \qquad (6.2)$$

The detailed formulation of the expression for the enthalpy departure, taking into account the variation with temperature of both parameters a and b, is given in Appendix V.

The enthalpy of mixing was then calculated as:

$$H^{E} = H_{mix} - \sum x_i H_i \qquad (6.3)$$

The enthalpy of pure CO_2 was obtained from the Peng-Robinson prediction in

order to be consistent. When this value was compared to that reported in the IUPAC Tables [27], the agreement was within 50 J/mol (0.5%) which we considered satisfactory.

6.3 Interaction Parameters.

The interaction parameter, δ_{ij}, required in the mixing rules of the equation of state, was not known for any of the (CO_2 + Physical Solvent) systems studied here. This interaction parameter characterizes the binary formed by component i and component j, and is usually determined in an empirical way.

The procedure followed was to assume $\delta_{ij} = 0$ and perform all the calculations. Then we matched the maximum value of the experimental enthalpy of mixing by letting δ_{ij} vary. After having done this for all the solvents at the three different pressures studied, we found a pressure dependence of δ_{ij}.

The values of δ_{ij} at 10.6 MPa and 12.6 MPa differed less than those at 7.5 and 10.6 MPa. In addition, δ_{ij}, is normally independent of pressure; therefore, in order to be able to report a single value for each solvent, we averaged the values at 10.6 and 12.6 MPa and recalculated all the data. In doing so we knew that at these pressures we were above the critical point of CO_2 and the variation of δ_{ij} with pressure was rather small, allowing us to use the same value of δ_{ij} for calculations at higher pressures, if necessary, without incurring large errors.

The final values of δ_{ij} used for the prediction of the experimental data are given in Table 5.

6.4 Discussion of Results.

The results obtained with the Peng-Robinson equation are plotted in Figures 25 to 32 for the same systems shown in Chapter V. All the predicted data is presented in Tables A6.1 to A6.8 of Appendix VI.

Now, we proceed to discuss the predicted results for the systems studied.

6.4.1 (CO_2 + Toluene) System.

The Peng-Robinson equation predicted the right shape for the enthalpy of mixing curves for this system at 298.15 K, but is not able to reproduce the endothermic effect at 308.15 K. Even though the equation at 298.15 K predicted the right shape, some of the predicted values differed by more than 100 J/mol when compared with the experimental ones. At 308.15 K the fit of the Peng-Robinson equation is best in the range $0.85 < x < 1.0$.

6.4.2 (CO_2 + Physical Solvent) Systems.

The Peng-Robinson equation gave enthalpy of mixing curves of the right shape for all these systems. The only exception was the (CO_2 + Methanol) system in which the endothermic region was not reproduced and will be discussed later on.

In general, the equation fitted the experimental data reasonably well in the solvent rich region, while in the CO_2 rich region the agreement was not as good. This may be due to the method employed for the determination of the pure component parameters of the solvents for which we used vapour pressure and liquid density data, hence forcing the equation to reproduce them, while the parameters for CO_2 were evaluated with the original rules given by Peng and Robinson [38].

It is also worth to mention that even though all these solvents are quite polar, the results obtained with the Peng-Robinson equation are reasonable and encouraging.

6.4.2.1 (CO_2 + Selexol) System.

The system (CO_2 + Selexol) was modeled as a two component system, but as we have mentioned before, Selexol is a mixture containing water, thus in a rigorous way

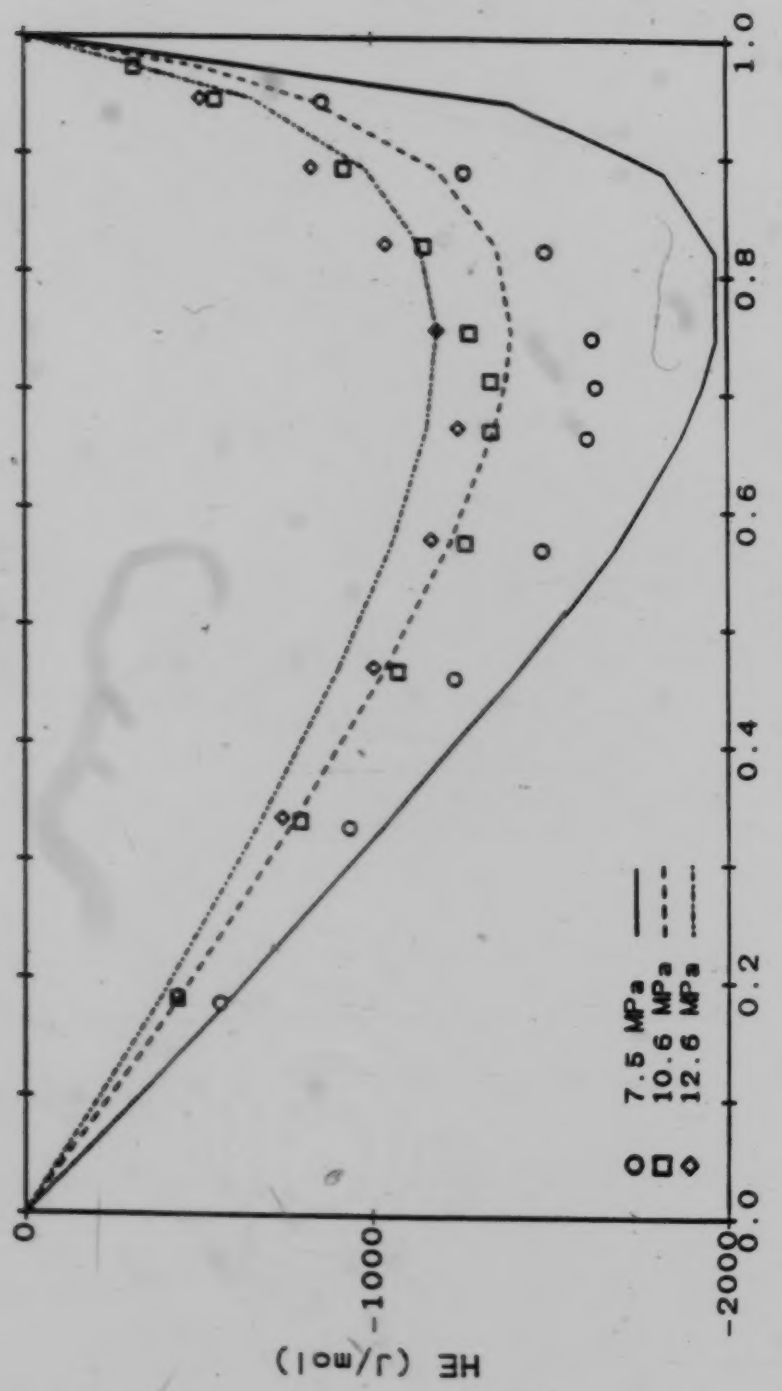

Figure 25. Comparison of Predicted and Experimental Enthalpy of Mixing of (CO_2 + N-Methyl Pyrrolidone) at 298.15 K

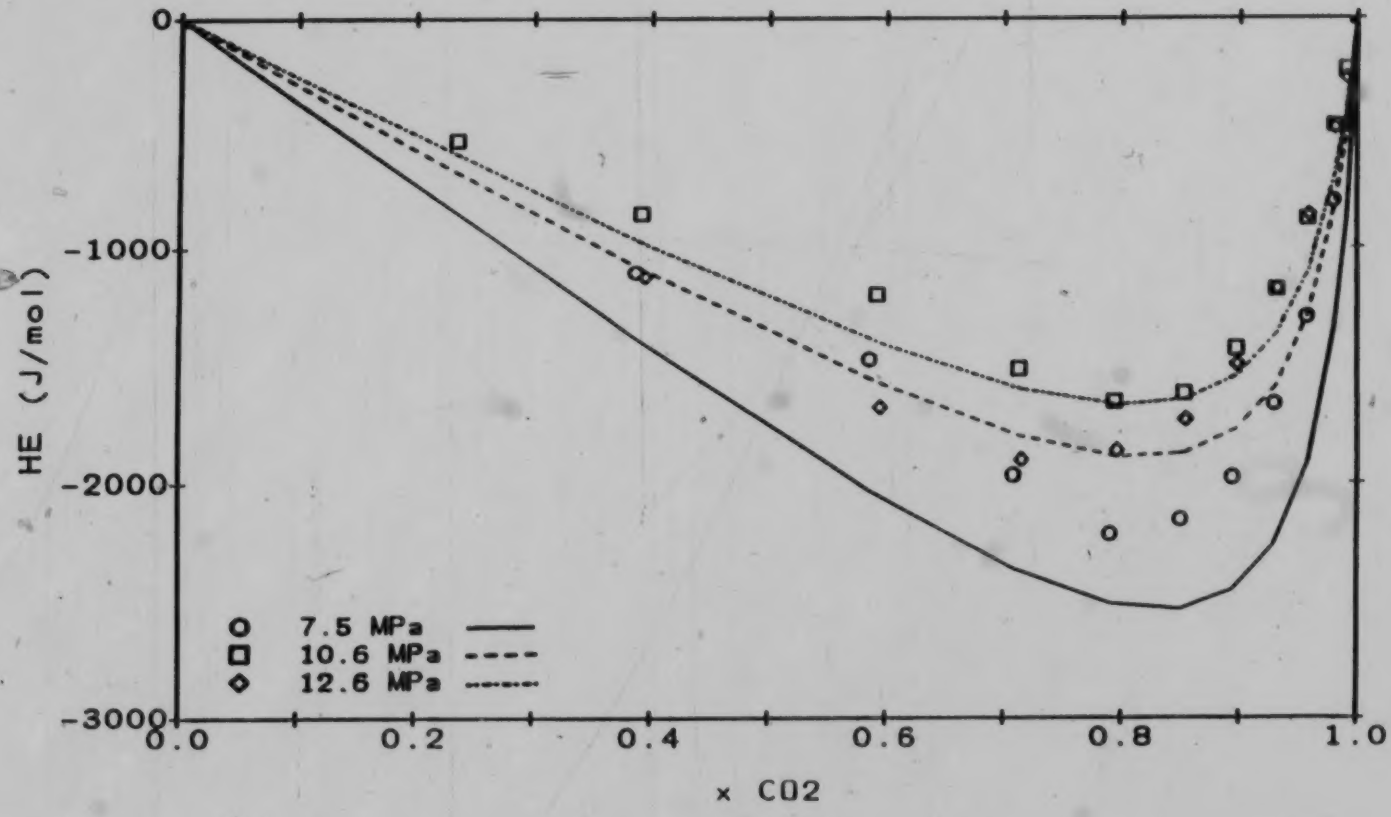

Figure 26. Comparison of Predicted and Experimental Enthalpy of Mixing of (CO_2 + Selexol) at 298.15 K. (0.83% wt. H_2O)

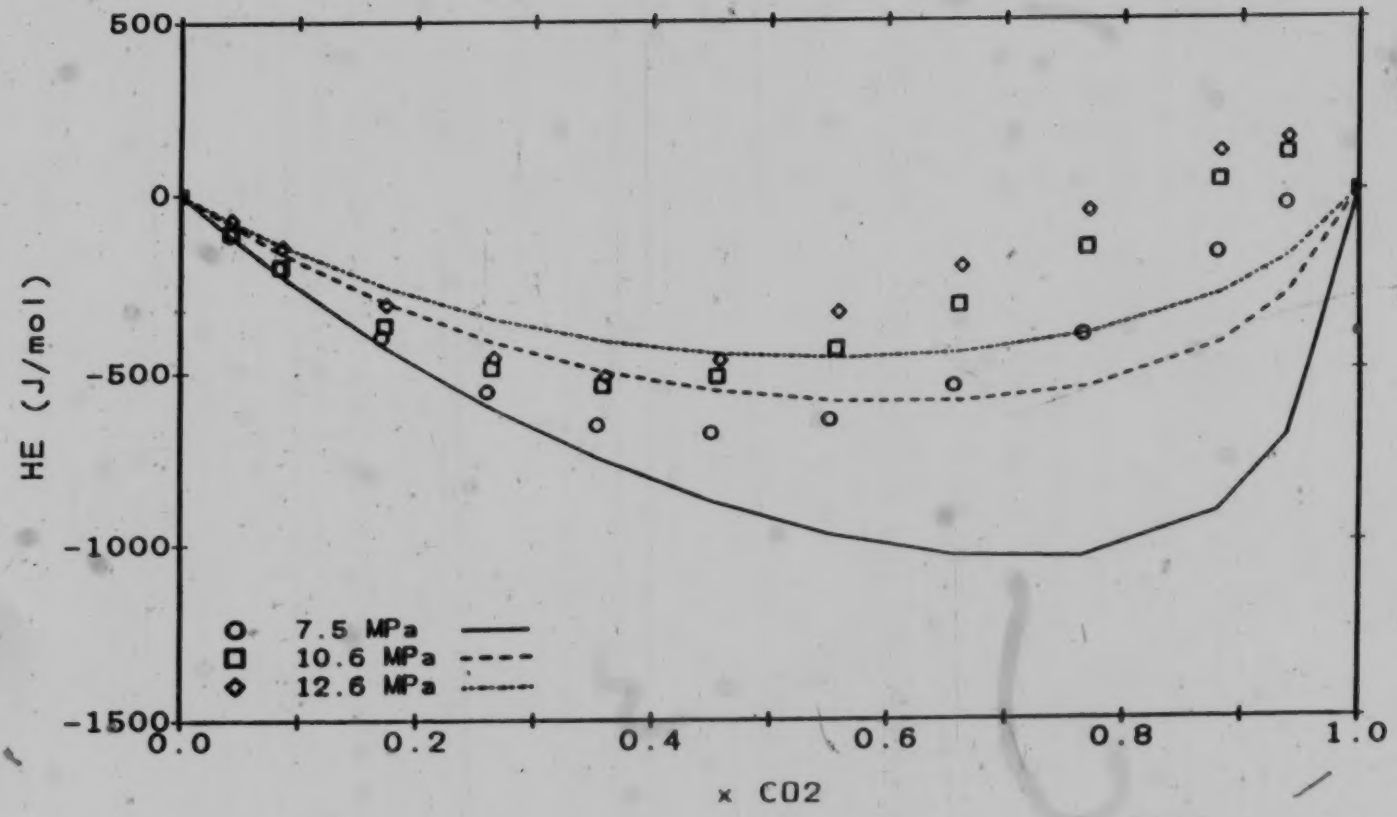

Figure 27. Comparison of Predicted and Experimental Enthalpy of Mixing of (CO_2 + Methanol) at 298.15 K

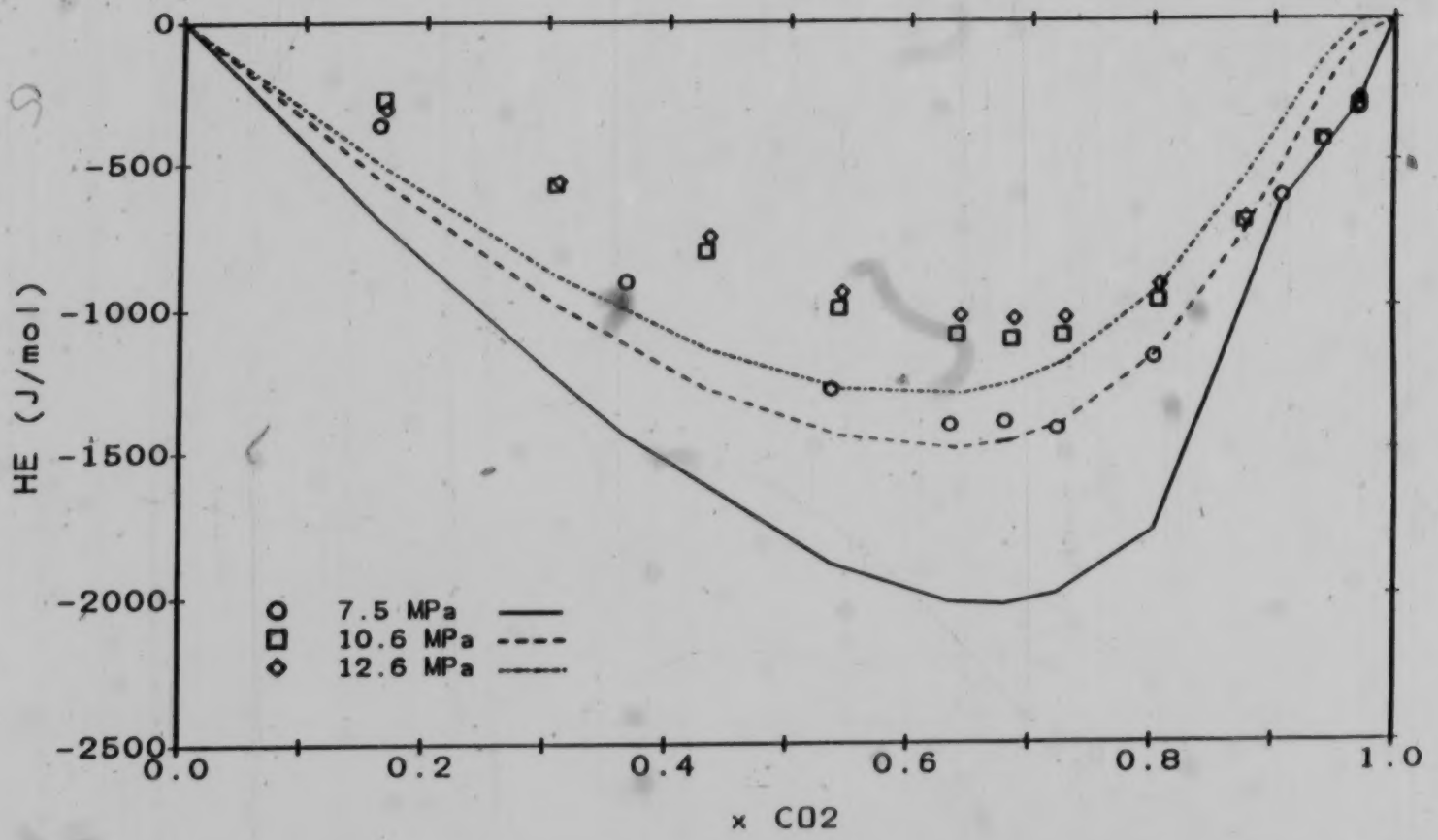

Figure 28. Comparison of Predicted and Experimental Enthalpy of Mixing of (CO_2 + Propylene Carbonate) at 298.15 K

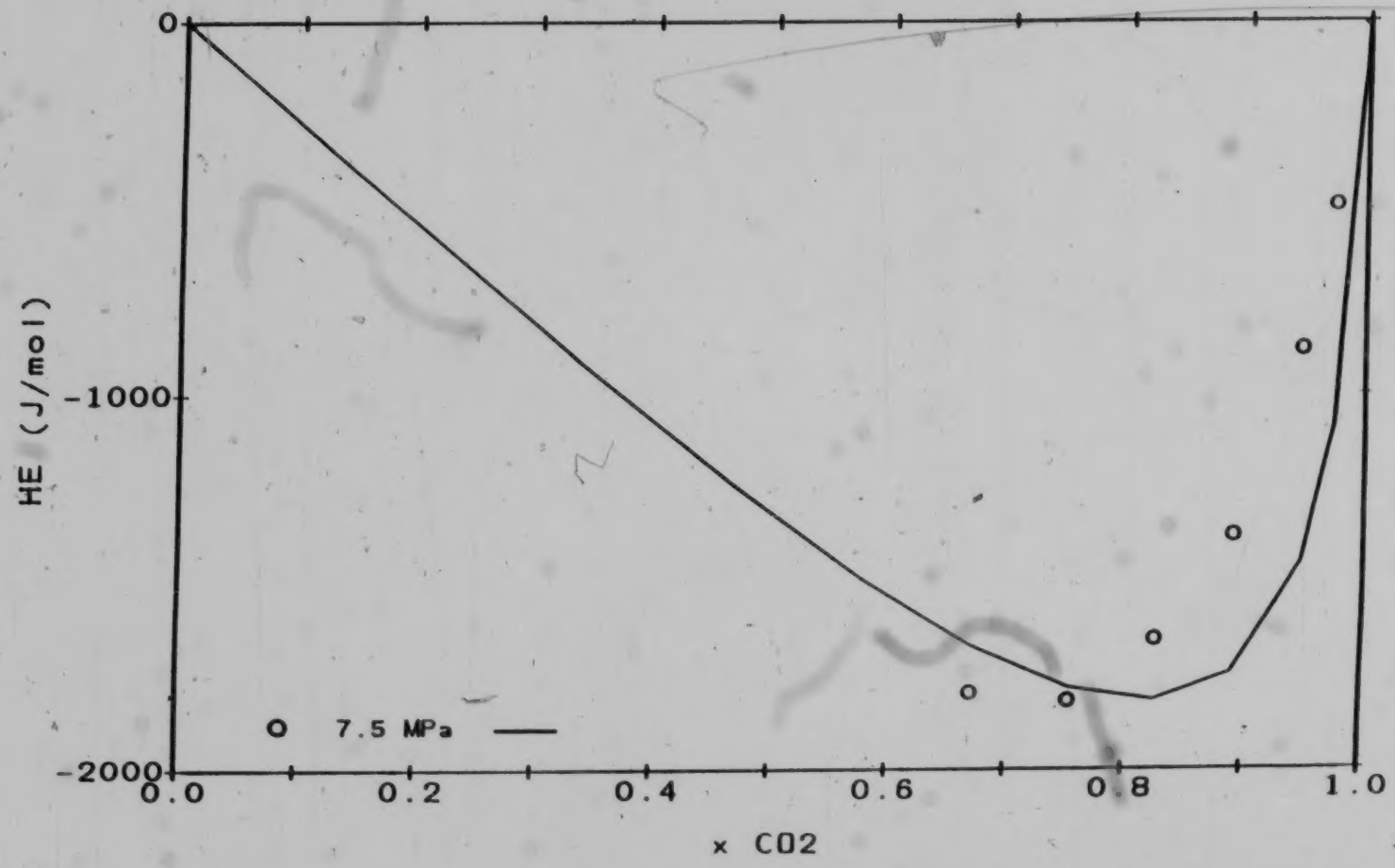

Figure 29. Comparison of Predicted and Experimental Enthalpy of Mixing of (CO_2 + N-Formyl Morpholine) at 298.15 K

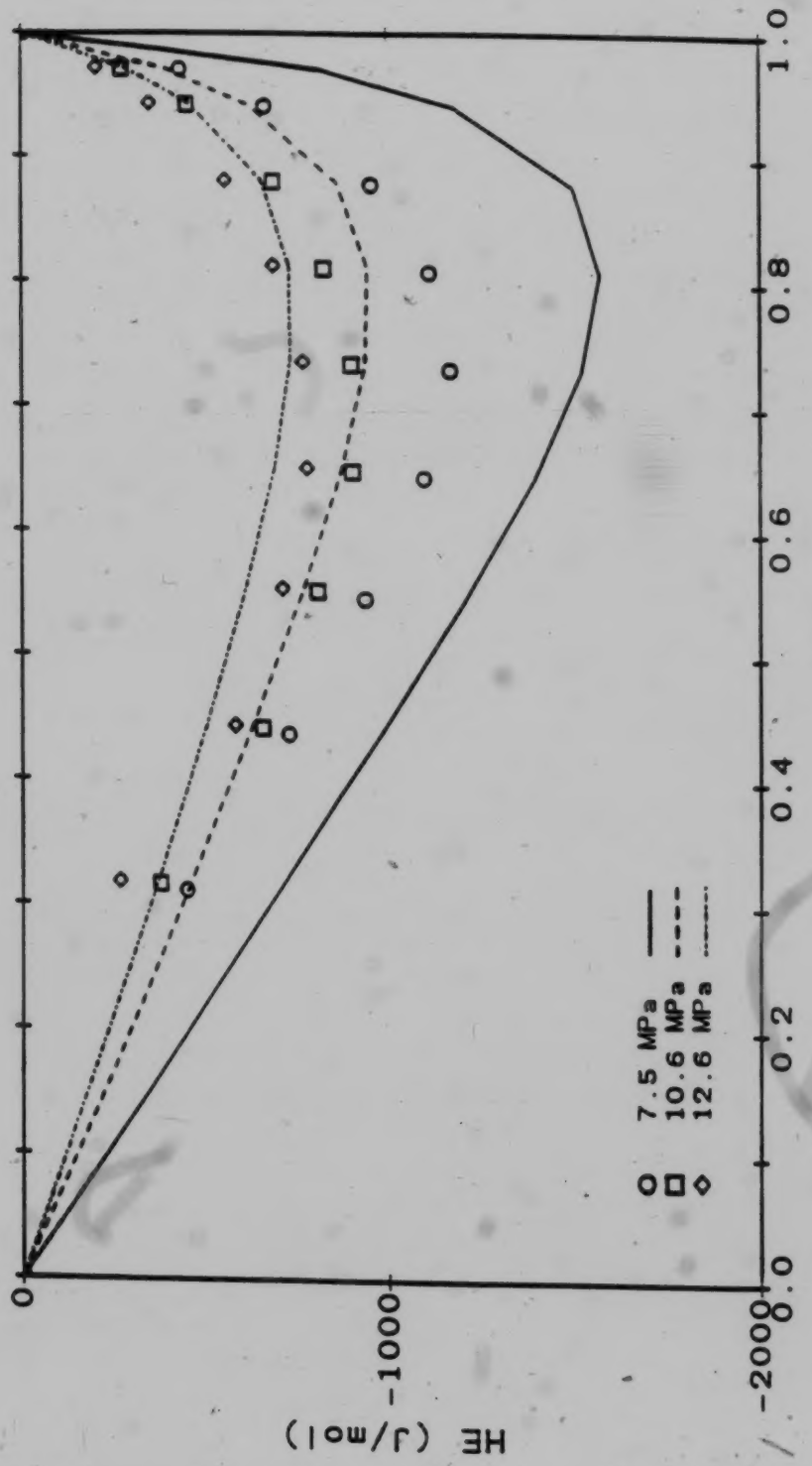

Figure 30. Comparison of Predicted and Experimental Enthalpy of Mixing of (CO_2 + Methyl Cyanoacetate) at 298.15 K

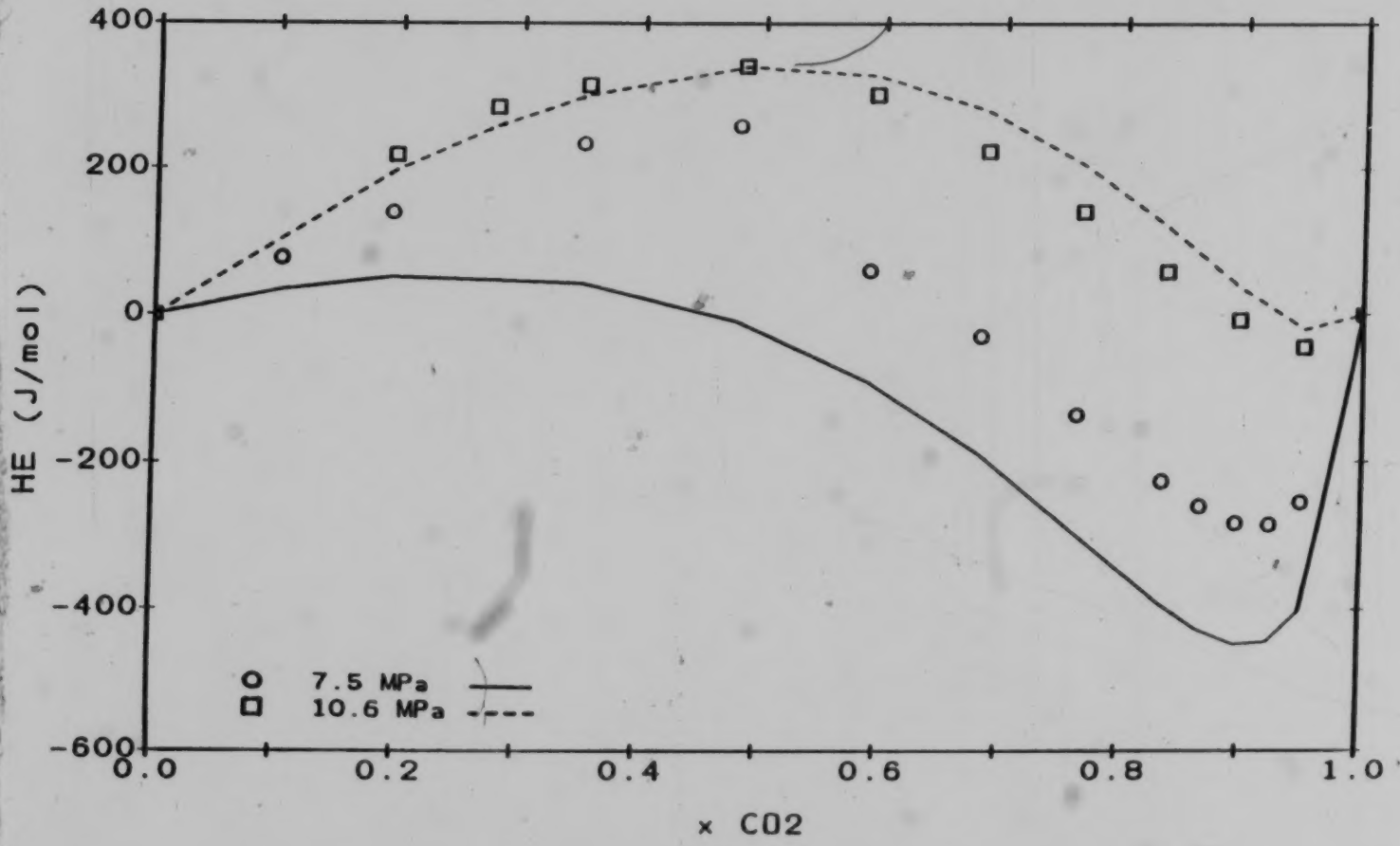

Figure 31. Comparison of Predicted and Experimental Enthalpy of Mixing of (CO_2 + Toluene) at 298.15 K

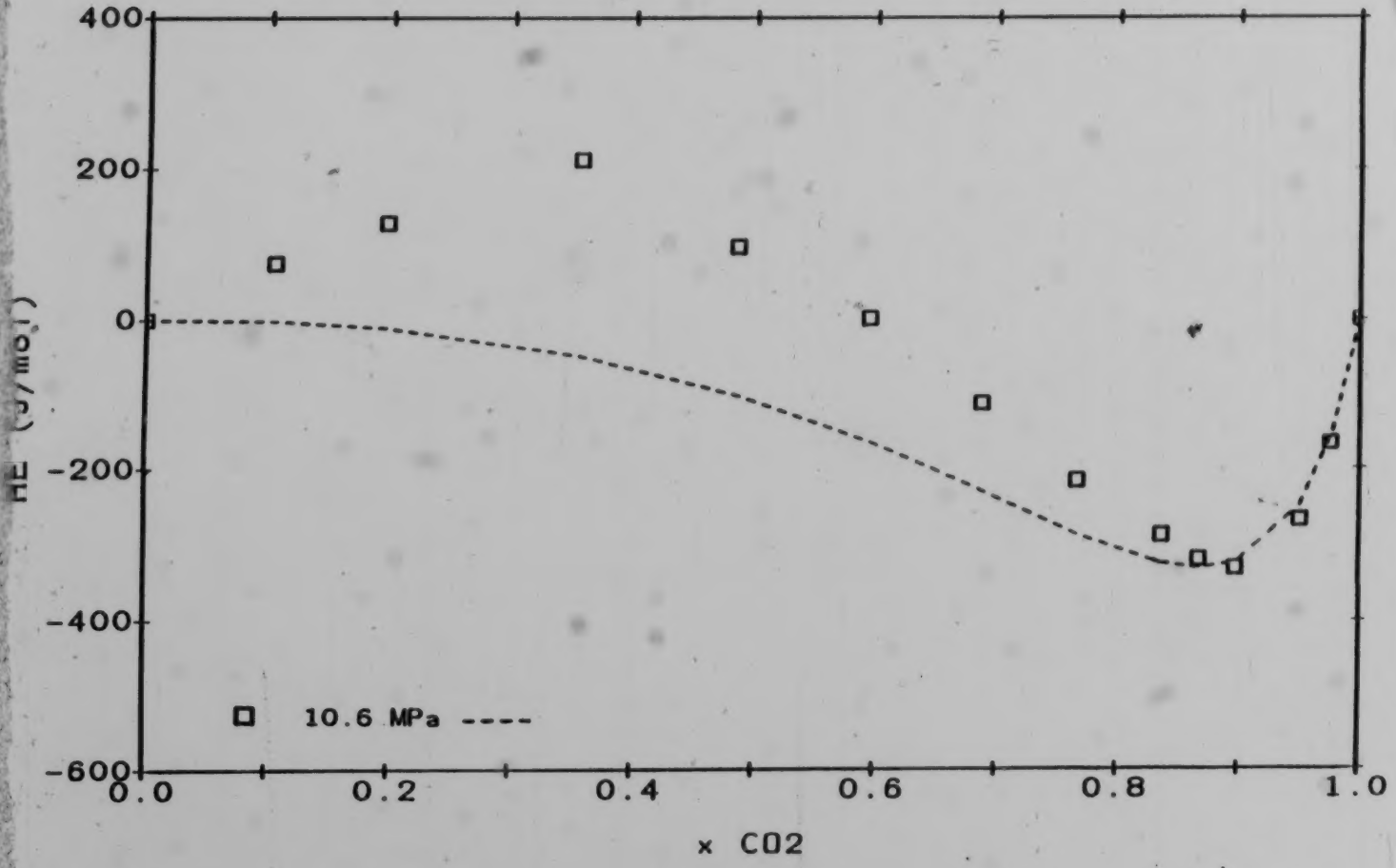

Figure 32. Comparison of Predicted and Experimental Enthalpy of Mixing of (CO_2 + Toluene) at 308.15 K

it should have been modeled as a three component system taking into account the three binaries formed: CO_2-Selexol, CO_2-H_2O, and Selexol-H_2O. In addition, the fact of Selexol being a polymer introduces one more factor to consider in the modeling of the system, which could be a separate project itself.

6.4.2.2 (CO_2 + Methanol) System.

The poorest fit of the Peng-Robinson equation was with the (CO_2 + Methanol) system. As we mentioned before, the equation predicted the wrong shape of the enthalpy of mixing curve and was unable to reproduce the endothermic region between $0.9 < x < 1.0$. The solvent in this particular system, besides being polar, has the characteristic of hydrogen bonding, which may be among the causes for obtaining a poor fit.

6.4.2.3 (CO_2 + Methyl Cyanoacetate) System.

We did not find in the literature vapour pressure and saturated liquid density data for Methyl Cyanoacetate at temperatures other than 298.15 K. We determined the Peng-Robinson parameters at this temperature and whenever we required the parameters at other temperatures (i.e. for evaluating (da/dT) and (db/dT) in equation (6.2)), we used the slope obtained for N-Methyl Pyrrolidone.

6.4.2.4 (CO_2 + Propylene Carbonate) System.

The data predicted with the interaction parameter obtained with the procedure given in Section 6.3, showed some endothermic effects in the CO_2 rich region at 10.6 and 12.6 MPa. Endothermic effects were never observed in the experimental runs; therefore, we varied the interaction parameter until and exothermic enthalpy of mixing curve in the entire composition range was obtained. This is the reason why the fit

TABLE 4

PENG-ROBINSON PARAMETERS FOR VARIOUS SOLVENTS

Solvent	Temperature (K)	a (Pa m^6/mol^2)	b x 10^6 (m^3/mol)
N-Methyl Pyrrolidone	293.15	5.4753	87.9998
	298.15	5.4661	88.1910
	303.15	5.4273	88.3176
Propylene Carbonate	298.15	5.4333	78.7922
	303.15	5.4518	79.0057
	308.15	5.3885	79.2317
Selexol	293.15	22.0602	260.3770
	298.15	21.9425	260.9284
	303.15	21.8248	261.4798
Methanol	293.15	1.4538	35.0277
	298.15	1.4402	35.0708
	303.15	1.4300	35.0883
Methyl Cyanoacetate	293.15	5.2045	80.9736
N-Formyl Morpholine	293.15	7.6281	93.5234
	298.15	7.3621	93.8463
	303.15	7.1928	93.7998
Toluene	293.15	4.0653	92.9945
	298.15	4.0149	92.5491
	303.15	3.9868	92.6413
	308.15	3.9677	92.9091
	313.15	3.9375	92.9255
CO_2	293.15	0.4066	26.6523
	298.15	0.4017	26.6523
	303.15	0.3969	26.6523
	308.15	0.3922	26.6523
	313.15	0.3875	26.6523

TABLE 5

INTERACTION PARAMETERS FOR VARIOUS SYSTEMS INVOLVING CARBON DIOXIDE AT 298.15 K

i	j	δ_{ij}
N-Methyl Pyrrolidone	CO_2	0.0787
Propylene Carbonate	CO_2	0.4150
Selexol	CO_2	-0.0631
Methanol	CO_2	-0.1389
Methyl Cyanoacetate	CO_2	0.1265
N-Formyl Morpholine	CO_2	-0.0821
Toluene	CO_2	0.1020 0.1526*

* This value is at 308.15 K

CHAPTER VII

CONCLUSIONS

We were able to achieve an acceptable operation of all the components of the isothermal flow calorimeter, including the flow system, for the determination of the enthalpy of mixing at high pressure.

The collection of the enthalpy of mixing data for systems involving CO_2 was a challenging task, involving a number of factors that one has to control in order to obtain meaningful results.

Enthalpies of mixing for various (CO_2 + Physical Solvent) systems were measured at 298.15 K and pressures ranging from 7.5 to 12.6 MPa.

All the (CO_2 + Physical Solvent) systems showed exothermic enthalpy of mixing throughout the entire composition range. This was not the case for the (CO_2 + Toluene) system. The only exception was the (CO_2 + Methanol) system which in the CO_2 rich region of the enthalpy of mixing curve exhibited an endothermic effect.

The effect of pressure on the enthalpy of mixing followed the same trend for all the systems in which physical solvents were involved. We noticed that the largest value of the enthalpy of mixing occured at the lowest pressure of those studied. As the pressure was increased, the magnitude of the enthalpy of mixing decreased. This can be explained in terms of the changes in various fluid properties of CO_2 near its critical point.

The presence of water in the solvents has an effect on the enthalpy of mixing. The modeling of such systems should be done taking into account all the binaries formed: CO_2-solvent, CO_2-H_2O, and H_2O-solvent.

A comparison of the experimental enthalpy of mixing data with those predicted by the Peng-Robinson equation of state was made. The equation reproduces for most of the solvents studied the main features observed but gives an approximate fit only.

So far, we were able to study the effect of pressure on the enthalpy of mixing at 298.15 K for several systems involving CO_2. Some more work remains to be done, such as the study of simultaneous effect of temperature and pressure on the enthalpy of mixing.

REFERENCES

1. American Petroleum Institute.
Technical Data Book. Petroleum Refining. (*Volume 1*).
Fourth Edition.
Washington, D.C.
1983.

2. Astarita, G.; Savage, D.W.; and Bisio, A.
Gas Treating with Chemical Solvents.
John Wiley & Sons.
1983.

3. Christensen, J.J.; Zebolsky, D.M.; and Izatt, R.M.
The excess enthalpies of (carbon dioxide + toluene) at 470.15 and 573.15 K from 7.60 to 12.67 MPa.
J. Chem. Thermodynamics *1985, 17, 1-10.*

4. Christensen, J.J.; Walker, T.A.C.; Schofield, R.S.; Faux, P.W.; Harding, P.R.; and Izatt, R.M.
The excess enthalpies of (carbon dioxide + hexane) at 308.15, 358.15, and 413.15 K from 7.50 to 12.50 MPa.
J. Chem. Thermodynamics *1984, 16, 445-451.*

5. Christensen, J.J.; Christensen, S.P.; Schofield, R.S.; Faux, P.W.; Harding, P.R.; and Izatt, R.M.
The excess enthalpies of (carbon dioxide + cyclohexane) at 308.15, 358.15, and 413.15 K from 7.50 to 12.50 MPa.
J. Chem. Thermodynamics *1983, 15, 1151-1157.*

6. Christensen, J.J.; Christensen, S.P.; Schofield, R.S.; Faux, P.W.; Harding, P.R.; and Izatt, R.M.
The excess enthalpies of (carbon dioxide + pyridine) at 308.15, 358.15, and 413.15 K from 7.50 to 12.50 MPa.
J. Chem. Thermodynamics *1984, 16, 249-255.*

7. Christensen, J.J.; Faux, P.W.; Cordray, D.; and Izatt, R.M.
The excess enthalpies of (carbon dioxide + pentane) at 348.15, 373.15, 413.15, 470.15, and 573.15 K from 7.58 to 12.45 MPa.
J. Chem. Thermodynamics *1986, 18, 1053-1064.*

8. Christensen, J.J.; Cordray, D.R.; Izatt, R.M.
The excess enthalpies of (carbon dioxide + decane) from 293.15 to 573.15 K at 12.50 MPa.
J. Chem. Thermodynamics *1986, 18, 53-61.*

9. Christensen, J.J.; Walker, T.A.C.; Cordray, D.R.; and Izatt, R.M.
The excess enthalpies of (carbon dioxide + cyclohexane) at 470.15, 553.15, and 573.15 K from 7.50 to 12.50 MPa.
J. Chem. Thermodynamics *1987, 19, 47-56.*

10. Christensen, J.J.; Zebolsky, D.M.; and Izatt, R.M.
The excess enthalpies of (carbon dioxide + pyridine) at 470.15 and 573.15 K from 7.50 to 12.50 MPa.
J. Chem. Thermodynamics 1985, 17, 785-795.

11. Christensen, J.J.; Zebolsky, D.M.; and Izatt, R.M.
The excess enthalpies of (carbon dioxide + hexane) at 470.15, 510.15, and 573.15 K from 7.50 to 12.50 MPa.
J. Chem. Thermodynamics 1985, 17, 183-192.

12. Christensen, J.J.; Izatt, R.M.; Eatough, D.J.; and Hansen, L.D.
The effect of pressure on the excess enthalpies of cyclohexane + n-hexane at 298.15 K.
J. Chem. Thermodynamics 1978, 10, 25-34.

13. Christensen, J.J.; Hansen, L.D.; Eatough, D.J.; Izatt, R.M.; and Hart, R.M.
Isothermal high pressure flow calorimeter.
Rev. Sci. Instrum. 1976, 47, 730-734.

14. Christensen, J.J.; Hansen, L.D.; Izatt, R.M.; Eatough, D.J.; and Hart, R.M.
Isothermal, isobaric, elevated temperature, high pressure, flow calorimeter.
Rev. Sci. Instrum. 1981, 52, 1226-1231.

15. Christensen, J.J. and Izatt, R.M.
An isothermal flow calorimeter designed for high temperature, high pressure operation.
Thermochim. Acta 1984, 73, 117-129.

16. Christensen, J.J.; Johnston, H.D.; and Izatt, R.M.
An isothermal titration calorimeter.
Rev. Sci. Instrum. 1968, 39, 1356-1359.

17. Christensen, J.J.; Gardner, J.W.; Eatough, D.J.; Izatt, R.M.; Watts P.J.; and Hart, R.M.
An isothermal titration microcalorimeter.
Rev. Sci. Instrum. 1973, 44, 481-484.

18. Cinelli, E.; Noe, S.; and Paret, G.
Extract Aromatics with FM.
Hydrocarbon Processing 1972, 51(4), 141-144.

19. Cordray, D.R.; Christensen, J.J.; and Izatt, R.M.
The excess enthalpies of (carbon dioxide + toluene) at 308.15, 358.15, and 573.15 K from 6.98 to 16.63 MPa.
J. Chem. Thermodynamics 1986, 18, 647-656.

20. Cordray, D.R.; Izatt, R.M.; and Christensen, J.J.
The excess enthalpies of (carbon dioxide + cyclohexane) at 390.15, 413.15, 438.15, 498.15, and 508.15 K from 7.50 to 14.39 MPa.
J. Chem. Thermodynamics 1988, 20, 225-234.

21. Faux, P.W.; Christensen, J.J.; Izatt, R.M.; Pando, C.; and Renuncio, J.A.R.
The excess enthalpies of (carbon dioxide + n-hexane + toluene) at 413.15 K and 7.50 and 12.50 MPa.
J. Chem. Thermodynamics 1988, 20, 503-512.

22. Freyer, E.B.; Hubbard, J.C.; and Andrews, D.H.
Sonic Studies of the Physical Properties of Liquids.
J. Am. Chem. Soc. 1929, 51, 759-770.

23. *Gas Conditioning Fact Book.*
The Dow Chemical Company.
Midland, Michigan.
1962.

24. Goodwin, R.D.
Methanol Thermodynamic Properties from 176 to 673 K at Pressures to 700 Bar.
J. Phys. Chem. Ref. Data 1987, 16(4), 799-892.

25. *Handbook of Chemistry and Physics.*
The Chemical Rubber Company.
63rd. Edition.
Boca Raton, Florida.
1982-1983.

26. Hong, C.S.; Wakslak, R.; Finston, H.; and Fried, V.
Some Thermodynamic Properties of Systems containing Propylene Carbonate and Ethylene Carbonate.
J. Chem. Eng. Data 1982, 27, 146-148.

27. *International Thermodynamic Tables of the Fluid State. Carbon Dioxide.*
IUPAC.
Pergamon Press.
Oxford, 1976.

28. *ISCO LC-5000 Syringe Pump Manual.*
ISCO, Inc.
Lincoln, Nebraska.
1986.

29. *ISCO Model 314 Metering Pump Manual.*
ISCO, Inc.
Lincoln, Nebraska.
1983.

30. Kneisl, P. and Zondlo, J.W.
Vapor Pressure, Liquid Density, and the Latent Heat of Vaporization as Functions of Temperature for Four Dipolar Aprotic Solvents.
J. Chem. Eng. Data 1987, 32, 11-13.

31. McCullough, J.P. and Scott, D.W.
Experimental Thermodynamics. (Volume I)
Butterworths.
London, 1968.

32. Michaeli, W.; Stein, W.H.; and Unland, H.
Das SELEXOL Verfahren Ein Beitrag zur selektiven Aufbereitung von saurem Erdgas.
Erdoel Erdgas Zeitschrift 1975, 91, 341-347.

33. Murrieta-Guevara, F. and Trejo Rodriguez, A.
Liquid Density as a Function of Temperature of Five Organic Solvents.
J. Chem. Eng. Data 1984, 29, 204-206.

34. Panagiotopoulos, A.Z. and Kumar, S.K.
A Generalized Technique to obtain Pure Component Parameters for two-parameter Equations of State.
Fluid Phase Equilibria 1985, 22, 77-88.

35. Pando, C.; Renuncio, J.A.R.; Schofield, R.S.; Izatt, R.M.; and Christensen, J.J.
The excess enthalpies of (carbon dioxide + toluene) at 308.15, 385.15, and 413.15 K from 7.60 to 12.67 MPa.
J. Chem. Thermodynamics 1983, 15, 747-755.

36. Pando, C.; Renuncio, J.A.R.; Izatt, R.M.; and Christensen, J.J.
The excess enthalpies of (carbon dioxide + pentane) at 308.15 and 323.15 K from 7.58 to 12.45 MPa.
J. Chem. Thermodynamics 1983, 15, 259-266.

37. Pando, C.; Renuncio, J.A.R.; McFall, T.A.; Izatt, R.M.; and Christensen, J.J.
The excess enthalpies of (carbon dioxide + decane) from 283.15 to 323.15 K at 7.58 MPa.
J. Chem. Thermodynamics 1983, 15, 173-180.

38. Peng, D.Y. and Robinson, D.B.
A New Two-Constant Equation of State.
Ind. Eng. Chem. Fundam. 1976, 15, 59-64.

39. Reid, R.C.; Prausnitz, J.M.; and Poling, B.E.
The Properties of Gases and Liquids.
McGraw Hill Book Company.
Fourth Edition.
1987.

40. Roberts, B.E.
M.Sc. Thesis. University of Alberta.
Edmonton, Alberta.
1983.

41. *SELEXOL Solvent Process.*
Norton Chemical Process Products.
Morristown, New Jersey.
1983.

42. Spiegel, M.R.
Mathematical Handbook of Formulas and Tables.
McGraw Hill Book Company.
1968.

43. *Tescom 26-3200 Series Back Pressure Regulator Catalog.*
Tescom Corporation.
Minneapolis, Minnesota.

44. *Tronac Model 1250 Calorimeter Manual.*
Tronac, Inc.
Orem, Utah.
1981.

45. Vetere, A.; De Simone, R.; and Ginnasi, A.
Methods of Estimation of Vapor-Liquid Equilibria for Multicomponent Systems. Application to the C_4 Hydrocarbons-Formylmorpholine-Water Systems.
Ind. Eng. Chem. Process Des. Dev. 1975, 14, 141-146.

46. Wallis, K.P.; Clancy, P.; Zollweg, J.A.; and Streett, W.B.
Excess thermodynamic properties for $\{xCO_2+(1-x)C_2H_6\}(l)$: experiment and theory.
J. Chem. Thermodynamics 1984, 16, 811-823.

47. Wolfer, W.
Helpful hints for Physical Solvent Absorption.
Hydrocarbon Processing 1982, 61(11), 193-197.

48. Wormald, C.J. and Eyears, J.M.
Excess molar enthalpies and excess molar volumes of $\{xCO_2+(1-x)C_6H_5CH_3\}$ at 298.15, 304.10, and 308.15 K from 7.5 to 12.6 MPa.
J. Chem. Thermodynamics 1987, 19, 845-856.

49. Wormald, C.J. and Eyears, J.M.
Excess molar enthalpies and excess molar volumes of $\{xCO_2+(1-x)C_2H_6\}$ up to 308.4 K and 11.0 MPa.
J. Chem. Thermodynamics 1988, 20, 323-331.

50. Wormald, C.J.
Heats and Volumes of Mixing in the Critical Region. An exploration using the Van der Waals Equation.
Fluid Phase Equilibria 1986, 28, 137-153.

APPENDIX I

PHYSICAL PROPERTIES

All the physical properties required for the computation of the enthalpy of mixing are given below. The properties are grouped by solvent and start with those for CO_2. A list of the Chemical Abstracts Registry Numbers for the solvents is provided on Table A1.2 at the end of this appendix.

The density of the solvents was corrected due to the effect of pressure by means of the isothermal compressibility. The isothermal compressibility, β_T , is defined as:

$$\beta_T = -\frac{1}{V}\left(\frac{\partial V}{\partial P}\right)_T \qquad \text{(A1.1)}$$

which can be approximated as:

$$\beta_T = -\left(\frac{d\ln V}{dP}\right)_T \qquad \text{(A1.2)}$$

Next, if we integrate equation (A1.2) we obtain:

$$\beta_T(P_2 - P_1) = \ln\left(\frac{V_1}{V_2}\right) \qquad \text{(A1.3)}$$

where: P_1 = Atmospheric Pressure. (101325.0 Pa)

P_2 = Pressure at which the density is to be evaluated.

V_1 = Specific volume of solvent at P_1.

V_2 = Specific volume of solvent at P_2.

We can obtain from equation (A1.3) V_2, and from V_2 the density.

The estimation of constants a and b of the Peng-Robinson equation of state required saturated liquid density and vapour pressure data. The references from which this data was taken are listed in table A1.1.

A) CO_2.

- Density.

The density of CO_2 was interpolated at 6°C from the IUPAC tables [27]. The values obtained from the interpolation were:

7.5 MPa ρ = 0.923 g/cm^3

10.6 MPa ρ = 0.946 g/cm^3

12.6 MPa ρ = 0.958 g/cm^3

B) N-Methyl Pyrrolidone.

- Density.

ρ = 1.023 g/cm^3 at 25°C, from Reference [25].

This value now has to be corrected for the effect of pressure using the isothermal compressibility. After this correction the density of the N-Methyl Pyrrolidone becomes:

7.5 MPa ρ = 1.027 g/cm^3

10.6 MPa ρ = 1.028 g/cm^3

12.6 MPa ρ = 1.029 g/cm^3

- Isothermal Compressibility.

β_T = 4.67 x 10^{-10} m^2/N at 25°C, from Reference [25].

No specific value of the isothermal compressibility for N-Methyl Pyrrolidone was found. The value of β_T reported here was obtained by analogy to the data for Aniline given in the same reference.

C) Propylene Carbonate.

- Density.

ρ = 1.189 g/cm^3 at 25°C, from Aldrich Chemicals.

Once this value is corrected for the effect of pressure, we obtain:

7.5 MPa	ρ = 1.192 g/cm^3
10.6 MPa	ρ = 1.194 g/cm^3
12.6 MPa	ρ = 1.195 g/cm^3

- Isothermal Compressibility.

β_T = 3.72 x 10^{-10} m^2/N at 25°C, from Reference [25].

No specific value of the isothermal compressibility for Propylene Carbonate was found. The value of β_T reported here was obtained by analogy to the data for Glycol given in the same refernce.

D) Selexol.

- Density (0.83 % weight of H_2O).

ρ = 1.027 g/cm^3 at 25°C, from Reference [41].

The correction of this value of density due to the effect of pressure yields:

7.5 MPa	ρ = 1.030 g/cm^3
10.6 MPa	ρ = 1.031 g/cm^3
12.6 MPa	ρ = 1.032 g/cm^3

- Density (3.62 % weight of H_2O).

ρ = 1.026 g/cm^3 at 25°C was estimated from the value for the mixture containing 0.83 % weight of H_2O, and considering no change in volume upon mixing. The densities at different pressures are:

7.5 MPa ρ = 1.029 g/cm^3

10.6 MPa ρ = 1.030 g/cm^3

12.6 MPa ρ = 1.031 g/cm^3

- Isothermal Compressibility.

β_T = 3.72 x 10^{-10} m^2/N at 25°C, from Reference [25].

No specific value of the isothermal compressibility for Selexol was found. The value of β_T reported here was obtained by analogy to the data for Glycol given in the same reference.

E) Methanol.

- Density.

ρ = 0.7865 g/cm^3 at 25°C, from Reference [22].

Once this value is corrected for the effect of pressure using the isothermal compressibility, we obtain:

7.5 MPa ρ = 0.794 g/cm^3

10.6 MPa ρ = 0.797 g/cm^3

12.6 MPa ρ = 0.799 g/cm^3

- Isothermal Compressibility.

β_T = 12.58 x 10^{-10} m^2/N at 25°C, from Reference [22].

F) Methyl Cyanoacetate.

- Density.

ρ = 1.1026 g/cm^3 at 25°C, extrapolated from the values at 15°C and 20°C given by Aldrich Chemicals and Reference [25], respectively. The correction of the density for the effect of pressure yields:

7.5 MPa ρ = 1.112 g/cm^3

10.6 MPa ρ = 1.116 g/cm^3

12.6 MPa ρ = 1.119 g/cm^3

- Isothermal Compressibility.

β_T = 11.84 x 10^{-10} m^2/N at 25°C, from Reference [25].

No specific value of the isothermal compressibility for Methyl Cyanoacetate was found. The value of β_T reported here was obtained by analogy to the data for Ethyl acetate given in the same reference.

G) N-Formyl Morpholine.

- Density.

ρ = 1.144 g/cm^3 at 25°C, determined experimentally using a Sodev high precision flow densimeter. Once this value is corrected for the effect of pressure we obtain:

7.5 MPa ρ = 1.148 g/cm^3

- Isothermal Compressibility.

β_T = 4.67 x 10^{-10} m^2/N at 25°C, from Reference [25].

No specific value of the isothermal compressibility for N-Formyl Morpholine was found. The value of β_T reported here was obtained by analogy to the data for Aniline given in the same reference.

H) Toluene.

- Density.

ρ = 0.861 g/cm^3 at 25°C, from Reference [22].

ρ = 0.852 g/cm^3 at 35°C, from Reference [22].

The correction of these values due to the effect of pressure yields:

25°C

7.5 MPa ρ = 0.867 g/cm^3

10.6 MPa ρ = 0.868 g/cm^3

35°C

10.6 MPa ρ = 0.861 g/cm^3

- Isothermal Compressibility.

β_T = 9.28 x 10^{-10} m^2/N at 25°C, from Reference [25].

β_T = 9.97 x 10^{-10} m^2/N at 35°C, from Reference [25].

I) Cyclohexane.

- Density.

ρ = 0.779 g/cm^3 at 20°C, from Reference [25].

Once this value is corrected for the effect of pressure we obtain:

7.0 MPa ρ = 0.785 g/cm^3

14.0 MPa ρ = 0.791 g/cm^3

- Isothermal Compressibility.

β_T = 11.40 x 10^{-10} m^2/N at 25°C, from Reference [25].

J) n-Hexane.

- Density.

ρ = 0.660 g/cm^3 at 20°C, from Reference [25].

Once this value is corrected for the effect of pressure we obtain:

7.0 MPa ρ = 0.668 g/cm^3

14.0 MPa ρ = 0.676 g/cm^3

- Isothermal Compressibility.

β_T = 16.72 x 10^{-10} m^2/N at 25°C, from Reference [25].

TABLE A1.1

References for Vapour Pressure and Density Data for various Solvents.

Solvent	Density	Vapour Pressure
N-Methyl Pyrrolidone	[30] [33]	[30] [47]
Propylene Carbonate	[23] [33]	[23] [26]
Selexol	[32] [41] [47]	[47]
Methanol	[24]	[24]
Methyl Cyanoacetate	[25]	*
N-Formyl Morpholine	[18]	[18] [45]
Toluene+	[1]	[1]

* Data obtained from Aldrich Chemicals.
+ Not experimental data; it was calculated with the equations given in this reference.

TABLE A1.2

Chemical Abstracts Registry Number
for various Solvents.

Solvent	Registry No.
N-Methyl Pyrrolidone	872-50-4
Propylene Carbonate	108-32-7
Selexol	24991-55-7
Methanol	67-56-1
Methyl Cyanoacetate	105-34-0
N-Formyl Morpholine	4394-85-8
Toluene	108-88-3

APPENDIX II

SAMPLE CALCULATION

The sample calculation shown below corresponds to the experimental run of (CO_2+Methanol) at 298.15 K and 10.6 MPa.

A) Physical Properties.

The physical properties of CO_2 and methanol can be obtained from Appendix I. The densities at these conditions of pressure and temperature are:

ρ = 0.946 g/cm^3 for CO_2.

ρ = 0.797 g/cm^3 for methanol.

The molecular weights are:

MW = 44.01 g/mol for CO_2.

MW = 32.04 g/mol for methanol.

B) Experimental Data.

The data collected throughout the run is shown in Table A2.1.

C) Determination of the Power of the Calibration Heater.

The heating power of the calibration heater is calculated by the equation:

$$W = (HTRI \times HTRV)/R_s \qquad (A2.1)$$

where W is the power in Watts, HTRI and HTRV are voltage readings taken during the experimental run, and R_s is the resistance in ohms of the standard resistor connected to the heater.

The readings for this run were:

HTRI = 2.9538 V

HTRV = 2.9433 V

R_s = 100.03 Ω

therefore, the power is:

$$W = (2.9538)(2.9433)/(100.03) = 0.086913 \text{ J/s}$$

Next, we determine the energy per count using the following equation:

$$E = W/\{(C_b + C_a)/2 - C_h\} \qquad (A2.2)$$

where E is the energy per count, W is the heating power of the calibration heater, C_b is the number of counts per second before the heater is turned on, C_a is the number of counts per second after the heater is turned off, and C_h is the number of counts per second while the heater is on.

From Table A2.1 we have:

C_b = 21475.52 counts/s

C_a = 21461.31 counts/s

C_h = 8775.03 counts/s

Hence, the energy per count is:

$$E = 0.086913/(21468.41 - 8775.03) = 6.847108 \times 10^{-6} \text{ (J/s)/count}$$

D) Determination of the Enthalpy of Mixing.

In order to obtain the enthalpy of mixing from the data shown in Table A2.1 we have to perform the following calculations:

- Molar Flow Rates.

The molar flow rates for both CO_2 and methanol are given by:

$$M = v\rho/MW \qquad (A2.3)$$

where M is the molar flow rate in mol/s, v is the volumetric flow rate in ml/s, ρ is the density in g/cm^3, and MW the molecular weight. Hence, if we take the data for the point where we have 5% of CO_2 and 95% of methanol by volume we have:

Total volumetric flow rate = 0.4 ml/min

For CO_2:

$v = (0.4\ ml/min)\ (0.05)\ (1/60) = 3.333 \times 10^{-4}$ ml/s

For methanol:

$v = (0.4\ ml/min)\ (0.95)\ (1/60) = 6.333 \times 10^{-3}$ ml/s

The correction of the volumetric flow rates with equation (A3.1) gives:

$v = 3.362 \times 10^{-4}$ ml/s for CO_2

$v = 6.554 \times 10^{-3}$ ml/s for methanol

Now we are able to determine the molar flow rates and the mole fractions:

For CO_2:

$M = (3.362 \times 10^{-4})(0.946)/(44.01) = 7.22 \times 10^{-6}$ mol/s

For methanol:

$M = (6.554 \times 10^{-3})(0.797)/(32.04) = 1.63 \times 10^{-4}$ mol/s

Total molar flow rate = 1.702×10^{-4} mol/s

Mole fraction for CO_2:

$$x = \frac{7.220 \times 10^{-6}\ mol/s}{1.702 \times 10^{-4}\ mol/s} = 0.042$$

Mole fraction for methanol:

$$x = \frac{1.630 \times 10^{-4}\ mol/s}{1.702 \times 10^{-4}\ mol/s} = 0.958$$

- Enthalpy of Mixing.

The heat involved in the interaction is given by:

$$Q = (C_e - C_{bla})(E) \qquad (A2.4)$$

where Q is the heat of the interaction in J/s, E is the energy per count in (J/s)/count, C_e is the average number of counts per second at the point where the enthalpy of mixing is going to be determined, and C_{bla} is given by:

$$C_{bla} = (C_{bls} + C_{ble})/2 \qquad (A2.5)$$

where C_{bls} and C_{ble} are the counts per second for the base line at the begining and at the end of the run, respectively.

From Table A2.1:

C_e = 18949.33

C_{bls} = 21461.31

C_{ble} = 21708.00

and C_{bla} can be calculated:

C_{bla} = 21584.65

therefore, the heat of the interaction is:

$$Q = (18949.33 - 21584.65)\ (6.847108 \times 10^{-6}) = -1.80443 \times 10^{-2}\ J/s$$

The enthalpy of mixing is obtained dividing the heat of the interaction by the total molar flow rate:

$$H^E = \frac{-1.80443 \times 10^{-2}\ J/s}{1.702 \times 10^{-4}\ mol/s} = -106.0\ J/mol$$

The same procedure outlined above is followed for the determination of the enthalpy of mixing for each one of the remaining points in Table A2.1.

Figure 33 shows the plot obtained from the chart recorder. All the points shown correspond to those given in Table A2.1.

TABLE A2.1

Basic Experimental Data for the System (CO_2 + Methanol)

Point	% vol CO_2	% vol Methanol	Average Number of Counts
1	0.0	100.0	21475.52[1]
2	0.0	100.0	8775.03[2]
3	0.0	100.0	21461.31[3]
4	5.0	95.0	18949.33
5	10.0	90.0	16612.70
6	20.0	80.0	12703.70
7	30.0	70.0	9952.63
8	40.0	60.0	8959.40
9	50.0	50.0	9784.73
10	60.0	40.0	11766.27
11	70.0	30.0	14642.37
12	80.0	20.0	18168.63
13	90.0	10.0	22229.17
14	95.0	5.0	23875.37
15	100.0	0.0	21708.00[4]

[1] Counts before heater is turned on.
[2] Counts while heater is on.
[3] Counts after heater is turned off and for the base line at the beginning of the run.
[4] Counts for the base line at the end of the run.

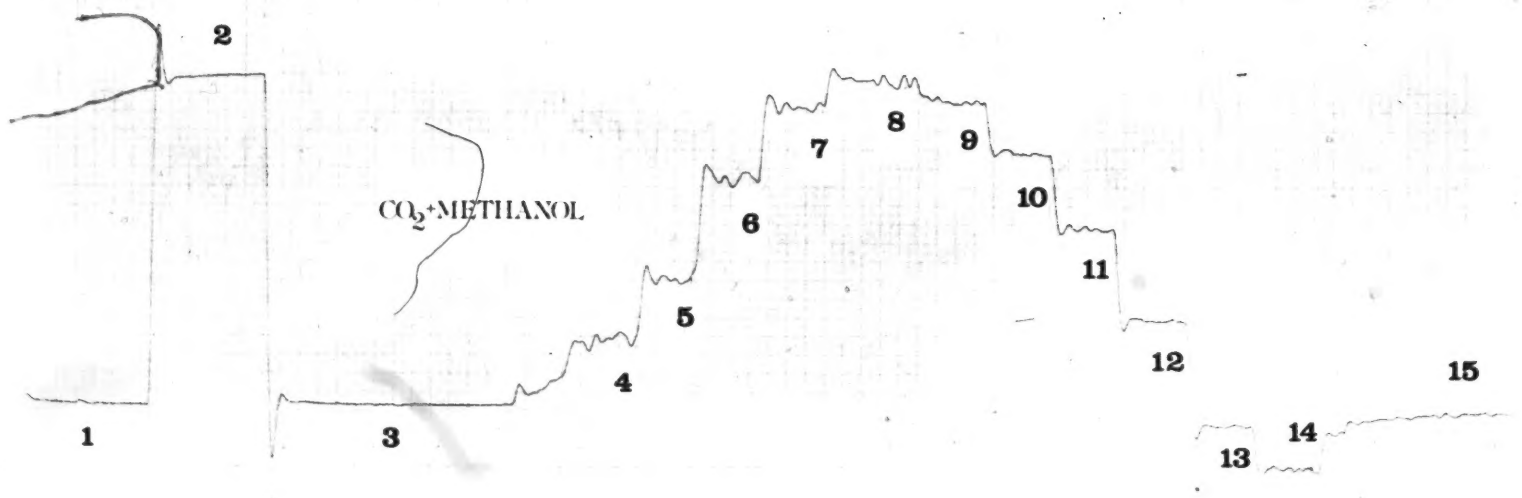

Figure 33. Chart Recorder Output.

APPENDIX III

CALIBRATION OF PUMPS

The syringe pumps, LC-5000 and 314, were calibrated in the flow rate range employed to obtain the experimental data. Once the total flow rate to be used during the course of an experimental run is known, the appropriate setting of the two knobs in each of the pumps which regulate the flow rate can be determined.

All the experimental runs throughout this work were carried out at a total flow rate of 0.4 ml/min (24 ml/h), and the settings selected for each of the pumps were:

LC-5000	15 ml/h and 40 ml/h	(0-100%)
314	8 ml/h and 20 ml/h	(0-100%)

For the calibration, the LC-5000 and 314 pumps were filled with cyclohexane and n-hexane, respectively. The liquid was collected in a clean, dry and previously weighed bottle. Liquid was allowed to flow for a period of time long enough for an accurate determination of its mass. The time allowed for this was precisely measured with the aid of a stopwatch. The weight of the liquid collected enables us to determine, along with the elapsed time, the actual flow rate delivered by the pump.

This procedure was repeated several times for all the settings selected for each pump. The flow rates determined in different calibrations were averaged and doing a least squares fit, equations for correcting the nominal flow rates were obtained.

The results are shown in Tables A3.1 to A3.3.

TABLE A3.1

Calibration of the ISCO LC-5000 Syringe Pump.

Pump Settings	Nominal Flow Rate (ml/min)	Calibration 1 (ml/min)	Calibration 2 (ml/min)	Calibration 3 (ml/min)	Calibration 4 (ml/min)	Mean (ml/min)	Standard Deviation
15 ml/h 25 %	0.0625	0.0604	0.0632	0.0625	0.0615	0.0619	0.0012
15 ml/h 50 %	0.1250	0.1273	0.1257	0.1254	0.1261	0.1261	0.0008
15 ml/h 75 %	0.1875	0.1891	0.1887	0.1874	0.1896	0.1887	0.0010
15 ml/h 100 %	0.2500	0.2529	0.2506	0.2500	0.2518	0.2513	0.0013
40 ml/h 25 %	0.1667	0.1694	0.1631	0.1639	0.1656	0.1655	0.0028
40 ml/h 50 %	0.3333	0.3325	0.3369	0.3298	0.3315	0.3327	0.0030
40 ml/h 75 %	0.5000	0.5004	0.5047	0.4992	0.5008	0.5013	0.0024
40 ml/h 100 %	0.6667	0.6606	0.6693	0.6703	0.6663	0.6666	0.0044

TABLE A3.2

Calibration of the ISCO 314 Syringe Pump

Pump Settings	Nominal Flow Rate (ml/min)	Calibration 1 (ml/min)	Calibration 2 (ml/min)	Calibration 3 (ml/min)	Mean (ml/min)	Standard Deviation
8 ml/h 25 %	0.0333	0.0350	0.0359	0.0343	0.0351	0.0008
8 ml/h 50 %	0.0667	0.0710	0.0702	0.0677	0.0696	0.0017
8 ml/h 75 %	0.1000	0.1049	0.1067	0.1023	0.1046	0.0023
8 ml/h 100 %	0.1333	0.1388	0.1393	0.1367	0.1382	0.0014
20 ml/h 25 %	0.0833	0.0846	0.0875	0.0856	0.0859	0.0015
20 ml/h 50 %	0.1667	0.1728	0.1730	0.1725	0.1728	0.0003
20 ml/h 75 %	0.2500	0.2608	0.2606	0.2610	0.2608	0.0002
20 ml/h 100 %	0.3333	0.3435	0.3443	0.3436	0.3438	0.0004

The equations obtained for correcting the nominal flow rates in each pump are of the type:

$$y = A_1 + A_2 x \qquad \text{(A3.1)}$$

where: y = corrected flow rate (ml/min)

x = nominal flow rate (ml/min)

The values of the coefficients A_1 and A_2 for each pump are given in Table A3.3.

TABLE A3.3

Coefficients for the correction of the Flow Rate by Equation (A3.1)

Pump	A_1	A_2
ISCO LC-5000	0.16388×10^{-3}	1.0005
ISCO 314	0.71976×10^{-3}	1.0329

APPENDIX IV

EXPERIMENTAL AND CALCULATED DATA

TABLE A4.1

Enthalpy of Mixing of (Cyclohexane + n-Hexane)
at 298.15 K and 0.1, 7.0, and 14.0 MPa

0.1 MPa		7.0 MPa		14.0 MPa	
x cyclohexane	H^E exp. (J/mol)	x cyclohexane	H^E exp. (J/mol)	x cyclohexane	H^E exp. (J/mol)
(0.128)	(29.9)	(0.144)	(31.6)	(0.212)	(30.2)
0.205	108.0	0.206	113.7	(0.272)	(93.9)
0.280	146.8	0.266	145.0	0.359	175.6
0.353	176.3	0.324	170.1	0.416	192.8
0.425	199.4	0.382	187.4	0.472	204.4
0.460	208.4	0.438	202.4	0.527	212.9
0.494	215.3	0.466	206.5	0.553	215.8
0.528	219.9	0.520	213.1	0.580	215.6
0.562	222.6	0.547	216.4	0.606	214.6
0.595	224.0	0.574	216.4	0.632	211.0
0.628	223.5	0.652	212.9	0.658	205.0
0.660	221.1	0.702	202.5	0.709	192.6
0.723	208.3	0.752	190.1	0.734	184.6
0.785	185.7	0.801	167.7	0.759	176.0
0.846	152.1	0.849	136.2	0.807	151.9
0.904	90.5	0.896	95.9	0.855	122.6
0.933	40.0	0.919	53.1	0.879	106.1
0.962	7.8	0.942	10.7	0.902	79.7

TABLE A4.2

Comparison of Calculated and Experimental Enthalpy of Mixing of (CO_2 + Toluene) at 298.15 and 308.15 K and 10.6 MPa

298.15 K			308.15 K		
x CO_2	H^E exp. (J/mol)	H^E calc. (J/mol)	x CO_2	H^E exp. (J/mol)	H^E calc. (J/mol)
0.196	218.8	221.2	0.105	75.3	78.6
0.279	284.7	282.6	0.197	128.9	140.9
0.354	315.0	315.2	0.356	212.2	179.7
0.484	341.0	341.1	0.486	97.4	120.2
0.593	302.0	299.4	0.595	2.2	9.0
0.686	224.6	227.6	0.688	-110.8	-114.5
0.766	140.6	142.0	0.767	-215.1	-221.5
0.836	58.0	57.1	0.837	-286.4	-296.7
0.897	-7.4	-10.6	0.868	-318.2	-315.9
0.951	-44.4	-41.8	0.898	-330.0	-319.9
			0.951	-266.9	-261.9
			0.976	-166.4	-174.6

TABLE A4.3

Comparison of Calculated and Experimental Enthalpy of Mixing of (CO_2 + Toluene) at 298.15 K and 7.5 MPa

x CO_2	H^E exp. (J/mol)	H^E calc. (J/mol)
0.103	76.6	67.0
0.194	138.9	150.8
0.351	234.6	244.3
0.480	259.5	213.5
0.590	59.4	104.2
0.683	-29.8	-28.5
0.763	-135.6	-148.2
0.834	-225.7	-235.0
0.866	-258.7	-261.1
0.896	-281.6	-274.7
0.924	-283.9	-274.6
0.950	-253.6	-259.2

TABLE A4.4

Comparison of Calculated and Experimental Enthalpy of Mixing of (CO_2 + N-Methyl Pyrrolidone) at 298.15 K and 7.5, 10.6, and 12.6 MPa

7.5 MPa			10.6 MPa			12.6 MPa		
x CO_2	H^E exp. (J/mol)	H^E calc. (J/mol)	x CO_2	H^E exp. (J/mol)	H^E calc. (J/mol)	x CO_2	H^E exp. (J/mol)	H^E calc. (J/mol)
0.179	-554.6	-529.2	0.183	-429.8	-420.5	0.185	-430.2	-412.3
0.329	-933.3	-947.6	0.334	-791.5	-798.7	0.337	-738.0	-756.9
0.456	1234.7	-1257.9	0.462	-1073.5	-1082.5	0.465	-1002.8	-1009.5
0.566	-1472.9	-1466.8	0.572	-1264.6	-1258.2	0.575	-1170.0	-1164.6
0.662	-1591.4	-1579.4	0.667	-1335.6	-1326.9	0.670	-1244.4	-1223.6
0.705	-1613.9	-1599.8	0.710	-1334.4	-1322.5	0.752	-1185.8	-1188.3
0.746	-1605.2	-1595.3	0.750	-1276.7	-1292.7	0.825	-1038.6	-1057.8
0.820	-1482.0	-1503.9	0.823	-1149.9	-1156.8	0.890	-825.7	-827.4
0.886	-1262.1	-1275.7	0.889	-919.1	-913.1	0.947	-498.8	-484.9
0.946	-856.7	-840.6	0.947	-542.1	-544.8			
			0.974	-306.4	-302.3			

TABLE A4.5

Comparison of Calculated and Experimental Enthalpy of Mixing of (CO_2 + Propylene Carbonate) at 298.15 K and 7.5, 10.6, and 12.6 MPa

7.5 MPa			10.6 MPa			12.6 MPa		
x CO_2	H^E exp. (J/mol)	H^E calc. (J/mol)	x CO_2	H^E exp. (J/mol)	H^E calc. (J/mol)	x CO_2	H^E exp. (J/mol)	H^E calc. (J/mol)
0.162	-363.6	-359.0	0.165	-271.6	-273.0	0.167	-304.9	-299.3
0.367	-902.9	-904.0	0.308	-571.0	-570.8	0.311	-560.3	-566.1
0.537	-1275.5	-1291.6	0.433	-799.6	-799.6	0.435	-751.4	-751.8
0.634	-1408.1	-1401.7	0.542	-997.4	-999.8	0.545	-941.7	-947.5
0.679	-1397.2	-1405.7	0.640	-1091.2	-1093.4	0.643	-1024.7	-1023.0
0.722	-1420.7	-1374.2	0.685	-1107.1	-1102.2	0.687	-1036.3	-1031.3
0.802	-1170.0	-1203.7	0.727	-1095.8	-1085.0	0.729	-1032.6	-1018.1
0.907	-624.3	-622.7	0.805	-977.0	-971.3	0.807	-922.7	-923.5
0.970	-320.4	-324.4	0.876	-709.0	-752.5	0.877	-696.5	-730.5
			0.940	-426.5	-430.6	0.941	-428.4	-429.6
			0.970	-304.7	-231.9	0.971	-282.8	-234.7

TABLE A4.6

Comparison of Calculated and Experimental Enthalpy of Mixing of (CO_2 + Selexol)* at 298.15 K and 7.5, 10.6, and 12.6 MPa

7.5 MPa			10.6 MPa			12.6 MPa		
w CO_2	H^E exp. (J/g)	H^E calc. (J/g)	w CO_2	H^E exp. (J/g)	H^E calc. (J/g)	w CO_2	H^E exp. (J/g)	H^E calc. (J/g)
0.088	-5.7	-4.7	0.045	-2.3	-2.0	0.091	-5.9	5.9
0.178	-10.2	-11.1	0.090	-4.4	-4.2	0.184	-11.8	11.8
0.271	-17.1	-17.5	0.182	-8.4	-8.9	0.278	-16.8	-16.7
0.366	-23.3	-22.9	0.276	-13.3	-13.4	0.374	-20.0	-20.2
0.464	-26.7	-26.5	0.372	-17.7	-17.4	0.473	-21.9	-21.8
0.565	-28.4	-28.2	0.470	-20.4	-20.1	0.573	-21.8	-21.6
0.668	-27.3	-27.6	0.571	-20.7	-21.0	0.676	-19.5	-19.6
0.775	-24.0	-24.2	0.674	-19.5	-19.7	0.781	-15.8	-15.8
0.885	-16.3	-16.3	0.779	-16.2	-15.9	0.888	-9.7	-9.7
0.941	-10.0	-9.6	0.887	-9.5	-9.3	0.943	-5.5	-5.5
			0.942	-4.7	-5.0			

* 0.83 % weight of H_2O in the solvent.

TABLE A4.7

Comparison of Calculated and Experimental Enthalpy of Mixing of (CO_2 + Selexol)* at 298.15 K and 7.5, 10.6, and 12.6 MPa

7.5 MPa			10.6 MPa			12.6 MPa		
w CO_2	H^E exp. (J/g)	H^E calc. (J/g)	w CO_2	H^E exp. (J/g)	H^E calc. (J/g)	w CO_2	H^E exp. (J/g)	H^E calc. (J/g)
0.088	-6.9	-6.4	0.090	-2.0	-2.1	0.091	-3.4	-3.5
0.179	-12.1	-12.4	(0.182)	(-4.7)	-	0.184	-8.4	-8.4
0.271	-17.2	-17.6	0.276	-12.2	-12.2	0.278	-13.2	-13.1
0.366	-22.1	-21.6	0.372	-16.6	-16.6	0.375	-16.8	-16.8
0.464	-24.3	-24.2	0.470	-19.5	-19.4	0.473	-18.8	-18.8
0.565	-25.1	-25.1	0.571	-19.9	-20.0	0.574	-18.8	-18.9
0.669	-24.1	-24.2	0.674	-18.3	-18.4	0.676	-17.2	-17.3
0.775	-20.6	-20.7	0.779	-15.1	-14.9	0.781	-14.1	-13.8
0.885	-13.6	-13.5	0.887	-9.0	-9.0	0.889	-8.3	-8.4
0.941	-7.9	-7.9	0.942	-4.8	-5.0	0.943	-4.6	-4.7

* 3.62 % weight of H_2O in the solvent.

TABLE A4.8

Comparison of Calculated and Experimental Enthalpy of Mixing of (CO_2 + Methanol) at 298.15 K and 7.5, 10.6, and 12.6 MPa

7.5 MPa			10.6 MPa			12.6 MPa		
x CO_2	H^E exp. (J/mol)	H^E calc. (J/mol)	x CO_2	H^E exp. (J/mol)	H^E calc. (J/mol)	x CO_2	H^E exp. (J/mol)	H^E calc. (J/mol)
0.042	-111.2	-103.1	0.042	-106.0	-102.7	0.043	-70.3	-60.5
0.084	-202.8	-208.0	0.085	-201.6	-201.0	0.086	-145.5	-146.4
0.170	-398.2	-402.4	0.173	-366.2	-371.2	0.175	-306.7	-323.4
0.260	-555.6	-553.6	0.264	-487.9	-486.3	0.266	-456.6	-449.6
0.353	-654.2	-648.0	0.358	-538.8	-534.1	0.360	-511.6	-496.8
0.450	-677.7	-679.0	0.455	-512.5	-515.0	0.458	-465.5	-462.0
0.551	-640.6	-644.8	0.556	-434.1	-437.1	0.558	-331.3	-356.7
0.656	-542.4	-546.8	0.660	-312.6	-312.1	0.663	-206.5	-204.1
0.765	-397.9	-389.2	0.769	-156.7	-152.6	0.770	-54.8	-37.1
0.879	-172.5	-176.2	0.881	30.1	26.7	0.882	113.0	102.6
0.938	-39.0	-38.5	0.939	108.1	109.1	0.940	151.0	153.0

TABLE A4.9

Comparison of Calculated and Experimental Enthalpy of Mixing of (CO_2 + Methyl Cyanoacetate) at 298.15 K and 7.5, 10.6, and 12.6 MPa

7.5 MPa			10.6 MPa			12.6 MPa		
x CO_2	H^E exp. (J/mol)	H^E calc. (J/mol)	x CO_2	H^E exp. (J/mol)	H^E calc. (J/mol)	x CO_2	H^E exp. (J/mol)	H^E calc. (J/mol)
(0.168)	(-40.1)	-	(0.171)	(-106.6)	-	(0.172)	(-21.7)	-
0.311	-450.3	-454.3	0.316	-374.8	-378.1	0.318	-264.5	-266.7
0.437	-735.0	-723.6	0.442	-662.5	-651.7	0.444	-586.5	-577.3
0.546	-940.3	-949.9	0.552	-814.5	-826.9	0.554	-718.8	-732.8
0.643	-1097.5	-1100.9	0.648	-907.6	-904.5	0.651	-786.5	-782.2
0.730	-1167.1	-1158.8	0.734	-905.9	-902.5	0.736	-776.3	-767.1
0.808	-1112.8	-1114.4	0.811	-833.2	-834.0	0.813	-694.9	-699.6
0.878	-957.8	-960.0	0.880	-695.0	-696.0	0.881	-561.5	-568.3
0.941	-670.4	-669.3	0.942	-454.1	-455.8	0.943	-348.4	-347.5
0.971	-434.7	-434.9	0.971	-273.0	-270.4	0.972	-203.7	-193.9

TABLE A4.10

Comparison of Calculated and Experimental Enthalpy of Mixing of (CO_2 + N-Formyl Morpholine) at 298.15 K and 7.5 MPa

x CO_2	H^E exp. (J/mol)	H^E calc. (J/mol)
(0.185)	(-265.1)	-
(0.337)	(-641.6)	-
(0.466)	(-858.4)	-
(0.576)	(-1588.7)	-
0.670	-1791.3	-1791.4
0.753	-1812.8	-1812.0
0.825	-1645.9	-1648.2
0.890	-1370.0	-1369.0
0.947	-881.4	-878.1
0.974	-498.1	-503.7

TABLE A4.11

Comparison of the Enthalpy of Mixing of (CO_2 + Selexol)* at 298.15 and 10.6 MPa with Different Flow Rates

w CO_2	0.4 ml/min H^E exp. (J/g)	0.2 ml/min H^E exp. (J/g)
0.045	-2.3	-
0.090	-4.4	-4.5
0.182	-8.4	-9.5
0.276	-13.3	-14.0
0.372	-17.7	-17.7
0.470	-20.4	-20.9
0.571	-20.7	-21.3
0.674	-19.5	-19.5
0.779	-16.2	-16.2
0.887	-9.5	-10.6
0.942	-4.7	-

* 0.83 % weight of H_2O in the solvent

TABLE A4.12

Coefficients for least-squares representation of the enthalpy of mixing of CO_2 with several solvents by equation (5.1).

Solvent	Pressure (MPa)	C_0	C_1	C_2	C_3	D_1	D_2	D_3
				298.15 K				
N-Methyl Pyrrolidone	7.5	-5395.40	-341.13	436.44	-	0.7959	-	-
	10.6	-4608.70	218.75	986.67	-	0.7029	-	-
	12.6	-4266.00	434.33	439.70	-	0.6227	-	-
Propylene Carbonate	7.5	-4920.10	-7252.60	6798.50	-	2.2413	0.2332	-
	10.6	-3721.80	3332.10	-1191.60	-	-0.0062	-0.0120	-
	12.6	-3483.20	1930.00	-798.29	-	-0.2712	-	-
Selexol	7.5	-109.42	39.18	-4.05	38.88	-	-	-
(0.83 % wt. H_2O)	10.6	-82.34	26.89	15.56	-2.29	-	-	-
	12.6	-87.75	4.48	3.74	18.65	-	-	-
Selexol	7.5	-98.92	23.98	-13.47	16.27	-	-	-
(3.62 % wt. H_2O)	10.6	-79.21	21.05	31.71	28.06	-	-	-
	12.6	-76.02	11.63	17.87	22.09	-	-	-

Methanol	7.5	-2674.90	-2867.30	-8.19	-	0.8861	-	-
	10.6	-1945.80	-1898.00	1063.00	-	0.2012	-0.4042	0.3378
	12.6	-1744.60	-5244.20	-1574.30	4064.90	1.7784	-	-
Methyl Cyanoacetate	7.5	-3434.90	891.00	1956.30	-876.34	0.9369	-	-
	10.6	-2923.80	22589.00	-2252.40	-19884.00	-6.6258	-7.0793	-
	12.6	-2630.20	-396.18	3722.50	3933.40	1.3420	0.6493	-
N-Formyl Morpholine*	7.5	115.03	42803.00	72670.00	52510.00	-	-	-
Toluene	7.5	795.38	2374.00	-750.79	-1833.60	0.9864	-	-
	10.6	1342.20	1497.90	-417.95	-144.89	0.8161	-	-
				308.15 K				
Toluene	10.6	434.93	2088.80	-359.23	-882.89	0.8930	-	-

* Constants useful in the range $0.65 \leq x \leq 1.0$

APPENDIX V

Enthalpy Departure Formulation for the Peng-Robinson Equation of State

The Peng-Robinson equation of state has the form:

$$P = \frac{RT}{v-b} - \frac{a(T)}{v(v+b)+b(v-b)} \tag{A5.1}$$

and the enthalpy departure of a fluid is given by the thermodynamic equation:

$$H - H^* = RT(Z-1) + \int_{\infty}^{v} \left[T\left(\frac{\partial P}{\partial T}\right)_v - P \right] dv \tag{A5.2}$$

We can obtain $\left(\frac{\partial P}{\partial T}\right)_v$ from equation (A5.1), noting that both a and b are functions of temperature.

$$\left(\frac{\partial P}{\partial T}\right)_v = \frac{R}{v-b} - \frac{\left(\frac{da}{dT}\right)}{(v^2+2bv-b^2)} + \frac{2a(v-b)\left(\frac{db}{dT}\right)}{(v^2+2bv-b^2)^2} \tag{A5.3}$$

Next, we multiply both sides of equation (A5.3) by T:

$$T\left(\frac{\partial P}{\partial T}\right)_v = \frac{RT}{v-b} - \frac{T\left(\frac{da}{dT}\right)}{(v^2+2bv-b^2)} + \frac{2aT(v-b)\left(\frac{db}{dT}\right)}{(v^2+2bv-b^2)^2} \tag{A5.4}$$

and substitute equations (A5.1) and (A5.4) into equation (A5.2):

$$H - H^* = RT(Z-1) + \int_{\infty}^{v} \left[\frac{a - T\left(\frac{da}{dT}\right)}{(v^2+2bv-b^2)} + \frac{2aT(v-b)\left(\frac{db}{dT}\right)}{(v^2+2bv-b^2)^2} \right] dv \tag{A5.5}$$

For the integration, using formulas 14.272 and 14.273 from the Mathematical Handbook of Formulas and Tables [42], we obtain:

$$\int_{\infty}^{v}\left[\frac{a-T\left(\frac{da}{dT}\right)}{(v^2+2bv-b^2)}\right]dv=\frac{a-T\left(\frac{da}{dT}\right)}{\sqrt{8b^2}}\ln\left(\frac{2v+2b-\sqrt{8b^2}}{2v+2b+\sqrt{8b^2}}\right) \qquad \text{(A5.6)}$$

$$\begin{aligned}\int_{\infty}^{v}\left[\frac{2a(v-b)T\left(\frac{db}{dT}\right)}{(v^2+2bv-b^2)^2}\right]dv &= \frac{4abT\left(\frac{db}{dT}\right)}{8b^2}\left[\frac{v-b}{v^2+2bv-b^2}+\frac{1}{\sqrt{8b^2}}\ln\left(\frac{2v+2b-\sqrt{8b^2}}{2v+2b+\sqrt{8b^2}}\right)\right.\\ &\left.+\frac{v+b}{v^2+2bv-b^2}+\frac{1}{\sqrt{8b^2}}\ln\left(\frac{2v+2b-\sqrt{8b^2}}{2v+2b+\sqrt{8b^2}}\right)\right] \qquad \text{(A5.7)}\end{aligned}$$

Now if we substitute equations (A5.6) and (A5.7) in equation (A5.5) and simplify, the expression for the enthalpy departure becomes:

$$\begin{aligned}H-H^{*} &= RT(Z-1)+\frac{a-T\left(\frac{da}{dT}\right)}{2\sqrt{2}b}\ln\left(\frac{2(v+b)-2\sqrt{2}b}{2(v+b)+2\sqrt{2}b}\right)\\ &+\frac{aT\left(\frac{db}{dT}\right)}{2b}\left[\frac{2v}{v^2+2bv-b^2}-\frac{1}{\sqrt{2}b}\ln\left(\frac{2(v+b)-2\sqrt{2}b}{2(v+b)+2\sqrt{2}b}\right)\right] \qquad \text{(A5.8)}\end{aligned}$$

Next, we define:

$$B=\frac{bP}{RT} \qquad \text{(A5.9)}$$

and also, the compressibility factor:

$$Z = \frac{vP}{RT}. \qquad \text{(A5.10)}$$

Therefore, if we multiply and divide the logarithmic terms of equation (A5.8) by $\left(\frac{P}{RT}\right)$ and the first component of the third term by $\left(\frac{P}{RT}\right)^2$ we obtain after rearrangment an expression relating the enthalpy departure to B and Z:

$$H - H^* = RT(Z-1) + \frac{a - T\left(\frac{da}{dT}\right)}{2\sqrt{2}b}\ln\left(\frac{Z - 0.414B}{Z + 2.414B}\right)$$

$$+\frac{aT\left(\frac{db}{dT}\right)}{b}\left[\frac{\frac{ZP}{RT}}{Z^2 + 2BZ - B^2} - \frac{1}{2\sqrt{2}b}\ln\left(\frac{Z - 0.414B}{Z + 2.414B}\right)\right] \qquad \text{(A5.11)}$$

Notice that equation (A5.11) differs from that given by Peng and Robinson [38] because of the third term that takes into account the variation of b with temperature.

APPENDIX VI

EXPERIMENTAL AND PREDICTED DATA

TABLE A6.1

Comparison of Predicted and Experimental Enthalpy of Mixing of (CO_2 + Toluene) at 298.15 and 308.15 K and 10.6 MPa

298.15 K			308.15 K		
x CO_2	H^E exp. (J/mol)	H^E pred. (J/mol)	x CO_2	H^E exp. (J/mol)	H^E pred. (J/mol)
0.196	218.8	196.5	0.105	75.3	-1.2
0.279	284.7	258.7	0.197	128.9	-10.3
0.354	315.0	301.7	0.356	212.2	-46.8
0.484	341.0	339.8	0.486	97.4	-100.5
0.593	302.1	327.8	0.595	2.2	-163.7
0.686	224.6	279.0	0.688	-110.8	-228.5
0.766	140.6	205.3	0.767	-215.1	-285.9
0.836	58.0	119.3	0.837	-286.4	-323.8
0.897	-7.4	36.2	0.868	-318.2	-329.9
0.951	-44.4	-20.1	0.898	-330.0	-323.1
			0.951	-266.9	-247.5
			0.976	-166.4	-158.4

TABLE A6.2

Comparison of Predicted and Experimental Enthalpy of Mixing of (CO_2 + Toluene) at 298.15 K and 7.5 MPa

x CO_2	H^E exp. (J/mol)	H^E pred. (J/mol)
0.103	76.6	33.5
0.194	138.9	49.8
0.351	234.6	41.3
0.480	259.5	-9.6
0.590	59.4	-90.5
0.683	-29.8	-190.3
0.763	-135.6	-296.3
0.834	-225.7	-392.0
0.866	-258.7	-427.8
0.896	-281.6	-448.6
0.924	-283.9	-445.3
0.950	-253.6	-402.3

TABLE A6.3

Comparison of Predicted and Experimental Enthalpy of Mixing of (CO_2 + N-Methyl Pyrrolidone) at 298.15 K and 7.5, 10.6, and 12.6 MPa

7.5 MPa			10.6 MPa			12.6 MPa		
x CO_2	H^E exp. (J/mol)	H^E pred. (J/mol)	x CO_2	H^E exp. (J/mol)	H^E pred. (J/mol)	x CO_2	H^E exp. (J/mol)	H^E pred. (J/mol)
0.179	-554.6	-573.0	0.183	-429.8	-435.5	0.185	-430.2	-384.9
0.329	-933.3	-1029.3	0.334	-791.5	-774.1	0.337	-738.0	-680.8
0.456	1234.7	-1389.8	0.462	-1073.5	-1034.0	0.465	-1002.8	-904.2
0.566	-1472.9	-1665.4	0.572	-1264.6	-1223.1	0.575	-1170.0	-1062.7
0.662	-1591.4	-1859.0	0.667	-1335.6	-1343.7	0.670	-1244.4	-1158.6
0.705	-1613.9	-1923.9	0.710	-1334.4	-1377.2	0.752	-1185.8	-1187.4
0.746	-1605.2	-1965.3	0.750	-1276.7	-1391.0	0.825	-1038.6	-1136.7
0.820	-1482.0	-1965.4	0.823	-1149.9	-1350.1	0.890	-825.7	-979.1
0.886	-1262.1	-1813.3	0.889	-919.1	-1187.0	0.947	-498.8	-655.1
0.946	-856.7	-1382.9	0.947	-542.1	-823.7			
			0.974	-306.4	-508.0			

TABLE A6.4

Comparison of Predicted and Experimental Enthalpy of Mixing of (CO_2 + Propylene Carbonate) at 298.15 K and 7.5, 10.6, and 12.6 MPa

7.5 MPa			10.6 MPa			12.6 MPa		
x CO_2	H^E exp. (J/mol)	H^E pred. (J/mol)	x CO_2	H^E exp. (J/mol)	H^E pred. (J/mol)	x CO_2	H^E exp. (J/mol)	H^E pred. (J/mol)
0.162	-363.6	-688.3	0.165	-271.6	-560.1	0.167	-304.9	-511.7
0.367	-902.9	-1438.7	0.308	-571.0	-978.5	0.311	-560.3	-885.6
0.537	-1275.5	-1889.4	0.433	-799.6	-1271.5	0.435	-751.4	-1138.7
0.634	-1408.1	-2019.4	0.542	-997.4	-1444.6	0.545	-941.7	-1276.4
0.679	-1397.2	-2027.6	0.640	-1091.2	-1492.5	0.643	-1024.7	-1295.0
0.722	-1420.7	-1993.1	0.685	-1107.1	-1465.6	0.687	-1036.3	-1256.5
0.802	-1170.0	-1778.6	0.727	-1095.8	-1401.8	0.729	-1032.6	-1183.9
0.907	-624.3	-647.1	0.805	-977.0	-1154.0	0.807	-922.7	-932.6
0.970	-320.4	-304.8	0.876	-709.0	-748.1	0.877	-696.5	-553.6
			0.940	-426.5	-260.8	0.941	-428.4	-144.6
			0.970	-304.7	-67.0	0.971	-282.8	-9.0

TABLE A6.5

Comparison of Predicted and Experimental Enthalpy of Mixing of (CO_2 + Selexol)* at 298.15 K and 7.5, 10.6, and 12.6 MPa

7.5 MPa			10.6 MPa			12.6 MPa		
x CO_2	H^E exp. (J/mol)	H^E pred. (J/mol)	x CO_2	H^E exp. (J/mol)	H^E pred. (J/mol)	x CO_2	H^E exp. (J/mol)	H^E pred. (J/mol)
0.387	-1104.8	-1387.3	0.235	-522.9	-665.4	0.395	-1125.7	-981.9
0.586	-1478.5	-2032.0	0.392	-846.6	-1090.3	0.595	-1682.9	-1411.7
0.708	-1968.9	-2357.3	0.592	-1204.6	-1576.7	0.715	-1904.8	-1608.1
0.790	-2211.6	-2503.8	0.713	-1518.1	-1806.3	0.796	-1867.4	-1674.4
0.850	-2150.6	-2527.6	0.794	-1661.3	-1892.3	0.854	-1739.6	-1650.8
0.894	-1977.4	-2447.6	0.853	-1625.5	-1878.9	0.898	-1502.0	-1550.8
0.929	-1671.0	-2258.3	0.897	-1434.7	-1780.9	0.932	-1179.6	-1372.1
0.957	-1302.2	-1924.8	0.931	-1183.9	-1595.0	0.959	-854.5	-1097.0
0.980	-796.6	-1345.1	0.958	-874.1	-1298.0	0.981	-473.0	-680.9
0.991	-465.6	-861.3	0.981	-461.5	-828.6	0.991	-253.2	-391.3
			0.991	-215.0	-487.6			

* 0.83 % weight of H_2O in the solvent.

TABLE A6.6

Comparison of Predicted and Experimental Enthalpy of Mixing of (CO_2 + Methanol) at 298.15 K and 7.5, 10.6, and 12.6 MPa

7.5 MPa			10.6 MPa			12.6 MPa		
x CO_2	H^E exp. (J/mol)	H^E pred. (J/mol)	x CO_2	H^E exp. (J/mol)	H^E pred. (J/mol)	x CO_2	H^E exp. (J/mol)	H^E pred. (J/mol)
0.042	-111.2	-113.7	0.042	-106.0	-84.5	0.043	-70.3	-74.7
0.084	-202.8	-221.2	0.085	-201.6	-162.4	0.086	-145.5	-142.5
0.170	-398.2	-420.3	0.173	-366.2	-299.8	0.175	-306.7	-258.7
0.260	-555.6	-596.5	0.264	-487.9	-411.7	0.266	-456.6	-348.8
0.353	-654.2	-748.6	0.358	-538.8	-497.4	0.360	-511.6	-412.4
0.450	-677.7	-874.8	0.455	-512.5	-556.4	0.458	-465.5	-449.5
0.551	-640.6	-972.8	0.556	-434.1	-587.8	0.558	-331.3	-460.4
0.656	-542.4	-1035.5	0.660	-312.6	-588.6	0.663	-206.5	-445.9
0.765	-397.9	-1042.2	0.769	-156.7	-547.8	0.770	-54.8	-393.9
0.879	-172.5	-912.8	0.881	30.1	-424.1	0.882	113.0	-285.3
0.938	-39.0	-694.4	0.939	108.1	-286.4	0.940	151.0	-183.1

TABLE A6.7

Comparison of Predicted and Experimental Enthalpy of Mixing of (CO_2 + Methyl Cyanoacetate) at 298.15 K and 7.5, 10.6, and 12.6 MPa

7.5 MPa			10.6 MPa			12.6 MPa		
x CO_2	H^E exp. (J/mol)	H^E pred. (J/mol)	x CO_2	H^E exp. (J/mol)	H^E pred. (J/mol)	x CO_2	H^E exp. (J/mol)	H^E pred. (J/mol)
0.168	-40.1	-383.7	0.171	-106.6	-252.9	0.172	-21.7	-202.1
0.311	-450.3	-706.9	0.316	-374.8	-460.6	0.318	-264.5	-369.6
0.437	-735.0	-979.6	0.442	-662.5	-634.3	0.444	-586.5	-507.8
0.546	-940.3	-1205.3	0.552	-814.5	-774.6	0.554	-718.8	-617.8
0.643	-1097.5	-1383.2	0.648	-907.6	-879.5	0.651	-786.5	-698.0
0.730	-1167.1	-1506.0	0.734	-905.9	-942.5	0.736	-776.3	-742.4
0.808	-1112.8	-1554.8	0.811	-833.2	-948.7	0.813	-694.9	-738.5
0.878	-957.8	-1485.6	0.880	-695.0	-866.9	0.881	-561.5	-661.7
0.941	-670.4	-1179.3	0.942	-454.1	-626.2	0.943	-348.4	-460.5
0.971	-434.7	-821.3	0.971	-273.0	-394.2	0.972	-203.7	-280.2

TABLE A6.8

Comparison of Predicted and Experimental Enthalpy of Mixing of (CO_2 + N-Formyl Morpholine) at 298.15 K and 7.5 MPa

x CO_2	H^E exp. (J/mol)	H^E pred. (J/mol)
0.185	-265.1	-509.7
0.337	-641.6	-913.6
0.466	-858.4	-1233.5
0.576	-1588.7	-1481.5
0.670	-1791.3	-1662.7
0.753	-1812.8	-1776.6
0.825	-1645.9	-1812.3
0.890	-1370.0	-1737.0
0.947	-881.4	-1441.0
0.974	-498.1	-1073.7

APPENDIX VII

RAW EXPERIMENTAL DATA

TABLE A7.1

Raw Data - Enthalpy of Mixing of (Cyclohexane + n-Hexane) at 298.15 K and 0.1 MPa

Flow Rate of Cycl. (ml/min)	Flow Rate of n-Hexane (ml/min)	Molar Flow Rate of Cycl. x 10^6 (mol/s)	Molar Flow Rate of n-Hex. x 10^6 (mol/s)	x Cycl.	x Hex.	Total Heat x 10^3 (J/s)	H^E exp. (J/mol)
0.054	0.446	0.828	5.648	0.128	0.872	1.938	29.9
0.088	0.412	1.346	5.220	0.205	0.795	7.091	108.0
0.122	0.378	1.865	4.791	0.280	0.720	9.767	146.7
0.156	0.344	2.384	4.362	0.353	0.647	11.895	176.3
0.189	0.311	2.903	3.933	0.425	0.575	13.634	199.4
0.206	0.294	3.162	3.719	0.460	0.540	14.343	208.4
0.223	0.277	3.422	3.504	0.494	0.506	14.911	215.3
0.240	0.260	3.681	3.290	0.528	0.472	15.327	219.9
0.257	0.243	3.940	3.076	0.562	0.438	15.620	222.6
0.274	0.226	4.200	2.861	0.595	0.405	15.818	224.0
0.291	0.209	4.459	2.647	0.628	0.372	15.885	223.5
0.308	0.192	4.719	2.432	0.660	0.340	15.809	221.1
0.342	0.158	5.238	2.004	0.723	0.277	15.081	208.3
0.376	0.124	5.757	1.575	0.785	0.215	13.615	185.7
0.409	0.091	6.275	1.147	0.846	0.154	11.289	152.1
0.443	0.057	6.794	0.718	0.904	0.096	6.798	90.5
0.460	0.040	7.054	0.503	0.933	0.067	3.026	40.0
0.477	0.023	7.313	0.289	0.962	0.038	0.596	7.8

TABLE A7.2

Raw Data - Enthalpy of Mixing of (Cyclohexane + n-Hexane) at 298.15 K and 7.0 MPa

Flow Rate of Cycl. (ml/min)	Flow Rate of n-Hexane (ml/min)	Molar Flow Rate of Cycl. x 10^5 (mol/s)	Molar Flow Rate of n-Hex. x 10^5 (mol/s)	x Cycl.	x Hex.	Total Heat x 10^3 (J/s)	H^E exp. (J/mol)
0.061	0.439	0.937	5.558	0.144	0.856	2.055	31.6
0.088	0.412	1.350	5.217	0.206	0.794	7.464	113.7
0.115	0.385	1.763	4.876	0.266	0.734	9.627	145.0
0.142	0.358	2.175	4.534	0.324	0.676	11.412	170.1
0.169	0.331	2.588	4.193	0.382	0.618	12.710	187.4
0.196	0.304	3.001	3.852	0.438	0.562	13.867	202.4
0.209	0.291	3.208	3.681	0.466	0.534	14.224	206.5
0.236	0.264	3.620	3.340	0.520	0.480	14.830	213.1
0.250	0.250	3.827	3.170	0.547	0.453	15.144	216.4
0.263	0.237	4.033	2.999	0.574	0.426	15.219	216.4
0.304	0.196	4.653	2.487	0.652	0.348	15.198	212.9
0.331	0.169	5.066	2.146	0.702	0.298	14.603	202.5
0.357	0.143	5.478	1.805	0.752	0.248	13.846	190.1
0.384	0.116	5.891	1.464	0.801	0.199	12.331	167.7
0.411	0.089	6.304	1.123	0.849	0.151	10.114	136.2
0.438	0.062	6.717	0.782	0.896	0.104	7.193	95.9
0.452	0.048	6.924	0.611	0.919	0.081	4.002	53.1
0.465	0.035	7.130	0.440	0.942	0.058	0.811	10.7

TABLE A7.3

Raw Data - Enthalpy of Mixing of (Cyclohexane + n-Hexane)
at 298.15 K and 14.0 MPa

Flow Rate of Cycl. (ml/min)	Flow Rate of n-Hexane (ml/min)	Molar Flow Rate of Cycl. x 10^6 (mol/s)	Molar Flow Rate of n-Hex. x 10^6 (mol/s)	x Cycl.	x Hex.	Total Heat x 10^3 (J/s)	H^E exp. (J/mol)
0.091	0.409	1.392	5.181	0.212	0.788	1.990	30.2
0.118	0.382	1.806	4.839	0.272	0.728	6.242	93.9
0.158	0.342	2.427	4.326	0.359	0.641	11.860	175.6
0.185	0.315	2.841	3.984	0.416	0.584	13.156	192.8
0.212	0.288	3.255	3.642	0.472	0.528	14.094	204.3
0.239	0.261	3.669	3.300	0.526	0.474	14.837	212.9
0.253	0.247	3.876	3.129	0.553	0.447	15.116	215.8
0.266	0.234	4.083	2.958	0.580	0.420	15.177	215.6
0.280	0.220	4.290	2.787	0.606	0.394	15.185	214.6
0.293	0.207	4.497	2.616	0.632	0.368	15.007	211.0
0.307	0.193	4.704	2.445	0.658	0.342	14.656	205.0
0.334	0.166	5.118	2.103	0.709	0.291	13.910	192.6
0.347	0.153	5.325	1.932	0.734	0.266	13.395	184.6
0.361	0.139	5.532	1.761	0.759	0.241	12.838	176.0
0.388	0.112	5.946	1.419	0.807	0.193	11.190	151.9
0.415	0.085	6.360	1.077	0.855	0.145	9.118	122.6
0.428	0.072	6.567	0.906	0.879	0.121	7.930	106.1
0.442	0.058	6.773	0.735	0.902	0.098	5.981	79.7

TABLE A7.4

Raw Data - Enthalpy of Mixing of (CO_2 + Toluene) at 298.15 K and 7.5 MPa

Flow Rate of CO_2 (ml/min)	Flow Rate of Solvent (ml/min)	Molar Flow Rate of CO_2 x 10^6 (mol/s)	Molar Flow Rate of Solvent x 10^6 (mol/s)	x CO_2	x Solvent	Total Heat x 10^3 (J/s)	H^E exp. (J/mol)
0.020	0.393	7.049	61.658	0.103	0.897	5.263	76.6
0.040	0.373	14.043	58.418	0.194	0.806	10.065	138.9
0.080	0.331	28.030	51.940	0.351	0.649	18.761	234.6
0.120	0.290	42.016	45.463	0.480	0.520	22.701	259.5
0.160	0.249	56.005	38.983	0.590	0.410	5.642	59.4
0.200	0.207	69.995	32.502	0.683	0.317	-3.054	29.8
0.240	0.166	83.979	26.027	0.763	0.237	-14.917	-135.6
0.280	0.125	97.972	19.543	0.834	0.166	-26.523	-225.7
0.300	0.104	104.959	16.310	0.866	0.134	-31.372	-258.7
0.320	0.083	111.959	13.065	0.896	0.104	-35.207	-281.6
0.340	0.063	118.952	9.826	0.924	0.076	-36.560	-283.9
0.360	0.042	125.946	6.587	0.950	0.050	-33.610	-253.6

TABLE A7.5

Raw Data - Enthalpy of Mixing of (CO_2 + Toluene) at 298.15 K and 10.6 MPa

Flow Rate of CO_2 (ml/min)	Flow Rate of Solvent (ml/min)	Molar Flow Rate of CO_2 x 10^6 (mol/s)	Molar Flow Rate of Solvent x 10^6 (mol/s)	x CO_2	x Solvent	Total Heat x 10^3 (J/s)	H^E exp. (J/mol)
0.040	0.373	14.390	58.991	0.196	0.804	16.056	218.8
0.060	0.352	21.560	55.717	0.279	0.721	22.001	284.7
0.080	0.331	28.727	52.447	0.354	0.646	25.570	315.0
0.120	0.290	43.060	45.907	0.484	0.516	30.338	341.0
0.160	0.249	57.398	39.362	0.593	0.407	29.231	302.1
0.200	0.207	71.734	32.819	0.686	0.314	23.483	224.6
0.240	0.166	86.069	26.278	0.766	0.234	15.796	140.6
0.280	0.125	100.401	19.739	0.836	0.164	6.968	58.0
0.320	0.083	114.730	13.203	0.897	0.103	-0.946	-7.4
0.360	0.042	129.075	6.651	0.951	0.049	-6.026	-44.4

TABLE A7.6

Raw Data - Enthalpy of Mixing of (CO_2 + Toluene) at 308.15 K and 10.6 MPa

Flow Rate of CO_2 (ml/min)	Flow Rate of Solvent (ml/min)	Molar Flow Rate of CO_2 x 10^6 (mol/s)	Molar Flow Rate of Solvent x 10^6 (mol/s)	x CO_2	x Solvent	Total Heat x 10^3 (J/s)	H^E exp. (J/mol)
0.020	0.393	7.224	61.834	0.105	0.895	5.200	75.3
0.040	0.373	14.391	58.585	0.197	0.803	9.407	128.9
0.080	0.331	28.729	52.083	0.356	0.644	17.148	212.2
0.120	0.290	43.057	45.592	0.486	0.514	8.634	97.4
0.160	0.249	57.389	39.096	0.595	0.405	0.212	2.2
0.200	0.207	71.721	32.600	0.688	0.312	-11.559	-110.8
0.240	0.166	86.059	26.099	0.767	0.233	-24.125	-215.1
0.280	0.125	100.387	19.607	0.837	0.163	-34.366	-286.4
0.300	0.104	107.556	16.356	0.868	0.132	-39.429	-318.2
0.320	0.083	114.728	13.103	0.898	0.102	-42.184	-330.0
0.360	0.042	129.060	6.607	0.951	0.049	-36.210	-266.9
0.380	0.021	136.221	3.364	0.976	0.024	-23.227	-166.4

TABLE A7.7

Raw Data - Enthalpy of Mixing of (CO_2 + N-Methyl Pyrrolidone) at 298.15 K and 7.5 MPa

Flow Rate of CO_2 (ml/min)	Flow Rate of Solvent (ml/min)	Molar Flow Rate of CO_2 x 10^6 (mol/s)	Molar Flow Rate of Solvent x 10^6 (mol/s)	x $(CO)_2$	x Solvent	Total Heat x 10^3 (J/s)	H^E exp. (J/mol)
0.040	0.373	14.039	64.304	0.179	0.821	-43.449	554.6
0.080	0.331	28.029	57.167	0.329	0.671	-79.513	-933.3
0.120	0.290	42.011	50.039	0.456	0.544	-113.654	-1234.7
0.160	0.249	56.000	42.904	0.566	0.434	-145.676	-1472.9
0.200	0.207	69.980	35.778	0.662	0.338	-168.303	-1591.4
0.220	0.187	76.975	32.210	0.705	0.295	-176.214	-1613.9
0.240	0.166	83.963	28.649	0.746	0.254	-180.765	-1605.2
0.280	0.125	97.950	21.516	0.820	0.180	-177.049	-1482.0
0.320	0.083	111.932	14.388	0.886	0.114	-159.429	-1262.1
0.360	0.042	125.915	7.258	0.946	0.054	-114.089	-856.7

TABLE A7.8

Raw Data - Enthalpy of Mixing of (CO_2 + N-Methyl Pyrrolidone) at 298.15 K and 10.6 MPa

Flow Rate of CO_2 (ml/min)	Flow Rate of Solvent (ml/min)	Molar Flow Rate of CO_2 x 10^6 (mol/s)	Molar Flow Rate of Solvent x 10^6 (mol/s)	x CO_2	x Solvent	Total Heat x 10^3 (J/s)	H^E exp. (J/mol)
0.040	0.373	14.395	64.395	0.183	0.817	-33.864	-429.8
0.080	0.331	28.728	57.258	0.334	0.666	-68.058	-791.5
0.120	0.290	43.068	50.113	0.462	0.538	-100.030	-1073.5
0.160	0.249	57.405	42.971	0.572	0.428	-126.936	-1264.6
0.200	0.207	71.739	35.832	0.667	0.333	-143.683	-1335.7
0.220	0.187	78.907	32.261	0.710	0.290	-148.343	-1334.4
0.240	0.166	86.075	28.691	0.750	0.250	-146.522	-1276.7
0.280	0.125	100.411	21.550	0.823	0.177	-140.243	-1149.9
0.320	0.083	114.755	14.401	0.889	0.111	-118.707	-919.1
0.360	0.042	129.084	7.267	0.947	0.053	-73.916	-542.1
0.380	0.021	136.254	3.695	0.974	0.026	-42.880	-306.4

TABLE A7.9

Raw Data - Enthalpy of Mixing of (CO_2 + N-Methyl Pyrrolidone) at 298.15 K and 12.6 MPa

Flow Rate of CO_2 (ml/min)	Flow Rate of Solvent (ml/min)	Molar Flow Rate of CO_2 x 10^6 (mol/s)	Molar Flow Rate of Solvent x 10^6 (mol/s)	x CO_2	x Solvent	Total Heat x 10^3 (J/s)	H^E exp. (J/mol)
0.040	0.373	14.583	64.459	0.185	0.815	-34.004	-430.2
0.080	0.331	29.106	57.312	0.337	0.663	-63.776	-738.0
0.120	0.290	43.633	50.162	0.465	0.535	-94.058	-1002.8
0.160	0.249	58.153	43.018	0.575	0.425	-118.370	-1170.0
0.200	0.207	72.684	35.864	0.670	0.330	-135.077	-1244.4
0.240	0.166	87.210	28.715	0.752	0.248	-137.464	-1185.8
0.280	0.125	101.736	21.565	0.825	0.175	-128.060	-1038.6
0.320	0.083	116.251	14.427	0.890	0.110	-107.901	-825.7
0.360	0.042	130.779	7.276	0.947	0.053	-68.862	-498.8

TABLE A7.10

Raw Data - Enthalpy of Mixing of (CO_2 + Propylene Carbonate) at 298.15 K and 7.5 MPa

Flow Rate of CO_2 (ml/min)	Flow Rate of Solvent (ml/min)	Molar Flow Rate of CO_2 x 10^6 (mol/s)	Molar Flow Rate of Solvent x 10^6 (mol/s)	x CO_2	x Solvent	Total Heat x 10^3 (J/s)	H^E exp. (J/mol)
0.040	0.373	14.041	72.522	0.162	0.838	-31.474	-363.6
0.100	0.311	35.022	60.458	0.367	0.633	-86.209	-902.9
0.160	0.249	56.010	48.388	0.537	0.463	-133.160	-1275.5
0.200	0.207	69.991	40.352	0.634	0.366	-155.374	-1408.1
0.220	0.187	76.987	36.329	0.679	0.321	-158.325	-1397.2
0.240	0.166	83.983	32.305	0.722	0.278	-165.210	-1420.7
0.280	0.125	97.970	24.263	0.802	0.198	-143.013	-1170.0
0.340	0.063	118.954	12.197	0.907	0.093	-81.878	-624.3
0.380	0.021	132.928	4.168	0.970	0.030	-43.926	-320.4

TABLE A7.11

Raw Data - Enthalpy of Mixing of (CO_2 + Propylene Carbonate) at 298.15 K and 10.6 MPa

Flow Rate of CO_2 (ml/min)	Flow Rate of Solvent (ml/min)	Molar Flow Rate of CO_2 x 10^6 (mol/s)	Molar Flow Rate of Solvent x 10^6 (mol/s)	x CO_2	x Solvent	Total Heat x 10^3 (J/s)	H^E exp. (J/mol)
0.040	0.373	14.389	72.605	0.165	0.835	-23.628	-271.6
0.080	0.331	28.729	64.548	0.308	0.692	-53.261	-571.0
0.120	0.290	43.060	56.500	0.433	0.567	-79.608	-799.6
0.160	0.249	57.399	48.445	0.542	0.458	-105.569	-997.4
0.200	0.207	71.728	40.399	0.640	0.360	-122.353	-1091.2
0.220	0.187	78.901	36.367	0.685	0.315	-127.613	-1107.1
0.240	0.166	86.060	32.350	0.727	0.273	-129.754	-1095.8
0.280	0.125	100.403	24.290	0.805	0.195	-121.825	-977.0
0.320	0.083	114.735	16.241	0.876	0.124	-92.862	-709.0
0.360	0.042	129.065	8.194	0.940	0.060	-58.541	-426.5
0.380	0.021	136.231	4.170	0.970	0.030	-42.780	-304.7

TABLE A7.12

Raw Data - Enthalpy of Mixing of (CO_2 + Propylene Carbonate) at 298.15 K and 12.6 MPa

Flow Rate of CO_2 (ml/min)	Flow Rate of Solvent (ml/min)	Molar Flow Rate of CO_2 x 10^6 (mol/s)	Molar Flow Rate of Solvent x 10^6 (mol/s)	x CO_2	x Solvent	Total Heat x 10^3 (J/s)	H^E exp. (J/mol)
0.040	0.373	14.576	72.655	0.167	0.833	-26.597	-304.9
0.080	0.331	29.091	64.598	0.311	0.689	-52.494	-560.3
0.120	0.290	43.604	56.544	0.435	0.565	-75.251	-751.4
0.160	0.249	58.122	48.485	0.545	0.455	-100.392	-941.7
0.200	0.207	72.645	40.421	0.643	0.357	-115.859	-1024.7
0.220	0.187	79.895	36.400	0.687	0.313	-120.517	-1036.3
0.240	0.166	87.157	32.367	0.729	0.271	-123.421	-1032.6
0.280	0.125	101.668	24.315	0.807	0.193	-116.245	-922.7
0.320	0.083	116.191	16.251	0.877	0.123	-92.246	-696.5
0.360	0.042	130.705	8.195	0.941	0.059	-59.505	-428.4
0.380	0.021	137.966	4.164	0.971	0.029	-40.194	-282.8

TABLE A7.13

Raw Data - Enthalpy of Mixing of (CO_2 + Selexol)* at 298.15 K and 7.5 MPa

Flow Rate of CO_2 (ml/min)	Flow Rate of Solvent (ml/min)	Mass Flow Rate of CO_2 x 10^3 (g/s)	Mass Flow Rate of Solvent x 10^3 (g/s)	w CO_2	w Solvent	Total Heat x 10^3 (J/s)	H^E exp. (J/g)
0.040	0.373	0.618	6.395	0.088	0.912	-39.974	-5.7
0.080	0.331	1.234	5.685	0.178	0.822	-70.574	-10.2
0.120	0.290	1.849	4.977	0.271	0.729	-116.725	-17.1
0.160	0.249	2.465	4.267	0.366	0.634	-156.856	-23.3
0.200	0.207	3.080	3.558	0.464	0.536	-177.235	-26.7
0.240	0.166	3.696	2.849	0.565	0.435	-185.878	-28.4
0.280	0.125	4.311	2.140	0.668	0.332	-176.112	-27.3
0.320	0.083	4.927	1.430	0.775	0.225	-152.568	-24.0
0.360	0.042	5.542	0.722	0.885	0.115	-102.103	-16.3
0.380	0.021	5.850	0.367	0.941	0.059	-62.792	-10.1

* 0.83 % weight of H_2O in the solvent.

TABLE A7.14

Raw Data - Enthalpy of Mixing (CO_2 + Selexol)* at 298.15 K and 10.6 MPa

Flow Rate of CO_2 (ml/min)	Flow Rate of Solvent (ml/min)	Mass Flow Rate of CO_2 x 10^3 (g/s)	Mass Flow Rate of Solvent x 10^3 (g/s)	w CO_2	w Solvent	Total Heat x 10^3 (J/s)	H^E exp. (J/g)
0.020	0.393	0.318	6.757	0.045	0.955	-16.273	-2.3
0.040	0.373	0.633	6.403	0.090	0.910	-30.958	-4.4
0.080	0.331	1.265	5.692	0.182	0.818	-58.439	-8.4
0.120	0.290	1.896	4.982	0.276	0.724	-91.477	-13.3
0.160	0.249	2.526	4.272	0.372	0.628	-120.325	-17.7
0.200	0.207	3.158	3.562	0.470	0.530	-137.088	-20.4
0.240	0.166	3.788	2.852	0.571	0.429	-137.448	-20.7
0.280	0.125	4.419	2.142	0.674	0.326	-127.940	-19.5
0.320	0.083	5.050	1.432	0.779	0.221	-104.360	-16.1
0.360	0.042	5.681	0.722	0.887	0.113	-60.829	-9.5
0.380	0.021	5.997	0.367	0.942	0.058	-29.274	-4.6

* 0.83 % weight of H_2O in the solvent.

TABLE A7.15

Raw Data - Enthalpy of Mixing of (CO_2 + Selexol)* at 298.15 K and 12.6 MPa

Flow Rate of CO_2 (ml/min)	Flow Rate of Solvent (ml/min)	Mass Flow Rate of CO_2 x 10^3 (g/s)	Mass Flow Rate of Solvent x 10^3 (g/s)	w CO_2	w Solvent	Total Heat x 10^3 (J/s)	H^E exp. (J/g)
0.040	0.373	0.641	6.407	0.091	0.909	-41.583	-5.9
0.080	0.331	1.280	5.697	0.184	0.816	-82.329	-11.8
0.120	0.290	1.920	4.985	0.278	0.722	-116.004	-16.8
0.160	0.249	2.559	4.275	0.374	0.626	-136.680	-20.0
0.200	0.207	3.197	3.565	0.473	0.527	-148.088	-21.9
0.240	0.166	3.836	2.854	0.573	0.427	-145.842	-21.8
0.280	0.125	4.475	2.144	0.676	0.324	-129.071	-19.5
0.320	0.083	5.114	1.433	0.781	0.219	-103.443	-15.8
0.360	0.042	5.753	0.723	0.888	0.112	-62.817	-9.7
0.380	0.021	6.072	0.368	0.943	0.057	-35.420	-5.5

* 0.83 % weight of H_2O in the solvent.

TABLE A7.16

Raw Data - Enthalpy of Mixing of (CO_2 + Selexol)* at 298.15 K and 7.5 MPa

Flow Rate of CO_2 (ml/min)	Flow Rate of Solvent (ml/min)	Mass Flow Rate of CO_2 x 10^3 (g/s)	Mass Flow Rate of Solvent x 10^3 (g/s)	w CO_2	w Solvent	Total Heat x 10^3 (J/s)	H^E exp. (J/g)
0.040	0.373	0.618	6.387	0.088	0.912	-48.335	-6.9
0.080	0.331	1.234	5.678	0.179	0.821	-83.635	-12.1
0.120	0.290	1.850	4.970	0.271	0.729	-117.304	-17.2
0.160	0.249	2.465	4.262	0.366	0.634	-148.667	-22.1
0.200	0.207	3.080	3.554	0.464	0.536	-161.206	-24.3
0.240	0.166	3.696	2.845	0.565	0.435	-164.179	-25.1
0.280	0.125	4.312	2.137	0.669	0.331	-155.421	-24.1
0.320	0.083	4.927	1.429	0.775	0.225	-130.934	-20.6
0.360	0.042	5.542	0.721	0.885	0.115	-85.177	-13.6
0.380	0.021	5.850	0.367	0.941	0.059	-49.114	-7.9

* 3.62 % weight of H_2O in the solvent.

TABLE A7.17

Raw Data - Enthalpy of Mixing of (CO_2 + Selexol)* at 298.15 K and 10.6 MPa

Flow Rate of CO_2 (ml/min)	Flow Rate of Solvent (ml/min)	Mass Flow Rate of CO_2 x 10^3 (g/s)	Mass Flow Rate of Solvent x 10^3 (g/s)	w CO_2	w Solvent	Total Heat x 10^3 (J/s)	H^E exp. (J/g)
0.040	0.373	0.633	6.395	0.090	0.910	-14.056	-2.0
0.080	0.331	1.264	5.686	0.182	0.818	-32.665	-4.7
0.120	0.290	1.895	4.977	0.276	0.724	-83.838	-12.2
0.160	0.249	2.527	4.267	0.372	0.628	-112.780	-16.6
0.200	0.207	3.157	3.558	0.470	0.530	-130.943	-19.5
0.240	0.166	3.788	2.849	0.571	0.429	-132.076	-19.9
0.280	0.125	4.419	2.140	0.674	0.326	-120.030	-18.3
0.320	0.083	5.051	1.430	0.779	0.221	-97.863	-15.1
0.360	0.042	5.681	0.722	0.887	0.113	-57.627	-9.0
0.380	0.021	5.996	0.367	0.942	0.058	-30.542	-4.8

* 3.62 % weight of H_2O in the solvent.

TABLE A7.18

Raw Data - Enthalpy of Mixing of (CO_2 + Selexol)* at 298.15 K and 12.6 MPa

Flow Rate of CO_2 (ml/min)	Flow Rate of Solvent (ml/min)	Mass Flow Rate of CO_2 x 10^3 (g/s)	Mass Flow Rate of Solvent x 10^3 (g/s)	w CO_2	w Solvent	Total Heat x 10^3 (J/s)	H^E exp. (J/g)
0.040	0.373	0.641	6.400	0.091	0.909	-23.939	-3.4
0.080	0.331	1.280	5.690	0.184	0.816	-58.548	-8.4
0.120	0.290	1.919	4.980	0.278	0.722	-91.067	-13.2
0.160	0.249	2.558	4.271	0.375	0.625	-114.727	-16.8
0.200	0.207	3.197	3.561	0.473	0.527	-127.050	-18.8
0.240	0.166	3.836	2.851	0.574	0.426	-125.716	-18.8
0.280	0.125	4.475	2.141	0.676	0.324	-113.795	-17.2
0.320	0.083	5.114	1.431	0.781	0.219	-92.285	-14.1
0.360	0.042	5.753	0.722	0.889	0.111	-53.743	-8.3
0.380	0.021	6.072	0.367	0.943	0.057	-29.619	-4.6

* 3.62 % weight of H_2O in the solvent.

TABLE A7.19

Raw Data - Enthalpy of Mixing of (CO_2 + Methanol) at 298.15 K and 7.5 MPa

Flow Rate of CO_2 (ml/min)	Flow Rate of Solvent (ml/min)	Molar Flow Rate of CO_2 x 10^6 (mol/s)	Molar Flow Rate of Solvent x 10^6 (mol/s)	x CO_2	x Solvent	Total Heat x 10^3 (J/s)	H^E exp. (J/mol)
0.020	0.393	7.048	162.382	0.042	0.958	-18.841	-111.2
0.040	0.373	14.036	153.857	0.084	0.916	-34.049	-202.8
0.080	0.331	28.036	136.782	0.170	0.830	-65.631	-398.2
0.120	0.290	42.021	119.722	0.260	0.740	-89.864	-555.6
0.160	0.249	56.010	102.658	0.353	0.647	-103.801	-654.2
0.200	0.207	69.986	85.607	0.450	0.550	-105.445	-677.7
0.240	0.166	83.976	68.542	0.551	0.449	-97.703	-640.6
0.280	0.125	97.960	51.483	0.656	0.344	-81.058	-542.4
0.320	0.083	111.942	34.426	0.765	0.235	-58.240	-397.9
0.360	0.042	125.940	17.353	0.879	0.121	-24.718	-172.5
0.380	0.021	132.925	8.831	0.938	0.062	-5.528	-39.0

TABLE A7.20

Raw Data - Enthalpy of Mixing of (CO_2 + Methanol) at 298.15 K and 10.6 MPa

Flow Rate of CO_2 (ml/min)	Flow Rate of Solvent (ml/min)	Molar Flow Rate of CO_2 x 10^6 (mol/s)	Molar Flow Rate of Solvent x 10^6 (mol/s)	x CO_2	x Solvent	Total Heat x 10^3 (J/s)	H^E exp. (J/mol)
0.020	0.393	7.218	163.017	0.042	0.958	-18.045	-106.0
0.040	0.373	14.385	154.453	0.085	0.915	-34.038	-201.6
0.080	0.331	28.726	137.318	0.173	0.827	-60.805	-366.2
0.120	0.290	43.065	120.184	0.264	0.736	-79.649	-487.9
0.160	0.249	57.395	103.060	0.358	0.642	-86.453	-538.8
0.200	0.207	71.720	85.941	0.455	0.545	-80.801	-512.5
0.240	0.166	86.059	68.807	0.556	0.444	-67.227	-434.1
0.280	0.125	100.398	51.674	0.660	0.340	-47.538	-312.6
0.320	0.083	114.719	34.558	0.769	0.231	-23.392	-156.7
0.360	0.042	129.052	17.431	0.881	0.119	4.409	30.1
0.380	0.021	136.221	8.865	0.939	0.061	15.684	108.1

TABLE A7.21

Raw Data - Enthalpy of Mixing of (CO_2 + Methanol) at 298.15 K and 12.6 MPa

Flow Rate of CO_2 (ml/min)	Flow Rate of Solvent (ml/min)	Molar Flow Rate of CO_2 x 10^6 (mol/s)	Molar Flow Rate of Solvent x 10^6 (mol/s)	x CO_2	x Solvent	Total Heat x 10^3 (J/s)	H^E exp. (J/mol)
0.020	0.393	7.326	163.430	0.043	0.957	-12.004	-70.3
0.040	0.373	14.588	154.842	0.086	0.914	-24.652	-145.5
0.080	0.331	29.103	137.677	0.175	0.825	-51.151	-306.7
0.120	0.290	43.625	120.504	0.266	0.734	-74.941	-456.6
0.160	0.249	58.149	103.330	0.360	0.640	-82.613	-511.6
0.200	0.207	72.664	86.164	0.458	0.542	-73.934	-465.5
0.240	0.166	87.194	68.984	0.558	0.442	-51.742	-331.3
0.280	0.125	101.712	51.815	0.663	0.337	-31.703	-206.5
0.320	0.083	116.235	34.642	0.770	0.230	-8.268	-54.8
0.360	0.042	130.750	17.476	0.882	0.118	16.750	113.0
0.380	0.021	138.013	8.888	0.940	0.060	22.182	151.0

TABLE A7.22

Raw Data - Enthalpy of Mixing of (CO_2 + Methyl Cyanoacetate) at 298.15 K and 7.5 MPa

Flow Rate of CO_2 (ml/min)	Flow Rate of Solvent (ml/min)	Molar Flow Rate of CO_2 x 10^6 (mol/s)	Molar Flow Rate of Solvent x 10^6 (mol/s)	x CO_2	x Solvent	Total Heat x 10^3 (J/s)	H^E exp. (J/mol)
0.040	0.373	14.044	69.700	0.168	0.832	-3.358	-40.1
0.080	0.331	28.026	61.973	0.311	0.689	-40.527	-450.3
0.120	0.290	42.016	54.239	0.437	0.563	-70.747	-735.0
0.160	0.249	56.002	46.509	0.546	0.454	-96.391	-940.3
0.200	0.207	69.981	38.786	0.643	0.357	-119.372	-1097.5
0.240	0.166	83.967	31.056	0.730	0.270	-134.243	-1167.1
0.280	0.125	97.957	23.322	0.808	0.192	-134.959	-1112.8
0.320	0.083	111.937	15.598	0.878	0.122	-122.153	-957.8
0.360	0.042	125.924	7.867	0.941	0.059	-89.693	-670.4
0.380	0.021	132.921	3.998	0.971	0.029	-59.519	-434.7

TABLE A7.23

Raw Data - Enthalpy of Mixing of (CO_2 + Methyl Cyanoacetate) at 298.15 K and 10.6 MPa

Flow Rate of CO_2 (ml/min)	Flow Rate of Solvent (ml/min)	Molar Flow Rate of CO_2 x 10^6 (mol/s)	Molar Flow Rate of Solvent x 10^6 (mol/s)	x CO_2	x Solvent	Total Heat x 10^3 (J/s)	H^E exp. (J/mol)
0.040	0.373	14.390	69.960	0.171	0.829	-8.992	-106.6
0.080	0.331	28.723	62.202	0.316	0.684	-34.079	-374.8
0.120	0.290	43.057	54.444	0.442	0.558	-64.594	-662.5
0.160	0.249	57.399	46.678	0.552	0.448	-84.771	-814.5
0.200	0.207	71.725	38.928	0.648	0.352	-100.429	-907.6
0.240	0.166	86.057	31.171	0.734	0.266	-106.197	-905.9
0.280	0.125	100.393	23.411	0.811	0.189	-103.154	-833.2
0.320	0.083	114.734	15.646	0.880	0.120	-90.614	-695.0
0.360	0.042	129.067	7.889	0.942	0.058	-62.192	-454.1
0.380	0.021	136.233	4.011	0.971	0.029	-38.287	-273.0

TABLE A7.24

Raw Data - Enthalpy of Mixing of (CO_2 + Methyl Cyanoacetate).
at 298.15 K and 12.6 MPa

Flow Rate of CO_2 (ml/min)	Flow Rate of Solvent (ml/min)	Molar Flow Rate of CO_2 x 10^6 (mol/s)	Molar Flow Rate of Solvent x 10^6 (mol/s)	x CO_2	x Solvent	Total Heat x 10^3 (J/s)	H^E exp. (J/mol)
0.040	0.373	14.576	70.121	0.172	0.828	-1.838	-21.7
0.080	0.331	29.086	62.350	0.318	0.682	-24.185	-264.5
0.120	0.290	43.609	54.566	0.444	0.556	-57.580	-586.5
0.160	0.249	58.122	46.792	0.554	0.446	-75.412	-718.8
0.200	0.207	72.641	39.012	0.651	0.349	-87.815	-786.5
0.240	0.166	87.148	31.244	0.736	0.264	-91.908	-776.3
0.280	0.125	101.669	23.462	0.813	0.187	-86.954	-694.9
0.320	0.083	116.178	15.692	0.881	0.119	-74.045	-561.5
0.360	0.042	130.695	7.914	0.943	0.057	-48.291	-348.4
0.380	0.021	137.961	4.018	0.972	0.028	-28.921	-203.7

TABLE A7.25

Raw Data - Enthalpy of Mixing of (CO_2 + N-Formyl Morpholine) at 298.15 K and 7.5 MPa

Flow Rate of CO_2 (ml/min)	Flow Rate of Solvent (ml/min)	Molar Flow Rate of CO_2 x 10^6 (mol/s)	Molar Flow Rate of Solvent x 10^6 (mol/s)	x CO_2	x Solvent	Total Heat x 10^3 (J/s)	H^E exp. (J/mol)
0.040	0.373	14.046	61.917	0.185	0.815	-20.138	-265.1
0.080	0.331	28.032	55.051	0.337	0.663	-53.306	-641.6
0.120	0.290	42.017	48.187	0.466	0.534	-77.431	-858.4
0.160	0.249	56.011	41.314	0.576	0.424	-154.620	-1588.7
0.200	0.207	69.989	34.456	0.670	0.330	-187.092	-1791.3
0.240	0.166	83.976	27.590	0.753	0.247	-202.247	-1812.8
0.280	0.125	97.964	20.722	0.825	0.175	-195.345	-1645.9
0.320	0.083	111.956	13.851	0.890	0.110	-172.356	-1370.0
0.360	0.042	125.936	6.992	0.947	0.053	-117.163	-881.4
0.380	0.021	132.939	3.549	0.974	0.026	-67.985	-498.1